Role of fms-like tyrosine kinase 3 in cardiac health and disease

Inauguraldissertation

Zur

Erlangung der Würde eines Doktors der Philosophie vorgelegt der

Philosophisch-Naturwissenschaftlichen Fakultät

der Universität Basel

von

Giacomo Della Verde

aus **Italien**

Basel, 2018

Genehmigt von der Philosophisch-Naturwissenschaftlichen Fakultät
auf Antrag von

Prof. Christoph Handschin, PD Dr. med. Gabriela Kuster Pfister, Prof. Aleksandra Wodnar-Filipowicz

Basel, 27.02.2018

Prof. Dr. Martin Spiess

The Dean of Faculty

Table of content

Summary

The fms-like tyrosine kinase 3 receptor (flt3) and ligand (flt3L) are important regulators of early haematopoiesis (*1*). Uncontrolled activity of flt3 is associated with acute myeloid leukaemia, making flt3 a major target of receptor tyrosine kinase inhibitors (TKIs) (*2*). TKIs are currently used in a variety of malignancies and patients have experienced cardiotoxicity under some of them. We recently demonstrated that exogenous activation of flt3 through intramyocardial injection of flt3L is cardioprotective and improves post-myocardial infarction remodeling and function in mice (*3*).

Based on this background, we wanted to assess how endogenous disruption of flt3-signaling affects the healthy and the injured heart. We also hypothesized that lack of flt3L has an impact on the adult cardiac progenitor cell pool, and, hence, on their contribution to cardiac homeostasis.

We isolated cardiac progenitor cells (CPCs) according to the side population (SP) phenotype (SP-CPCs) from 12 week-old wt and flt3L-/- mice (*4*) and we further expanded the SP-CPC fraction positive for Sca1 and negative for CD31 in culture (*5*). Our *in vivo* findings showed a reduced number of SP-CPCs in flt3L-/- hearts, suggesting an untimely activation of a proportion of this physiologically quiescent population. In line with this finding, transcriptional comparison revealed a reduced CD31- progenitor cell signature in flt3L-/- SP-CPCs, with downregulation of transcripts involved in cell cycle arrest and stemness. Expanded SP-CPCs do express functional flt3 receptor and secrete flt3L allowing for an autocrine and/or paracrine activation of the receptor. SP-CPCs maintained the capacity to differentiate into different cardiac lineages when expanded under progenitor potential-preserving culturing conditions. However, in this context, flt3L-/- SP-CPCs showed enhanced proliferation capacity associated with reduced differentiation potential towards all three major cardiac lineages, i.e., cardiomyocytes, smooth muscle and endothelial cells.

Echocardiography showed that disruption of flt3-signaling leads to significant systolic dysfunction and subtle structural alterations of the heart. Specifically, flt3L-/- hearts are smaller and exhibit reduced microvascularization within the ventricular wall. Together, these findings support that flt3-signaling is important for the maintenance of a functional CPC pool and cardiac homeostasis of the healthy heart. We further

investigated the implications of the lack of a functional flt3 system in a model of myocardial infarction. Given the importance of flt3 in cardiomyocyte survival (*3*) and myocardial microvascularization, we hypothesized that flt3-disruption may aggravate post-infarct myocardial damage and dysfunction. Contrary to this hypothesis, however, flt3L ablation mitigated the functional decline during the acute and post-acute phase after myocardial infarction. This protective effect may involve potential immunomodulatory properties related to flt3-signaling as supported by our most recent RNA sequencing data.

In summary, this thesis work shows that in a context of a potential prospective use of CPCs for cardiac cell therapy, careful adjustments of culturing conditions are pivotal to preserve the CPC potential, and thus the capability for multi-lineage commitment and differentiation, during *ex vivo* expansion.

Furthermore, this work uncovers a so-far unrecognized role of flt3 signaling in the regulation of adult CPC homeostasis and function. In particular we showed that flt3 contributes to the maintenance of a pool of quiescent, functional cardiac progenitor cells *in vivo* and their balanced proliferation and differentiation *in vitro*.

Finally, our most recent data suggest that the systemic inhibition of flt3 may be protective during the early phase post-myocardial infarction. In view of the increasing use of TK targeting cancer therapies, improved understanding of the roles of such TK in cardiac health and disease is important in order to anticipate potential cardiac side effects. This work uncovers so far unknown functions of flt3 signaling in the healthy and injured heart that raise both awareness of potential cardiac toxicity, but also of a possible therapeutic effect of the systemic inhibition of flt3 in the post-acute phase after myocardial infarction.

List of abbreviation

ABC: ATP-binding cassette
Abcb1b: TP-binding cassette, sub-family B (MDR/TAP), member 1B
Abcg2: ATP-binding cassette sub-family G member 2
α-MHC: α Myosin Heavy Chain
AML: acute myloide leukemia
ACTN2: α-sarcomeric-actinin
ATP: Adenosine triphosphate
BM: Bone marrow
BSA: bovine serum albumin
CFU: colony forming unit
CHF: congestive heart failure
CPC: cardiac progenitor cell
CSC: cardiac stem cell
CSP: cardiac side population
CMC: cardiomyocyte
DAPI: 4',6-diamidino-2-phenylindole
DC: dendritic cell
DCM: Diabetic cardiomyopathy
DMEM: Dulbecco's Modified Eagle's Medium
EGF: epidermal growth factor
EthBr: ethidiumbromide
EtOH: ethanol
FGF: fibroblast growth factor
FBS: fetal bovine serum
FDR: false discovery rate
flt3: Fms-like tyrosine kinase 3
flt3L: Fms-like tyrosine kinase 3 ligand
GSEA: Gene Set Enrichment Analysis
HBSS: Hank's buffered salt solution
HF: heart failure
Hoechst: bisBenzimide H33342 trihydrochloride
HSCT: hematopoietic stem cells transplantation
IL: interleukin
IMDM: Iscove's Modified Dulbecco's Medium
Kdr: Kinase insert domain receptor
KI: kinase ihnibitor
KO: knock-out
LAD: left anterior descending
LS: longitudinal strain
LV: left ventricular
LVEF: left ventricular ejection fraction
LVEDD: left ventricular end-diastolic diameter
mA: milliAmpere
M-CSF: macrophage colony-stimulating factor
MI: myocardial infarction
MP: main population
MRI: magnetic resonance imaging
Myh6: Myosin heavy chain 6

NRVM: Neonatal Rat Ventricular Myocytes
ON: over-night
PBS: phosphate buffered saline
PCR: polymerase chain reaction
PDGFR: platelet derived growth factor receptors
PFA: paraformaldehyde
PI3K: phosphoinositol-3-kinase
PY: Pyronin Y
Rn18s: 18s ribosomal RNA
RS: radial strain
RT: room temperature
RTK: receptor tyrosine kinase
RT-PCR: reverse transcription PCR
s.c.: sub-cutaneous
SCF: stem cell factor
SMC: smooth muscle cell
SP: side population
TKD: tyrosine kinase domain
TKI: tyrosine kinases inhibitor
TNNI3: troponin I type 3
V: Volt
VEGF: vascular endothelial growth factor
VEGFR: vascular endothelial growth factor receptor
vWF: von Willebrand factor
WGA: Wheat germ agglutinin
wt: wild-type

Introduction

Chapter 1. Role of fms-like tyrosine kinase 3 receptor in health and disease

Cancer kinome and its cardiotoxicity

The human kinome is an ensemble defining above 500 kinases in the human genome. A clinical study screened 518 protein kinase genes for somatic mutations in varying types of human cancer. Excluding gene "passenger" mutations (random neutral mutation, which it is believed to have no role in cancer), they identified approximately 120 genes as plausible cause for the observed tumours (*6*). These protein kinases that can carry mutations, which may act as cancer "drivers" (or contribute to tumour growth), are defined as cancer kinome and are recognised as an attractive target for therapy against cancer via the use of the so-called kinase inhibitors (KIs).

KI therapy has shown high efficiency with regard to cancer treatment (*7, 8*). Despite their beneficial effects, KIs are responsible for a simultaneous inhibition of the same kinases in the whole organism, including the heart, where these kinases may be important for cardiac cell homeostasis, and hence leading to cardiotoxic effects.

Cardiotoxicity is a term used to describe a broad range of adverse effects on heart function induced by therapeutic molecules. These adverse events may impact on hemodynamics, electrical activity, or interfere with myocytes and progenitor cell function, and facilitate the development of cardiomyopathies.

We distinguish two general types of cardiotoxicity. "On target" cardiotoxicity is induced by the inhibition of kinases that are specifically targeted by a chosen KI. In contrast, "off-target" cardiotoxicity is the cardiotoxic effect due to inhibition of kinases, for which the drug was not designed for, since none of these small-molecule inhibitors seem to be truly selective (*9*).

Although past studies of cardiotoxicity have mainly focused on anthracyclines and radiotherapy (*10*), the increasing use of targeted therapies, such as KIs in general or receptor tyrosine kinase inhibitors (TKIs) in particular, for a variety of solid and hematologic malignancies has increased the need to investigate their related cardiotoxic effects (*11*).

Several KIs have been shown to evoke adverse cardiac events, some of them being transient and/or reversible. The susceptibility to KIs to experience cardiotoxicity may

vary from patient to patient, making it difficult to identify patients truly at risk.
An improved understanding of the cardiac functions of specific kinases targeted by KIs and of the underlying cellular and molecular mechanisms may help anticipate potential cardiotoxicity and identify and improve the management of high risk patients (*12, 13*).

Cardiovascular risk in cancer patients

The leading non cancer-related cause of morbidity and mortality in long-term cancer survivors is cardiovascular disease. Improvements in childhood cancer therapy have led to a growing number of long-term cancer survivors, but compared to age-matched healthy control subjects, they experience a 7-fold higher incidence of cardiovascular abnormalities or diseases and an 8-fold higher cardiac-related mortality rate (*14-17*).
Cardiotoxicity related to cancer treatment may manifest as acute, when it occurs within the first week of treatment, early onset or late onset. Acute cardiotoxicity is mainly characterized by transient electrophysiological abnormalities, rare fatal arrhythmia or left ventricular (LV) dysfunction and, if resolved, patients remain at high risk for late cardiotoxic effects (*18*). Early or late onset cardiotoxicity occurs within a year or more respectively, and is characterized by persistent damage, mostly leading to heart failure (HF) due to loss of functional cardiomyocytes (CMCs) and reduced LV contractility (*19*). However, the degree and progression of the disease remains unpredictable due to a widely various susceptibility to anthracyclines or KIs among individuals and depends on concomitant additional cardiovascular risk factors such as smoking, diabetes, obesity, aging, et cetera. This accentuates the need for a cardiovascular program, which offers preventive care during and after cancer treatment, together with sensitive screening strategies to detect early subclinical cardiac dysfunction.
To date, no agreed-upon preventive strategies to avoid cardiotoxicity exist. However, the pre-emptive initiation of standard HF therapy, such as the administration of angiotensin converting enzyme inhibitors or beta-blockers, has shown to reduce early acute cardiotoxicity in high risk patients (*20*). Dexrazoxane, a cardioprotective agent, which decreases oxygen free radicals through intracellular iron chelation, can decrease tissue damage induced by anthracyclines (*21*). However, reports of an increased incidence in hematologic malignancies later in life of young patients treated with dexrazoxane has limited its routine clinical use (*22*).

Nowadays several sensitive screening strategies exist, although the precise roles and the frequency of monitoring cardiac function is not clear. To date, cardiac magnetic resonance imaging (MRI) and echocardiography approaches are used as reference standard to detect LV dysfunction, but they lack sufficient sensitivity and specificity to detect early cardiac injury. Screening guidelines also suggest monitoring of biomarkers such as brain natriuretic peptide (BNP) (*23*) or serum cardiac troponin I, which are indicative of HF and cardiac injury respectively, and have shown to be elevated under chemotherapy (*24*).

Flt3 signaling in haematopoiesis

In this study we focused on the fms-like tyrosine kinase 3 (flt3) system, also known as fetal liver kinase 2 (flk2). Flt3 receptor exerts a functional role in early haematopoiesis upon binding with its own ligand (flt3L) (to date the only one identified), controlling proliferation and differentiation of hematopoietic progenitor cells.

Flt3 belongs to the type III family of receptor tyrosine kinases (RTKs). It is expressed as a monomeric transmembrane receptor. Upon flt3L binding, two flt3 receptor molecules assemble to form a homodimer. Flt3 dimerization results in the phosphorylation of the tyrosine kinase domain (TKD), which triggers the activation of signal transduction pathways through activation of cytoplasmic molecules such as phosphoinositol-3-kinase (PI3K), Ras GTPase, phospholipase C-γ, Shc, growth factor receptor bound protein (Grb2) and Src family tyrosine kinase (Fig.1). Phosphorylation of these proteins affects further downstream signalling including Akt, Erk, and Stat3 and 5, which are involved in several cellular processes (*25*) (Fig.2).

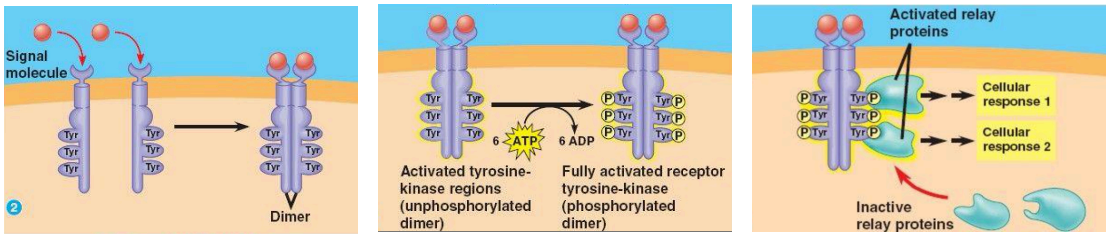

Fig.1: flt3 receptor system triggered by flt3L binding (https://www.slideshare.net)

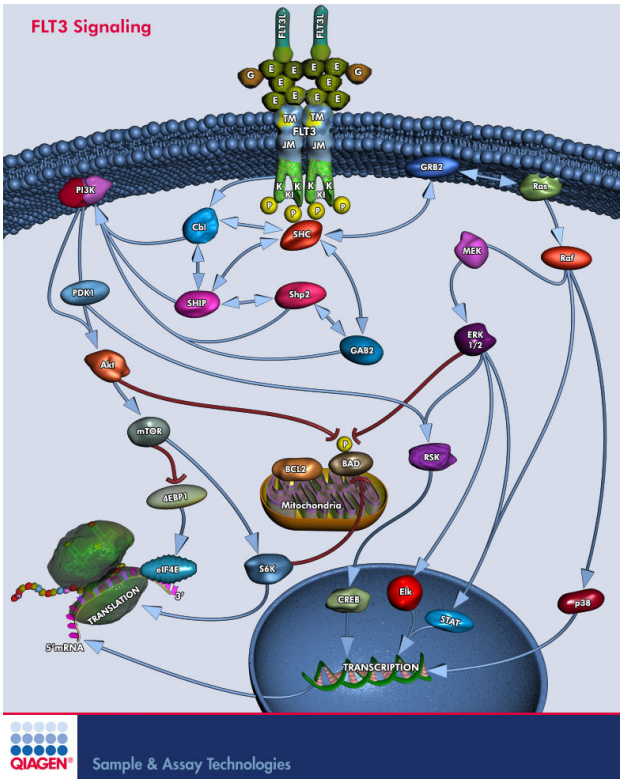

Fig.2: Intracellular pathways involved in flt3 signaling (http://www.qiagen.com)

Numerous studies have demonstrated that flt3L, supplemented *in vitro* (in synergy with other cytokines such as interleukin (IL) 3, granulocyte colony-stimulating factor, granulocyte macrophage colony-stimulating factor, stem cell factor (SCF), and IL-6) or administered *in vivo* (as single agent), stimulates the expansion and mobilization of hematopoietic progenitor cells (*26-29*).

Mice that are knock-out (KO) for flt3 receptor (flk2-/-) or its ligand (flt3L-/-) exhibit hematologic defects, which are more severe in mice lacking the flt3L. Flk2-/- mice do not have variations in monocyte, granulocyte, and erythrocyte levels but B lymphoid precursor are reduced. Also the ability of mutant flk2-/- stem cells to reconstitute haematopoiesis in irradiated hosts is 5-fold reduced compared to wild-type (wt) competitors (*30*). Flt3L-/- mice exhibit reduced leucocyte cellularity in bone marrow (BM), peripheral blood and lymph nodes, along with reduced numbers in myeloid and lymphoid progenitors. In contrast, erythrocyte and platelet production is not affected. In addition, flt3L-/- mice have a marked deficiency in natural killer and dendritic cells (DCs) (*31*). Different studies approached the role of flt3L in DC. A study in a mouse model shows that transplanted common lymphoid and common myeloid progenitors

increase their DC progeny when a subsequent flt3L injection is performed (*32*). Also the DC progenitor compartment in the BM is responsive to flt3L as it increases progenitor cell numbers, although it does not alter their ability to produce mature DCs. In contrast, DC homeostasis in the spleen depends on flt3-mediated signals.

Importantly, more recent work by the group of A. Rolink and colleagues suggests an instructive role of flt3L in the commitment of multipotent progenitor cells towards myeloid and lymphoid lineage (*33*) and a permissive role of flt3L on the B-cell progenitor compartment through enhancing proliferation and possibly survival of their non-committed precursors (*34*). These findings support previous notions that flt3L acts in a cell type specific manner and exerts very distinct effects during hematopoiesis that heavily depend on the stage and context.

Flt3 signaling in acute myeloid leukaemia

Different kind of mutations leading to constitutive activation of flt3 are associated (in the presence of at least another mutated gene) with the development of acute myeloid leukaemia (AML), making the flt3 receptor itself an attractive target for cancer therapy (*35*). These mutations include internal tandem duplications (ITD) or point mutations of the kinase domain (TKD), although enhanced expression levels of wt flt3 also contributes to leukaemia. ITDs can be found in 17-26% of AML cases. The ITD occurs near the juxta-membrane domain and may negatively affect the auto-inhibition of the catalytic activity of the receptor (Fig.3A). Flt3-TKD mutations, such as single-amino acid substitutions, are also associated with constitutive activation of the flt3 receptor. Usually, they encompass a missense point mutation at the D835 residue and point mutations, deletions and insertions in the codons surrounding D835 (Fig.3B). They are found in approximately 7% of AML patients (*36*). Likely this mutation favours an open ATP-binding conformation of the activation loop hence making the receptor prone to accept ATP molecules and exert its catalytic activity. Although flt3-ITD blasts express similar levels of flt3 receptor compared to wt leukemic blasts, the flt3-ITD receptor is flt3L non-responsive. Ligand independent flt3-ITD blasts express increased levels of p-Stat1, p-Stat3 and p-Stat5 but not increased basal levels of p-Erk and p-Akt (*37*).

It was recently shown that flt3-ITD knock-in mice develop myeloproliferative neoplasms. Concomitant with the uncontrolled expansion of multipotent progenitor cells, flt3-ITD perturbs hematopoietic stem cell quiescence causing a proportion of

physiologically quiescent stem cells, such as the side population (SP), to leave their state and enter the cell cycle (*38*).

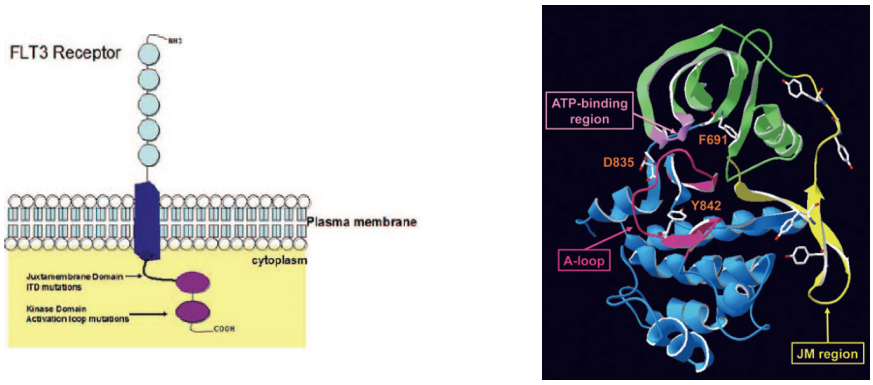

Fig.3: A. flt3 receptor domains (*35*). B. Activation loop mutations in the Tyrosine Kinase Domain (*36*).

Flt3–targeting tyrosine kinase inhibitors induce cardiotoxicity

Nowadays several TKIs targeting the flt3 receptor exist and cardiotoxicity has been observed under some of them. According to the modality of binding, TKIs can be classified in 4 different types. Type I inhibitors (e.g. sunitinib) recognize the ATP pocket of the kinase. This kind of TKIs are easy to design, but they are associated with a lack of selectivity due to the highly conserved structure of the ATP pocket across this class of human kinases. Type II inhibitors (e.g. sorafenib) target the ATP pocket and an adjacent site to it, thereby enhancing selectivity. A third class (type III) of inhibitors (quizartinib) is not competitive for the ATP pocket. They exhibit the highest specificity for the receptor binding, but insufficient knowledge of this unique portion of the receptor structure poses a challenge for drug design. Type IV inhibitors are designed to make a covalent bond with the kinase active site of the receptor (*39*).

The first generation TKI sunitinib is approved for metastatic renal-cell carcinoma and gastrointestinal stromal tumours. This drug shows a predominant inhibitory capacity for KIT, platelet derived growth factor receptor (PDGFR), vascular endothelial growth factor receptor-2 (VEGFR) and flt3 receptor. In a phase I/II trial on imatinib-resistant, metastatic, gastrointestinal stromal tumours, eight out of 75 patients experienced a cardiovascular event, with congestive HF (CHF) in 6 of them. Ten out of 36 patients receiving the approved dose of 50mg per day experienced an absolute reduction of the LV ejection fraction (LVEF) of at least 10%. Mechanisms of sunitinib cardiotoxicity were assessed in murine and rat cardiomyocytes. Murine

myocytes showed mitochondrial swelling and degeneration of the cristae. Being contractile units, myocytes have a high demand for ATP. Disturbance of the mitochondrial activity hence impairs energy generation and perturbs the contractile function. Sunitinib also causes cardiomyocyte apoptosis in mice and in cultured rat cardiomyocytes, likely via the mitochondrial death pathway (*40*).

The second-generation flt3 inhibitors, including sorafenib, quizartinib and crenolanib (CP-868596), are more potent and selective than the first-generation inhibitors.

Sorafenib is a multi-kinase inhibitor active against VEGFR, PDGFR, RAF-1, KIT, and flt3. Several AML studies have been conducted to assess sorafenib efficacy in combination with standard therapy. Again the treatment showed a higher impact on flt3 mutated-patients (*41, 42*).

A cardiac toxicity study (n=74) of sorafenib and sunitib in patients with metastatic renal cell carcinoma showed that 10% of patients experienced a cardiovascular event, which mostly consisted of changes in electrocardiography. However, elevation of troponin T or reduced LVEF (in three of them) were also observed (*43*). Following these clinical results, mechanisms of sorafenib toxicity have been evaluated in mice undergoing myocardial infarction (MI) after 1 week of treatment. Sorafenib significantly reduced the survival of mice in the two weeks following MI compared to vehicle treated mice. However, there were no differences regarding conventional functional parameters as LVEF and fractional shortening, but sorafenib-treated hearts were smaller and histological analysis showed an increased myocytes cross-sectional area suggesting loss of myocytes *in vivo.* Through BrdU incorporation strategy, they also showed that sorafenib reduced the number of myocytes and non-myocytes undergoing S-phase DNA replication in the infarct border zone. As for sunitinib, high dose of sorafenib induced myocyte necrotic death *in vitro (44).* These findings confirm previous clinical observations that cardiotoxicity might manifest and/or be more pronounced in the setting of aggravating factors, such as concomitant MI in this study.

Quizartinib (AC220) (Fig.4) is a novel non ATP-competitive compound developed to treat flt3-mutant AML. Quizartinib has a high flt3 binding affinity with a K_d 1.6nM (second only to Sunitib) and is the most potent cellular flt3-ITD inhibitor when tested in the human cell line MV4-11, which holds a homozygous flt3-ITD mutation. A screening through a 402 kinases binding assay, representing almost 80% of human

protein kinases revealed flt3 has the highest affinity for the drug. Although with a 10-fold higher K_d, the assay showed also binding affinity for other class III RTKs such as KIT, PDGFRA, PDGFRB, RET, and CSF1R (*45*). This off-target inhibition of mutant PDGFR and KIT isoforms was confirmed by an additional study (*46*). Quizartinib led to *in vitro* inhibition of cellular proliferation of mutant flt3, KIT or PDGFRA leukaemia cell lines in a dose dependent manner. The anti-proliferative effect was accompanied by a pro-apoptotic effect in cells harbouring activating-mutation on class III RTKs (*45*).

Quizartinib efficacy was evaluated *in vivo* in a xenograft tumour model, in which leukemic human MV4-11 cells were implanted subcutaneously into mice to establish the disease. Quizartinib was administrated for 28 days at 10mg/kg/day (to avoid cytotoxic effects but still to approach an IC_{50} during the course of the treatment). Mice treated with quizartinib showed complete regression of the tumour with no regrowth during the 60-days post-treatment observation period. In a more physiologically relevant model, in which leukemic MV4-11 cells were injected into BM-ablated mice, quizartinib showed a prolonged dose-dependent survival, with 80% survival at 10mg/kg/day administration (*45*).

A phase II study enrolled two cohorts of patients (n=333), including patients greater than 60 years old, who relapsed within <1 year or were refractory to first-line chemotherapy (cohort I), and patients greater than 18 yeas old refractory to second-line, salvage chemotherapy or relapsed after hematopoietic stem cells transplantation (HSCT) (cohort II, n=137). The majority of the patients were flt3-ITD and were treated with quizartinib continuously for 28 days. In cohort I, composite complete response (which includes complete remission with or without platelet and/or hematologic recovery) was demonstrated in 54% of patients harbouring flt3-ITD mutation compared with 31% in the flt3-wt group. Flt3-ITD patients in cohort II again demonstrated a higher composite complete remission rate: 44% versus 34% in the flt3-wt subset. Of note, in flt3-ITD population, which relapsed after their first AML therapy, 37% of patients were successfully bridged to HSCT. Taken together, these preclinical and clinical studies demonstrated the high efficacy of quizartinib in the treatment of wt as well as flt3-ITD-driven leukemia.

The side-effect profile of quizartinib showed primarily myelosuppression and QTc prolongation, which was transient and non-fatal (*47*).

Several clinical trials assessing quizartinib in patients are currently active or recruiting.

These trials address both the efficacy of quizartinib as monotherapy or in combination with conventional treatment or hematopoietic stem cell transplantation (*2*).

One of the major problems disclosed through early phases of clinical trial is the development of several resistance mechanisms against the flt3 inhibitor (*36, 48*). A primary resistance comprises of the low efficacy on mutations that differ from flt3-ITD, such as flt3-TKD mutation (although they correlate less with development of AML), and the compensatory up-regulation of parallel or downstream pathways. In contrast, secondary resistance arises from acquisition of new resistance mutations. It has been shown that D835Y, D835V, D835F or F691L mutations were additionally acquired in flt3-ITD patients treated with quizartinib monotherapy (*49*). Currently, there are two main ways to overcome acquired resistance during early phases of drug delivery. One way is the combinatorial use of different TKIs, since flt3 receptor could develop a point mutation and consequently resistance to a TKI, but still preserves sensitivity to a new agent. The other way consists of the use of an alternative flt3 inhibitor, which is selective and sensitive against both flt3-ITD and flt3-TKD mutations. At present, crenolanib is under clinical evaluation. In a phase II trial of patients with relapsed or refractory AML, crenolanib had better activity in flt3 inhibitor-naive patients compared with previously treated patients. Crenolanib was also tested against a panel of D835 mutant cell lines and showed superior cytotoxicity compared with other available flt3-TKIs such as quizartinib and sorafenib (*50, 51*).

Combinatorial therapy represents a solution not only to overcome resistance but may enhance efficacy given that results from monotherapy, although promising, are still far from optimal. At present, several studies combined quizartinib with conventional chemotherapy such as anthracyclines to minimize toxicity (avoiding cytotoxic effects resulting from high concentrations of a single agent) and to prompt a synergistic effect for better outcome (*52*).

In this setting, timing of flt3-TKI delivery is crucial, since flt3L levels dramatically increase in response to cytotoxic chemotherapy (*53*) and this might counteracts flt3-TKI efficacy (*2, 47, 52*).

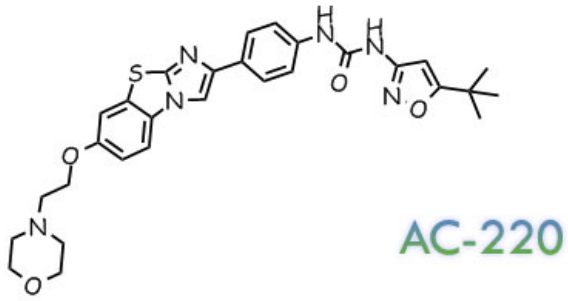

Fig.4: Quizartinib chemical structure (www.kinasepro.wordpress.com)

Flt3 signaling in skeletal muscle

A novel role for flt3/flt3L outside of the hematopoietic system has recently been reported in skeletal muscle. In this study using C2C12 myoblasts, flt3L was found to drive myogenesis. Specifically, these authors described a negative effect on myotube formation following flt3 or flt3L knock-down, which was partially rescued by exogenous flt3L delivery. They further showed that depletion of flt3/flt3L led to an increase in cell proliferation, and proposed that the absence of flt3/flt3L prevented cell cycle exit, which is required for promoting differentiation. Finally, in a skeletal muscle regeneration model, flt3L mRNA was increased during the early phases of regeneration and flt3L siRNA inhibited regeneration, supporting a role of flt3/Flt3L in muscle regeneration *in vivo (54)*. These findings are in agreement with an earlier study, which showed inhibition of proliferation of muscle-derived stem cells in the presence of flt3L through an increase in the length of the cell cycle (*55*).

Together, these papers point to a so far unrecognised role of flt3/flt3L in the regulation of skeletal muscle precursors. Whereas this novel role is distinct from the known role of flt3L as pro-proliferative agent in the permissive growth of B-cell precursors (*34*) and hematopoietic progenitor cells (*28, 29, 38*), it is consistent with the recently reported instructive role of flt3L in early lineage commitment of lymphoid/myeloid progenitor cells (*33*), supporting the notion that flt3 may regulate cell fate in a cell type-specific manner.

Flt3 signaling in the heart

Flt3 receptor and flt3L expression have been identified in whole heart homogenates in mice (*56*). Interestingly, mRNA levels of flt3L and Flt3 were up regulated between 3 and 7 days after MI. A recent study suggested that co-administration of exogenous flt3L with G-CSF into the peripheral circulation improves post-MI remodelling and LV systolic function. They supported the idea that, at least in part, the beneficial effect of this treatment was related to increased homing of BM-derived cells into the infarcted heart, which differentiate into newly formed myocytes and vascular cells (*57*).

Flt3L also exerts cytoprotective effects in the injured heart when administered exogenously at therapeutic concentrations. In 2014 Pfister *et al.* identified expression of flt3 by intrinsic cardiac cells, which was pronounced in CMCs exposed to hypoxia. Flt3 activation triggered by exogenous flt3L decreased CMC apoptosis *in vitro* and in the infarct border zone *in vivo* and ameliorated post-MI function and remodelling by limiting infarct size. The investigators also provided evidence for activation of pro-survival pathways involving Bcl-2 family protein regulation and inhibition of the mitochondrial death pathway (*3*), as it was previously shown for flt3-expressing leukemia cells (*58*).

Wang and colleagues examined the effect of flt3L in mice with multi-organ dysfunction syndrome, which affects different organs of the body, including the heart. They observed mitigated organ damage in the mice treated with flt3L as compared to control, an effect, which they attributed to a more favourable immune response in the flt3L group (5 μg/kg once a day for seven days) (*59*).

Chapter 2. Cardiac progenitor cells and regeneration

The adult mammalian heart has an extremely limited capacity to regenerate. Under homeostatic conditions, CMC turnover amounts to approximately 0.5-1.5% per year (*60-62*). Although multiple studies have demonstrated that renewal of CMCs based on complete cell cycle re-entry of pre-existing CMCs including karyokinesis and cytokinesis occurs in areas adjacent to myocardial injury, this is not sufficient to replenish the CMC pool and confer recovery of the necrotic, akinetic myocardium (*61, 63-65*). The discovery of cardiac progenitor cells (CPCs) opened new perspectives for therapeutic cardiac regeneration, aiming at activation of residential CPCs to proliferate and differentiate into CMCs and other cardiac cell types (*66*).

CPCs are multipotent as they can differentiate into all three main cardiac lineages: CMCs, endothelial cells and smooth muscle cells (SMCs). *In vitro*, they can self-renew to maintain a pool of undifferentiated clones (*66*). Such CPCs reside in the heart, which allows direct targeting of these cells, thereby circumventing problems like poor engraftment or immune rejection that accompany cell transplantation. CPCs are activated *in vivo* in response to cardiac injury to renew and maintain an undifferentiated cell pool (*67*). Numerous preclinical studies have shown that CPCs, either endogenously or upon *in vitro* expansion and transplantation, improve cardiac remodelling and function after cardiac injury (*61, 68-70*).

Interestingly, an impairment of the CPC pool is observed under anthracycline therapy, possibly contributing to chemotherapy-induced cardiomyopathy (*71, 72*). Specifically, administration of doxorubicin (DOXO) in rats has been shown to lead to dilated cardiomyopathy via a process that involves CPC alterations. DOXO promoted oxidative stress resulting in a dose-dependent reduction of CPC viability along with increased apoptosis and premature senescence. Administration of CPCs following anthracycline therapy ameliorated the DOXO-induced cardiomyopathy by regeneration of cardiomyocytes and vascular structures, which improved cardiac function and decreased animal mortality (*72*). These data propose that the functionality of CPCs is important to maintain cardiac cellular homeostasis and that weakening of CPC function can contribute to chemotherapy-induced cardiomyopathy. This notion is supported by major findings in human CPCs (hCPCs). In this study, the majority of hCPCs of DOXO-induced cardiomyopathic human hearts showed signs of senescence. Isolated hCPCs under DOXO showed increased apoptosis and DNA

damage due to accumulation of reactive oxygen species. DOXO also negatively affects hCPC differentiation into CMCs, smooth muscle cells and endothelial cells, suggesting a decline in regenerative capacity (*71*).

Another cardiac disease, in which functional alterations of progenitor cells have been implicated, is diabetic cardiomyopathy (DCM). DCM consists of a progressive structural and functional remodelling of the heart in diabetes, which occurs independently from coronary atherosclerosis and hypertension, and which eventually leads to HF. In a streptozotocin rat model following MI through coronary ligation, progenitor cell homing was markedly inhibited in hyperglycemic rats compared to normoglycemic rats. As expected, hemodynamic measurements showed that cardiac function was much more aggravated in diabetic rats following MI (*73*).

Different types of potential resident CPCs have been identified so far (*74*). C-kit+ CPCs and cardiosphere-derived cells have been widely explored and recently used for autologous transplantation in patients with ischemic cardiomyopathy. In both studies, intracoronary CPC transplantation was safe with no incidence of malignant arrhythmias or sudden cardiac death.

Briefly, the c-kit+ **S**tem **C**ell **I**nfusion in **P**atients with **I**schemic **C**ardiomyopathy (SCIPIO) trial (in which from a total of 20 patients enrolled in the treated arm, the analysis of cardiac MRI data were carried out in 9 treated patients) showed an improvement in LVEF at 4 and 12 months after transplantation, along with a reduction of the infarct size in a subset of patients. The most dramatic change instead was observed in the non-viable LV tissue, which was reduced by 50% after 12 months (*75*).

Similarly, in the intracoronary **CA**rdiosphere-**D**erived a**U**tologous Stem**CE**lls to reverse ventric**U**lar dy**S**function (CADUCEUS) trial, cardiac MRI did not show any change in global function at 1 year after cell delivery, but it revealed a reduction of the scar size, which correlated with a consistent 20% increment in viable mass compared to control patients (*76*).

Despite the significant reduction in myocardial scar mass in both studies and significant improvement in cardiac function and patient symptoms in SCIPIO, these results have to be taken with the great caution and placebo-controlled, double-blinded studies are needed. As in most preclinical studies showing low cardiomyogenic differentiation of administered CPCs, the mechanism of action remains unclear, and

paracrine effects appear more likely than true cardiomyogenesis.

In 2003, Oh *et al.* were the first to isolate Sca1+ CPCs from the adult mouse heart, which were negative for blood cell lineage markers, c-kit, flt1, flk1, CD34, and CD45, but expressed cardiac transcription factors such as Gata4, MEF2C and TEF-1. *In vitro*, these cells could express α-sarcomeric-actinin and cardiac troponin I upon stimulation with the demethylation agent 5-azacytidine. Labelled cardiac Sca1+ cells were injected after ischemia reperfusion injury. After 2 weeks, persistence of grafted cells was below 1% but donor-derived α-sarcomeric-actinin+ cells were abundant in the infarct border zone (*68*). In addition, murine cardiac Sca1+ cells treated with oxytocin differentiated in mature CMCs, with spontaneous beating, well-organized structures and electrical junctions *(77).* More recently, a study confirmed the intrinsic capacity of murine cardiac Sca1+ cells to give rise to endothelial cells, which was impaired during certain anti-cancer treatments such as DOXO (*78*).

An additional purification strategy takes advantage of the ability of CPCs to efficiently efflux vital dyes such as Hoechst through specific membrane ATP-binding cassette (ABC) transporters, including Abcg2 and Mdr1. ABC transporters utilize the energy of adenosine triphosphate (ATP) hydrolysis to carry out certain biological processes including translocation of various substrates across membranes such as cytotoxic compounds and therapeutic drugs (*79*).

These cells, firstly isolated in adult murine BM, showed a low Hoechst fluorescence and were referred to as side population (SP) as they fell to the "side" of the bulk of the positively stained cells in FACS analysis plots. The ability to efflux Hoechst was abolished by the presence of the ABC transporter inhibitor Verapamil, which confirmed that these cells are uniquely low in Hoechst fluorescence because of Mdr or a Mdr-like-mediated efflux of the dye (*80*) (Fig 5).

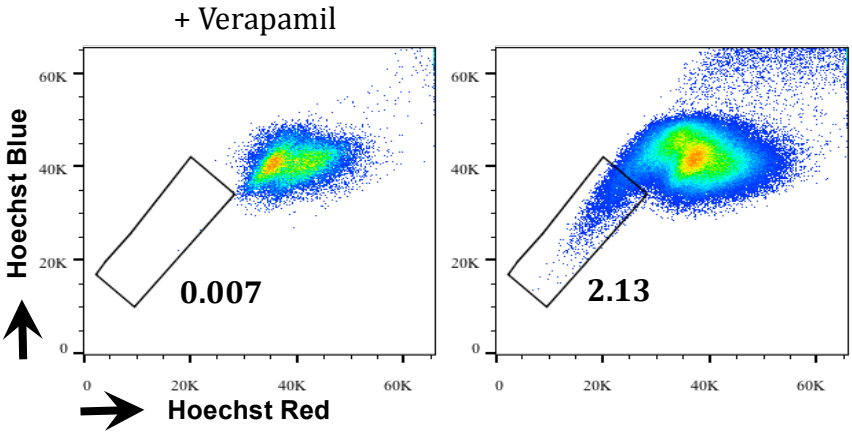

Fig.5: Cardiac Side Population.

Since this original discovery, SP-CPCs have been identified in a variety of tissues including umbilical cord blood (*81*), skeletal muscle (*82-84*), mammary glands (*85-87*), lung (*88-90*), liver (*91*), epidermis (*92, 93*), forebrain (*94*), testis (*95, 96*), kidney (*97*), limbal epithelium (*98, 99*), prostate (*100*), and endometrium (*101*). In normal tissues SP cells express high levels of stem-like genes and possess multipotent differentiation potential, and as such, they are thought to behave in a similar fashion to stem cells.

Hierlihy provided the first evidence that the adult myocardium contains a resident stem-like cardiac SP (CSP) (*102*). SP-CPCs localize ubiquitously in the four heart chambers mainly in perivascular areas and in interstitial space between CMCs (*103*) and the presence of this heterogeneous population within the adult heart was further confirmed in several studies. SP-CPCs were largely negative for hematopoietic markers CD45, CD34, and CD44 but exhibited expression of CD31 and Sca1. Notably, whereas the well-characterized BM-SP cells additionally expressed the SCF receptor c-kit, SP-CPCs were negative for it (*5*). Furthermore, they demonstrated that among Sca1+ SP-CPCs, the greatest potential for cardiomyogenic differentiation is restricted to cells negative for CD31 expression. Monoculture of Sca1+/CD31- SP-CPCs exhibited expression of the early cardiac transcription factor Gata4 and contractile protein α-sarcomeric-actinin and troponin I, although an organized structure and so a functional maturity was missing. Cellular coupling with neonatal rat ventricular myocytes was required to reach further biochemical and immune-histochemical features of mature CMCs, such as sarcomere organization and electromechanical coupling (Fig.6) (*5*).

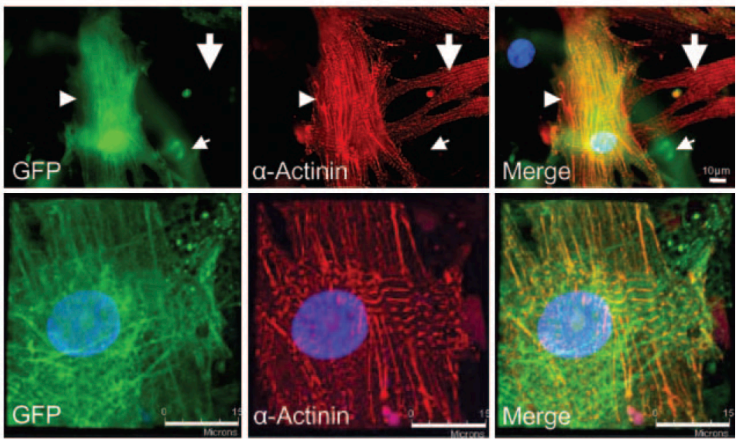

Fig.6: GFP-expressing Sca1+/CD31- CSP cells (green) co-cultured with adult CMCs: CSP cells (green), α-sarcomeric-actinin (red), dapi/nuclei (blue) (*5*).

In 2005 Oyama *et al.,* observed CSP cell differentiation capacity also in a rat model. SP-CPCs were isolated from neonatal hearts, which contained a larger amount of SP-CPCs compared to an adult heart. When treated with oxytocin, a small proportion of SP-CPCs expressed contractile proteins such as α-sarcomeric-actinin and showed spontaneous beating. When transplanted in a MI rat model via the tail vein, these cells migrated and homed to the injured region of the heart abounding in the border zone and contributing to cardiac regeneration (*103*).

Subsequently several groups assessed the endothelial differentiation potential of murine CSP. Yoon *et al.* observed that after treatment with vascular endothelial growth factor (VEGF) for 28 days, SP-CPCs demonstrated morphological changes and differentiated into endothelial cells, which were positively stained for CD31 and von Willebrand factor (vWF). Transplantation of these cells into the ischemic thigh muscle area showed a greater ratio of ischemic/normal hindlimb blood flow compared to the saline-treated group (*104*).

A further investigation confirmed Sca1+/CD31+ SP-CPCs as the sub-fraction with the highest potential to migrate in the injured region of the myocardium and form a vascular tube-like structure (*105*).

Liang *et al.* were the first to prove Sca1+/CD31- CSP progenitor cell commitment *in vivo* following MI. A proportion of these cells, transplanted into non-infarct myocardium, expressed myogenic and endothelial markers and participated in regeneration of the ischemic areas, although at a minimal rate due to a still incomplete differentiation. They proposed a model in which SDF-1α induces chemotaxis of

Sca1+/CD31- SP-CPCs to the infarcted area via CXCR4 receptor, which is up-regulated in Sca1+/CD31- SP-CPCs of ischemic hearts (*106*).

Recently the group turned its interest on the characterization of the Sca1-/CD31- CSP sub-population. These cells, expanded *in vitro,* were injected in the mouse heart following experimental MI. In a similar way to Sca1+/CD31- SP-CPCs (*106*), this cells, upon injection in a non-infarcted area could migrate from to the injured region and form tube-like structures positive for the endothelial marker vWF (*107*).

An intense work to understand the origin and potential of SP-CPCs was carried out by Noseda *et al.* Within the Sca1+ CSP, they identified a stricter profile, in which PDGFRα-positivity demarcates the clonogenic cardiogenic progenitor cells. They assessed tri-lineage differentiation capacity of expanded SP-CPCs in a murine MI model. Although cell retention already declined to 0.1–0.5% at 2 weeks, after 12 weeks 50% of the donor-derived cells were expressing troponin I and 5-15% were positive for vascular markers. Of note and new, multipotential properties were assessed on a single cell progeny clone expanded and labelled *in vitro* prior to injection (Fig.7).

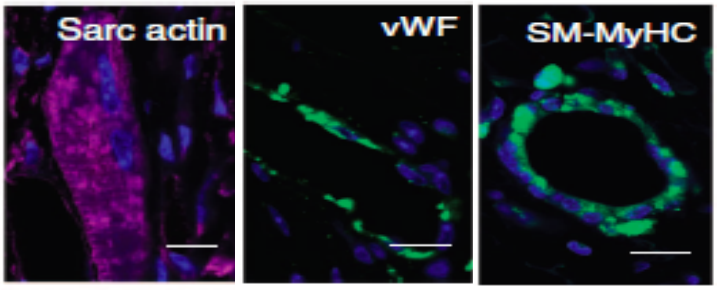

Fig.7: Cloned cardiac SP cells show tri-lineage potential after cardiac grafting (*69*).

Via Cre/lox fate mapping, they evaluated the potential origin of SP-CPCs. As all cardiac cells, they have a mesodermal origin as they derived from Mesp1+ precursors. No CSP cell was derived from pre-existing myocytes. Although Nkx2.5 and Isl1 were expressed rarely in fresh single cells and cloned cardiac SP cells, they largely contributed to the fate map profile, suggesting that CSP cells originate from Nkx2.5+ and Isl1+ precursors, contributors to the epicardium, the first and the second heart field (*69*).

Despite this considerable amount of work already performed on CPCs, overall understanding of CPC biology and behaviour is still insufficient to judge their therapeutic potential through either endogenous stimulation or transplantation.

Chapter 3. Myocardial infarction

MI is the leading cause for the development of CHF. MI occurs when the blood flow to the heart falls below a certain threshold due to a coronary artery blockage and it manifests as sudden and dramatic loss of contractile heart muscle cells that are later replaced by a fibrotic scar. A sophisticated inflammatory response and adaptive mechanisms initiate repair and remodeling processes aimed to compensate for the loss of myocytes, and maintain heart elasticity and cardiac function to pump sufficient blood to meet the need of the body.

Repair of the infarcted heart evolves in three overlapping phases: the inflammatory phase; the proliferative phase; and the maturation phase (*108*).

During the inflammatory phase, acute CMC necrosis (with subsequent release of all cellular components in the circulation) and matrix damages generate endogenous signals transducing an intense inflammatory response in the infarcted heart. Release of endogenous danger associated molecular patterns by ruptured cells promotes the activation of the complement cascade and activation of innate immune cells by binding to patter recognition receptors as toll-like receptors expressed by macrophages, DC cells and neutrophils (*109-111*). Reactive oxygen species are also important contributors to inflammatory signals in the infarcted myocardium during the acute phase. All these mechanisms trigger a diffuse chemokine and cytokine expression and secretion by several cellular populations (immune cells, fibroblasts, smooth muscle cells, endothelial cells), which contribute to a chemotactic gradient to recruit leucocyte populations within the first 24 hours (*112*). In particular, pro-inflammatory cytokines such as tumor necrosis factor, IL-1β and members of the IL-6 family are important regulators in protecting surviving CMCs at remote and boarder zones from apoptosis and inducing the synthesis of endothelial adhesion molecules and leukocyte integrin activation that ultimately lead to the extravasation of inflammatory cells into the infarct zone (*113*). Recruited neutrophils participate in the maintenance of a chemotactic gradient over time during the inflammatory phase and initiate the release of matrix metalloproteinases, which degrade the inter-myocyte collagen struts while monocytes and macrophages remove dead cells and matrix debris by phagocytosis (*114, 115*). Due to these processes, the region is more bound to distension, and consequently, more susceptible to deformations. Therefore, CMCs may slide on the infarcted wall resulting in wall thinning and ventricular dilation.

CMC lengthening may as well contribute to this deformation process, which further drives myocardial disarray (*116*).

Timely suppression of the inflammatory phase is pivotal to avoid accentuated cardiac damage and dysfunction. The repression of pro-inflammatory signaling is not a passive process, but requires an induction of inhibitory molecules and an activation of suppressive pathways (such as TGF-β, IL-10, pro-inflammatory-resolving lipid mediators, which inhibit matrix degradation) (*117-120*). In this context, macrophages acquire an inhibitory profile and phagocytize apoptotic neutrophils (*121, 122*). Also, a pericyte coat of new vessels stabilizes the vasculature and prevents the recruitment of leukocytes. Prolonged inflammatory signaling is detrimental: the continued secretion of proteases and cytokines by immune cells enhances matrix-degrading processes and loss of CMCs resulting in worsening of chamber dilation, loss of ventricular wall integrity and, hence, suppression of systolic function.

The suppression of the inflammatory phase overlaps with the activation of a pro-fibrotic repair program. Once the wound is cleared from dead cells and matrix debris, growth factors released by mononuclear cells and macrophages (such as TGF-β) promote activation of mesenchymal reparative cells such as vascular cells, which contribute to neovasculogenesis and angiogenesis to the infarcted boarder zone and interstitial and perivascular fibroblasts, which trans-differentiate into myofibroblasts.

Myofibroblasts secrete matrix proteins (mainly type I-III collagen) for the formation of a collagen-based scar aimed to preserve structural integrity of the ventricular wall, despite the loss of muscle elasticity (*108*).

These alterations in ventricular structure are detrimental in the long run, eventually leading to symptomatic or asymptomatic ventricular dysfunction and, hence, to HF (Fig.8).

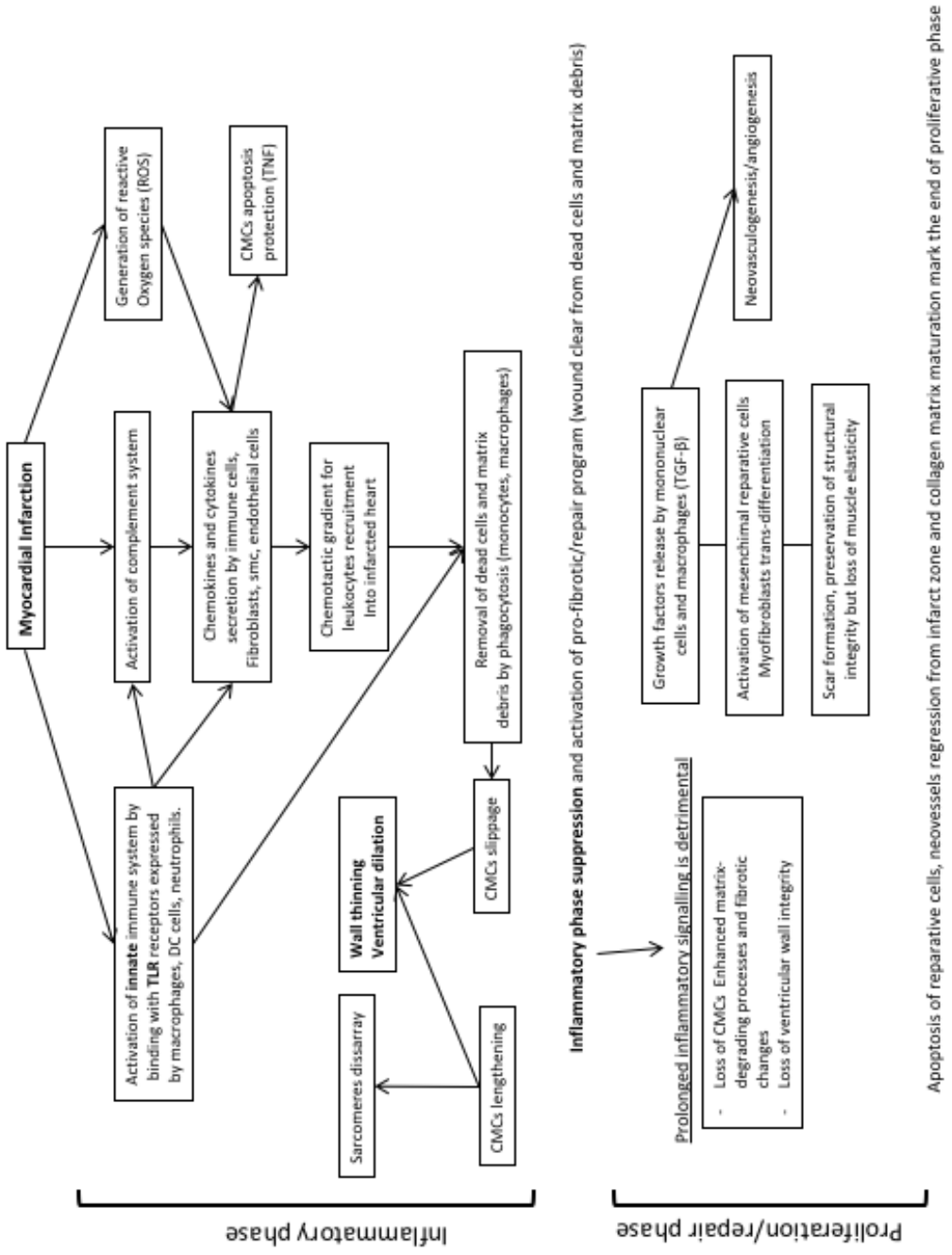

Fig.8: Myocardial post-MI remodelling.

Aim of the study

As in other organs, cardiac homeostasis defines any process involved in regulating and maintaining an internal steady state that makes the cells or the organ healthy.

This work is aimed to understand potential heart damages and disturbance of cardiac homeostasis deriving from TK-mediated inhibition of the flt3 receptor in a context of treatment of different malignancies, including AML. Flt3 is a cytoprotective system in the heart (*3*) and given that intrinsic, i.e. cardiac, flt3 activation is beneficial for CMC survival under ischemic conditions, the blockade of this signaling pathway might lead to CMC injury, resulting in cardiac dysfunction. In addition, flt3 is a regulator of hematopoietic progenitor cell proliferation and differentiation and may similarly be required for the regulation of cardiac progenitor cells.

For the current study we take advantage of two mouse models: a flt3L-/- model, in which we have the complete ablation of flt3 signaling since the embryonic stage and a time-defined (and partial) pharmacological inhibition of flt3 signaling via delivery of the TKI quizartinib.

Since Flt3/flt3L is an important regulator of progenitor cell function in different organs (*1, 54, 123*), in the first part of the project, we want to evaluate if and how flt3 signaling inhibition impacts on the progenitor cell pool of the heart, focusing on a specific multipotent CPC population, known as CSP.

In the second part of the project we want to investigate how endogenous flt3L ablation affects the structure and function of the heart at the whole organ level in a context of cardiac health and of ischemic disease.

Materials and Methods

Animals and in vivo models

Studies were conducted on 8-13 weeks-old C57BL/6NRj (wt), C57BL/6Flt3ltmlImx (flt3L-/-) (kindly provided by Prof. Aleksandra Wodnar-Filipowicz), 129S/SvEv-Flt3tm1Irl (flk2-/-) and C57BL/6-Tg(UBC-GFP)30Scha/J (kindly provided by Experimental Hematology research lab (Prof. Radek Skoda) (124). Flt3L-/- and flk2-/- mice were previously described by the original source laboratory (30, 31). The breeding and the animal care was carried out by the DBM Animal Facility Hebelstrasse (Basel, Switzerland).

Genotyping

A 0.5 cm tail biopsy was digested with lysis buffer (TRIS HCl 8.5pH + Proteinase K (Thermoscientific, #EO0491)) ON at 56°C. The lysate was centrifuged (2min, max speed, RT) to remove debris. DNA samples were heated at 95°C and used for PCR (see program below). 2% agarose was polymerised in TAE buffer (40mM Tris acetate and 1mM EDTA, pH 8.0-8.5) with Red Safe (Intron Biotech., #21141) addition. PCR products were then run for 40min at 100Volt. Bands were visualized with Gel Doc XR under UV using BenchTop 100bp DNA Ladder (Promega, #G8291) (Fig.9A-B).

		Program:		
5X FIREPol Master Mix (Solis BioDyne, 04-12-00115)	2µl			
Primer FOR (10µM)	0.5µl	2 min	94°C	
Primer REV (10µM)	0.5µl	30 sec	94°C	
ddH$_2$O	6µl	30 sec	60°C	
Tot	9.µl/tube + 1µl DNA	1 min	72°C	←step2 **37 cycles**
		10 min	72°C	
		∞	4°C	

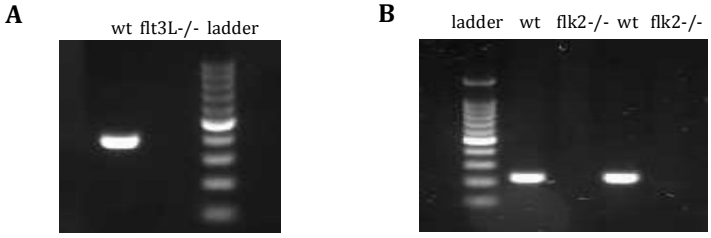

Fig.9: A. Genotyping for flt3L on wt and flt3L-/- mice; B. Genotyping for flt3 on wt and flk2-/- mice.

Quizartinib model: 2mg/ml of powdered quizartinib (Selleckchem, #S1526) was formulated in 15% polyanionic beta-cyclodextrin Captisol (Cidex pharmaceuticals) and administrated via oral gavage once daily. 48 wt mice were included in this

experiment. 24 mice (quizartinib-treated) were treated with quizartinib 10 mg/kg/day and 24 mice were treated with Captisol only (vehicle-treated) for 28 consecutive days. 2D-echocardiography was performed on 12-week-old wt 1 day before (baseline) and 28 days after quizartinib treatment as described. Body weight changes, physical condition and behaviour were monitored daily. Following treatment mice were subjected to echocardiography and then sacrificed for histology or CSP analysis (see below*)*. Heart weight was assessed based on the ventricular weight/tibia length ratio.

Myocardial infarction (MI) model: Baseline 2D-echocardiography was performed on 7-week-old wt and flt3L-/- mice, 1 week before MI. Wt and flt3L-/ were randomly assigned to sham or permanent LAD ligation. Anaesthesia for surgery was performed via intraperitoneal administration of ketamin/xylazine/acepromazin (65/15/2 mg/kg) and maintained with isoflurane 1-3%. Following left lateral thoracotomy at the fourth left intercostal space, MI was induced via permanent ligation of the left anterior descending (LAD) (*125, 126*). Sham-operated mice underwent an identical procedure except for LAD occlusion. Buprenorphin 0.1mg/kg in 0.9% NaCl solution was applied subcutaneously (s.c.) at the time of surgery, with subsequent additional s.c. doses every 6h after surgery and per os (buprenorphin 0.3 mg/ml (5ml) in 160 ml drinking water) over-night (ON) for two consecutive days. Body weight changes, physical condition and behaviour were monitored daily. Echocardiography was performed 1 week post-MI or post-sham and then mice were sacrificed for histology. Heart weight was assessed based on the ventricular weight/tibia length ratio.

Echocardiography: Transthoracic echocardiography was performed using a 40 MHz probe and the Vevo 2100 Ultrasound machine (VisualSonics, Toronto, ON, Canada). Mice were put under isoflurane anesthesia via a nose cone (2% in 100% oxygen) and placed on a heated platform to maintain body temperature at 37°C. Hair was removed from the chest with a depilatory agent (Nair). The heart was imaged in parasternal short and long-axis views both in 2D (B-mode) and M-mode. Data were transferred to an offline computer for analysis by an investigator blinded for animal group assignment. Left ventricular wall thickness and internal diameters were derived from M-Mode tracings acquired in a short axis image plane. Values were averages from three separate measurements. Left ventricular ejection fraction (EF) was calculated from derived volumes, which are computed based on the 'cubic' equations

(EF%=100%×[(LVID;d)^3-(LVID;s)^3)]/(LVID;d)^3). Echocardiographic 2D strain and strain rate measurement based on speckle-tracking was used to assess the global changes of left ventricular function.

Perfusion and paraffin embedding

350mM KCl (in water) was intravenously (jugular vein) injected to block the heart in diastole. The mouse chest was opened with scissors. A small cut was produced on the right atrium and a 29G needle was placed longitudinally into the apex of the LV. The heart was then perfused with 15 mL of cold 4% paraformaldehyde (PFA) under controlled pressure (70-90 mmHg). After removing the atria (and the right ventricle for some experiments), the perfused hearts were cleaned from surrounding non-heart tissue and left ON at 4°C in 4% PFA. The hearts were then transferred to 70% EtOH and cut transversally into three pieces (apex, middle, basis) using a sterile razor blade and processed for paraffin embedding. The embedded tissue was cut in 4µm sections on a Microm HM 340E Microtome and used for histology.

Immunohistochemistry

- von Willebrand factor (vWf), Wheat germ agglutinin (WGA), α-sarcomeric-actinin, Isolectin B4 (IB4) staining:

Tissue was deparaffinised and rehydrated. Tissue was then processed for antigen retrieval using Antigen Unmasking Solution (Vectorlabs, #H3300) at 97°C for 25min or using Proteinase K 20 mg/ml (Thermoscientific, #EO0491) for 25min. Tissue was washed with Tris-Buffered Saline Tween and blocked with 10% goat serum (Life Technologies, 50-062Z) for 1h. Immunostaining was performed using the following antibodies: vWf (1:50 Abcam, #6994), FITC-labelled WGA (1:100 Sigma, #4895), α-sarcomeric-actinin (1:20 Sigma, #A7811), DyLight 594 labelled IB4 (1:25 Vector labs, #DL-1207). Goat Alexa Fluor (Invitrogen) (1:100 to 1:800 according to primary) was used for secondary detection. Secondary antibody only was used as a negative control. 4',6-diamidino-2-phenylindole (DAPI) (Invitrogen, #D1306) was used to stain cell nuclei. Tissue was mounted with SlowFade Antifade kit (Invitrogen, #S2828). The stained samples were visualized using Widefield Fluorescence Olympus BX63 or Olympus BX61 and quantified with CellSens software (Olympus).

- TUNEL staining:

Tissue was deparaffinised and rehydrated. Tissue was then processed for antigen

retrieval using Antigen Unmasking Solution (Vectorlabs, #H3300) at 97°C for 25min. Tissue was washed with phosphate buffered saline (PBS) and incubated 2h at 37°C with In situ cell death detection kit, Fluorescein (Roche Diagnostics AG, #12-156-792-910). DAPI was used to stain the nuclei. Tissue was mounted with SlowFade Antifade kit.

The stained samples were visualized using Widefield Fluorescence Olympus BX63 or Olympus BX61 and quantified with CellSens software (Olympus).

- Fibrosis staining:

Tissue was deparaffinised and rehydrated. Tissue was treated 15min with preheated Bouin's solution (Sigma, #HT10132-1L) at 56°C and washed with running water. Tissue was subsequently treated with Weigerts iron Hematoxylin solution (Sigma, #HT1079) Biebrich Scarlet-Acid Fuchsin and Phosphotungstic/Phosphomolybdic acid solutions (Thricrome staining (Masson) kit, Sigma #HT15), respectively for 5, 5 and 20min, with washing in running water for 5min in between.

Then tissue was treated 10min with Aniline Blue Solution (Sigma, #HT15), 2min in 1% Acetic Acid (Sigma (Fluka), #45731) and rinse again in water. Tissue was then dehydrated and mounted with Cytoseal 60 (Thermoscientific, #8310-4)

Cardiac Side Population Isolation and Pyronin Y staining

SP-CPCs was isolated as previously described with some adjustments (*4*). 12-week-old mice were euthanized with 200mg/kg Pentobarbital i.p.. The heart was removed from the chest, minced with a razor blade and digested with Collagenase B 1mg/ml (Roche Diagnostics, #AG 11088807001) and 2.5mM CaCl2 at 37°C for 30min. Cardiac suspensions were filtered with 100 and 40μm cell strainers to eliminate undigested tissue and mature cardiomyocytes, and further treated with red blood lysis buffer (Biolegend, #420301) to deplete erythrocytes. Cardiomyocyte- and erythrocyte-depleted cardiac cells were suspended 1million/ml in DMEM (Gibco, #31885) supplemented with 10% FBS (Hyclone, #SH30071) and 25mM Hepes (Gibco, #15630) and stained with Hoechst 5μg/ml (Sigma, #B2261) at 37°C for 90min in the dark. Cells were washed with Hank's buffered salt solution (HBSS) and additionally incubated with Sca1-FITC (0.6 $\mu g/10^7$) (BD, #557405) and CD31-APC (0.25 $\mu g/10^7$) (BD, #551262) at 4°C for 30min in the dark. 7-Aminoactinomycin D (1$\mu g/10^7$ cells) (Invitrogen, #A1310) was added to the samples to exclude dead cells. The Sca1+/CD31- CSP fraction or whole CSP cells were sorted using Influx or

Sorpass AriaIII (BD) flow cytometer cell sorters.
To quantify RNA content of SP-CPCs, Pyronin Y (PY) 2µg/ml (Sigma, #P9172) was added for additional 15min after Hoechst incubation at 4°C in the dark. Cell sorting was performed by the DBM Flow cytometry Facility (Basel, Switzerland).

RNA sequencing from heart tissue and cardiac side population
RNA was isolated from a total of five sorts each of wt and flt3L-/- SP-CPCs (from 4 mice, the cells of which were pooled) or from 10 mg of heart tissue (ground with homogenizer using 5mm steel beads after atria removal, n=4 per group) using the NucleoSpin RNA XS kit (Macherey Nagel). RNA quality was controlled on an Agilent 2100 Bioanalyzer using RNA Pico CHIP (Agilent Technologies). RNA concentration was assessed using Quantus Fluorometer (Promega, #E6150) and QuantiFluor RNA System (Promega #E3310), a Fluorescence-based nucleic acid quantification method (See table 1-2).
RNA-seq library preparation and sequencing was performed at the Quantitative Genomics Facility of the Department of Biosystems Science and Engineering of the Swiss Federal Institute of Technology Zurich (Basel, Switzerland).
RNA-seq libraries from SP-CPC RNA samples were created with the SMART-Seq v4 kit from Clontech/Takara (*1, 2*). Sequencing was performed on an Illumina NextSeq 500 sequencer, and single-end 75bp unstranded reads were produced.
RNA-seq libraries from heart tissue RNA samples were created with the TruSeq RNA Library Prep Kit v2 (starting from 100ng per sample). Sequencing was performed on an Illumina NextSeq 500 sequencer, and single-end 75bp stranded reads were produced.
RNA-seq reads were mapped to the mm10 mouse genome assembly, with STAR (version 2.5.2a) (*3*). We allowed at most 10 hits to the genome per read. Reads were assigned to the best mapping location, or randomly across equally best mapping locations. Using the list of mouse Known Genes coordinates, obtained from http://genome.ucsc.edu in December 2015, and the qCount function from the Bioconductor package QuasR (version 1.18.0), we quantified gene expression as the number of reads that started within an annotated exon of a gene. The differentially expressed genes were identified using the Bioconductor package edgeR (version 3.18.1) (*4*). Sequencing analysis was performed in collaboration with the DBM Bioinformatics Core Facility (Basel, Switzerland).

Samples	SORT EVENTS	RIN	con. ng/µl
CPC_Bl6N_1	39119	9.1	1.315
CPC_Bl6N_2	40173	8.8	1.337
CPC_Bl6N_3	38486	8.3	1.375
CPC_Bl6N_4	50234	8.5	2.749
CPC_Bl6N_5	64612	6.7	2.674
CPC_FLKO_1	34222	6.8	2.235
CPC_FLKO_2	91495	7.2	3.497
CPC_FLKO_3	71757	8.2	1.475
CPC_FLKO_4	31261	7.4	1.479
CPC_FLKO_5	63091	7.9	1.201

Samples	RIN	con. ng/µl
WH_Bl6N_1	8.1	39.6
WH_FLKO_1	8.5	14.4
WH_Bl6N_2	8.4	25.2
WH_FLKO_2	8.1	24.0
WH_Bl6N_3	8	16.8
WH_FLKO_3	8.2	31.2
WH_Bl6N_4	8	22.2
WH_FLKO_4	8.6	10.5

Table1-2: Integrity and concentration values of RNA samples isolated from freshly sorted CSP cells (CPC) and heart (WH) homogenates.

Neonatal Rat Ventricular Myocyte (NRVM) Isolation

Neonatal rat pups were sacrificed by decapitation and hearts were quickly removed. Atria were removed and ventricles were transferred into Trypsin EDTA 0.05% (Gibco, #25300) over night (ON).

Hearts were washed with 7ml Medium3 (check below) and then digested with collagenase type 2 (36 mg/50ml HBSS) (Worthington, #LS004174). Suspension was filtered over a 100µm cell strainer to remove undigested tissue. Cells were suspended in Medium3 and pre-plated to remove most of the fibroblasts and endothelial cells (2x1h at 37°C). After preplating cells were counted and plated in Medium3 with 100µM Bromodeoxyuridine (Sigma, #B5002) to prevent proliferation of non-myocytes.

Culture media

Sca1+/CD31- SP-CPCs or NRVM were cultured *in vitro* at 37°C 5%CO2 in:

- **Medium1** (regular medium for CSP cells expansion): αMEM (Gibco, #32561) supplemented with 20% Fetal bovine serum (FBS) (Hyclone, #SH30071), 25 mM HEPES (Gibco, #15630), 1% penicillin and streptomycin (Gibco, #15140) and Sodium Pyruvate (Gibco, #11360).
- **Medium2** (regular medium for CSP cells expansion): 35% Iscove's Modified Dulbecco's Medium (IMDM) (Gibco, #12440), 65% Dulbecco's Modified

Eagle's Medium (DMEM)/Nutrient Mix F-12 Ham (Sigma #D8437), 3.5% FBS (Hyclone, #SH30071), 1.3% B27 supplement (Gibco, #17504044), 6.5 ng/ml recombinant human epidermal growth factor (EGF) (Peprotech, #AF-100-15), 13 ng/ml recombinant human fibroblast growth factor-basic (FGF) (Peprotech, #100-18B), 0.0005U/ml thrombin (Diagnotec AG, #100-125), 0.65 ng/ml Cardiothrophin-1 (Peprotech, #250-25), 1% penicillin and streptomycin (Gibco, #15140) and 0.2mM Glutathione (Sigma-Aldrich, #G6013) (*69*).

- **Medium3** (regular medium for NVRM): DMEM low Glucose, Pyruvate (Gico, #31885 supplemented with 7% FBS (Gibco, #10270), 25mM HEPES (Gibco, #15630), 1% penicillin and streptomycin (Gibco, #15140).
- **Medium4** (smooth muscle differentiation medium): 35% IMDM (Gibco, #12440), 65% Dulbecco's Modified Eagle's Medium (DMEM)/Nutrient Mix F-12 Ham (Sigma #D8437), 3.5% FBS (Hyclone, #SH30071), 1.3% B27 supplement (Gibco, #17504044), 10 ng/ml platelet-derived growth factor-beta (PDGF-β) (Peprotech, #100-14B), 0.0005U/ml thrombin, 0.65 ng/ml Cardiothrophin-1 (Peprotech, #250-25), 1% penicillin and streptomycin (Gibco, #15140) and 0.2mM Glutathione (Sigma-Aldrich, #G6013)
- **EGM-2** Bulletkit (Lonza, #CC-3162) (endothelial differentiation medium): Endothelial Basel medium (EBM-2) 500ml, human epidermal growth factor (hEGF) 0.5ml, vascular endothelial growth factor (VEGF) 0.5ml, R3-Insulin-like growth factor (R3-IGF-1) 0.5ml, Ascorbic acid 0.5ml, Hydrocortisone 0.2ml, human Fibroblast growth factor-basic (hFGF-β) 2ml, Heparin 0.5ml, FBS 10ml, Gentamicin/Amphotericin-B 0.5ml.

Proliferation assay

$1x10^4$ Sca1+/CD31- SP-CPCs (from passages P6-P8) were seeded with Medium1 or Medium2 (≈ 500cells/cm^2). Proliferation was assessed over 5 days by cell counting using Neubauer chamber. Trypan blue was used to exclude dead cells.

Colony formation assay

100 expanded Sca1+/CD31- SP-CPCs were plated in 3.5cm dishes with 1mL of Medium2. Medium was changed every 3 days. At 7, 10 and 14 days cells were fixed with 100% ice-cold MetOH for 10min on ice. Cells were then stained with 0.5%

crystal violet (1% Cristal violet (Sigma, #V5265):water 1:1) for 10min. Cells were carefully washed 5-6 times with water and let dry at RT ON (lid open).

Cardiostem spheres assay

$2x10^5$ Sca1+/CD31- SP-CPCs (P6-P8) were seeded in bacterial dishes (≈ 3000cells/cm^2) in Medium2 (without EGF, FGF). After 24h, 15 cardiostem spheres were collected with a pipette tip under the microscope under the flow desk and seeded in a LN-coated (10μg/ml) 24well-plate in Medium3. Cardiostem spheres were cultured for 2 weeks and medium was changed every 3 days. Expression of cardiac markers was assessed by immunocytochemistry (see below).

Immunocytochemistry

Freshly isolated or expanded SP-CPCs were cultured in non-coated, fibronectin (FN)-coated (10 μg/ml) or laminin (LN)-coated (10 μg/ml) dishes for 2 weeks with defined medium (see above) (FN: Sigma, #F4759; LN: Sigma, #L2020). Cells were washed with PBS and fixed in 3.7% PFA for 2-10min at room temperature (RT). Cells were then permeabilized with 0.1%-0.3% TritonX (Sigma (Fluka), #93420) in PBS, washed with PBS and blocked with 10% goat serum (Life Technologies, #50-062Z) for 1h. Immunostaining was performed using the following antibodies: von Willebrand Factor (1:100 Abcam, #6994), α-sarcomeric-actinin (1:25 Sigma, #A7811), troponinI (1:50 Santa Cruz, #15368), , α- Smooth Muscle Actin (1:50 Sigma, #A2547). Goat Alexa Fluor antibodies (Invitrogen) (1:500 to 1:800 according to primary) were used for secondary detection. DAPI was used to stain cell nuclei. Secondary antibody only was used as a negative control. The stained samples were visualized using Widefield Fluorescence Olympus BX63 or Olympus BX61 and quantified with CellSens software.

Tube formation assay

$3x10^5$ SP-CPCs were cultured in FN- and LN-coated (10 μg/ml) P10 dishes. After 24h in 0.1% FCS Medium1 (without EGF, FGF, Thrombin, Cardiothrophin-1, and B27) cells were cultured in EGM-2 medium for 3 weeks. Medium was changed every 3 days. Cells were collected and counted. $2x10^4$ SP-CPCs were then cultured in Matrigel Basement Membrane Matrix Growth Factor Reduced 10mg/ml (Corning, #354230). After 24h we evaluated tube formation capacity.

Flow Cytometry

Expanded Sca1+/CD31- SP-CPCs from passages P7-P9 were cultured in Medium1 or Medium2 in 75cm2 flask. After trypsinization cells were washed with HBBS and counted using a Neubauer chamber. Cells were incubated for 1h at the dark at 4°C using the following conjugated antibodies: Sca1-FITC (BD, #557405), FITC Rat IgG2a, κ Isotype Control (BD, #554688), CD31-APC (BD, #551262), APC Rat IgG2a κ Isotype Control (BD, #553932). After washing with HBBS, 7-Aminoactinomycin D (1μg/107 cells) (Invitrogen, #A1310) was added to the samples to exclude dead cells. Samples were analysed with BD Fortessa.

RNA interference

$1x10^5$ SP-CPCs were seeded in Medium1 (-antibiotics) ON. Medium was changed and cells were transfected with 40nM siRNA_flt3L (Mm_Flt3l_1 Qiagen, #SI01003695) or AllStars Negative Control siRNA (Qiagen, #SI03650318) for 72h (new medium with siRNA was added after 48h) using DharmaFECT1 (Dharmacon, #T2001) as a vehicle. Cells were collected for RNA or protein extraction using Trizol-Chloroform or Lysis/RIPA buffer respectively.

ELISA

$1x10^5$ SP-CPCs were seeded with regular Medium1 (-antibiotics for siRNA transfection) or Medium2 ON. Medium was changed every 48h. Supernatant was collected after 96h and centrifuged using Amicon Ultra-4 Centrifugal Filter Units (Millipore, #UFC801024) to achieve a retention volume of ≈150 μl.

Flt3L abundance in supernatant was detected using mouse Flt3 Ligand ELISA kit (R&Dsystems, #MFK00) and quantified by ELISA reader at delta 450-540nm. Concentrated medium only was used as blank.

For siRNA treatment Medium1 was substituted by phenol-free DMEM without FCS and antibiotics during the last 48h of culturing.

In vitro flt3L treatment for western blot

Wt, flt3L-/- and flk2-/- SP-CPCs were seeded and expanded in Medium1 or Medium2 till 90% confluence. Cells were then kept at 0.1% FCS ON. Cells were treated 5min with flt3L (R&Dsystems, #427-FL/CF) 100ng/ml and Akt phosphorylation was quantified by Western Blotting (see below). To evaluate the quizartinib inhibitory

effect on flt3L-dependent Akt phosphorylation, CSP cells were preincubated for 2h with 5nM DMSO diluited-quizartinib (Selleckchem, #S1526) prior to flt3L treatment. DMSO only was used as negative control.

Polymerase Chain Reaction (PCR)

RNA was extracted from expanded SP-CPCs using Trizol-Chloroform (Sigma) or Direct-zol RNA MiniPrep Plus (Zymo Research, #R2072) and cDNA was generated using the High Capacity cDNA Reverse Transcription Kit (Applied Biosystems, #4368814) (see program below). Normal PCR was performed using FIREpol Master Mix (Solis BioDyne, #04-12-00115) to assess expression of stemness, cardiomyogenic and vascular genes. Quantitative Real Time (RT-PCR) was performed using *Power* SYBR Green PCR Master Mix (Applied Biosystems, #4367659). Samples were run and expression was quantified Fast 7500 Real Time PCR systems.

Reverse transcriptase PCR:

RT-Buffer	2.0 µl
dNTP	0.8 µl
Random Primer	2.0 µl
Reverse Transcriptase	1.0 µl
RNasin (Promega, #N211B)	0.5 µl
H2O	3.7 µl
	+ 10 µl (up to 2 µg) RNA

Program:

10 min	94°C
120min	94°C
5 sec	60°C
∞	4°C

Normal PCR:

5X FIREPol Master Mix (Solis BioDyne, #04-12-00115)	2µl
Primer FOR (10µM):	0.5µl
Primer REV (10µM):	0.5µl
ddH$_2$O:	5µl
Tot	8.µl/tube
	+ 2µl cDNA (50ng)

Program:

2 min	94°C	
30 sec	94°C	
30 sec	60°C	
1 min	72°C	←step2 **25/30/38 cycles**
10 min	72°C	
∞	4°C	

To evaluate gene expression the following primers were used:

Gene	Forward 5'- 3	Reverse 5' – 3	Cycle Nr.
Pou5f1	GGAGTCCCAGGACATGAAAGC	TGCTGTAGGGAGGGCTTCG	38
Nanog	GGTGGCAGAAAAACCAGTGG	GCTTCCAGATGCGTTCACC	38
Klf4	GCCCAACTACCCTCCTTTCC	CTGGTCAGTTCATCGGAGCG	30
c-kit	CAGGACCTCGGCTAACAAAGG	ACTCTTGCCCACATCGTTGG	38

Nkx2-5	CCTGACCCAGCCAAAGACC	CACTTGTAGCGACGGTTCTGG	38
Gata4	GCCAACCCTG GAAGACACC	TTGCAAGAGGCCTGGGAA	38
Myh6	GCCGTATCATCACCAGAATCC	TCCAGCCTCTCGGTCATCTC	38
Actn2	AGGCCATGCAGAAGAAGCTG	GTCAGGGTCGCAGACTCGTAG	38
Tnni3	CTGCCAACTACCGAGCCTATG	CCCTCAGGTCCAAGGATTCC	38
Gapdh	CAGAACATCATCCCTGCATCC	AGGTCCACCACCCTGTTGC	38
flt3L (DNA)	GCCCAAATGTGCGTATACCT	CCCAGCACAGTATGGGAACT	38
flt3 rec (DNA)	CGT TGT TCC CTC TAC CTC AC	AATCAAAGTGCGGCTGGC	38

Real Time PCR

SYBR Green PCR Mix: 10µl
Primer FOR (10µM): 0.75µl
Primer REV (10µM): 0.75µl
ddH$_2$O: 3.5µl

10µl/tube
+ 5µl cDNA
(cDNA concentration according to the target)

Program:

20 sec 95°C
03 sec 95°C
30 sec 60°C ←step2 **40 cycles**
∞ 4°C

To evaluate gene expression the following primers were used:

Gene	**Forward 5'- 3**	**Reverse 5' – 3**
Nanog	GGTGGCAGAAAAACCAGT GG	GCTTCCAGATGCGTTCACC
Nkx2-5	CCTGACCCAG CCAAAGACC	ATCCGTCTCGGCTTTGTCC
Gata4	GCCAACCCTGGAAGACACC	GACATGGCCCCACAATTGAC
Myh6	GCCGTATCATCACCAGAATCC	TGGATAACCAGCAGGGCATC
Actn2	TTGGAGCACTTGGCTGAGAAG	GTCAGGGTCGCAGACTCGTAG
Tnni3	CTGCCAACTACCGAGCCTATG	CGTTCCATCTCCTGCTTCG
Tie2	TGCCCTCCTGGGTTTATGG	GGTCCTGCCAAATGTGTGC
Vwf	GATGGAGGGGAGCTTGAACTG	CGACTCCACCACCTCAAAGTG
Abcg2	CATGAAACCTGGCCTTAATGC	TCCCTTTGGATCTTTCCTTGC
Abcb1b	TCAACTACCCATCGAGAAGCG	TTGTGCTTTTTCCACAGCCAC
Kdr	GGGATGGTCCTTGCATCAGAA	ACTGGTAGCCACTGGTCTGGT TG
Trp63	AAGCAGCAAGTATCGGACAGC	TCATCATCTGGGGATCTCCG
flt3 rec. **Probe**	TGGCTCATCAGCGGGAAA TCGTACCGAATGGTGCGAGGATCC	GGGGCACACTGGAGGTCTT
flt3L	CACCTCATGTA CCTTCCAGCC	GTCTGGACGAATCGCAGACA
Klf4	CGGAAAAGAACAGCCACCC	CTGGTCAGTTCATCGGAGCG
αSMA	GGGAGTAATGGTTGGAATGGG	GCCAGATCTTTTCCATGTCGT
PECAM	CGTGAATGACACCCAAGCG	CGCAATGAGCCCTTTCTTCC
Vegfr2	GGGATG GTCCTTGCATCAGAA	ACTGGTAGCCACTGGTCTGGT TG
Rn18s	CCATTCGAACGTCTGCCC	GTCACCCGTGGTCACCA

Western blot

Protein samples were prepared from cell lysates and homogenised hearts using Lysis or RIPA buffer (Cell Signaling, #9803/9806) containing PhosSTOP (Roche, 04-906-845-001) and Complete Protease Inhibitor Cocktail (Roche, 11-697-498-001). Protein samples were reduced with β-mercaptoethanol or Dithiothreitol and heated at 95°C with shaking. Samples were loaded on 10% SDS-Page and run at 120 Volt. Protein samples were transferred onto PVDF membranes previously activated with Methanol. After blocking 1h with 4% bovine serum albumin (BSA), the immuno-blotting was performed using the following antibodies diluted in BSA: Stat5 (1:5000 Cell Signaling, #9358), p-Stat5^{Tyr694} (1:1000 Cell Signaling, #9359), Stat 3 (1:3000 Santa Cruz, #482/8019), p-Stat3^{Tyr705} (1:2000 Cell Signaling, #9145), Akt (1:7000 Cell Signaling, 9272), p-Akt^{Ser473} (1:2000 Cell Signaling, 4058), ERK (1:7000 Cell Signaling, #9102), p-ERK$^{Thr202/Tyr204}$ (1:2000 Cell Signaling, #9101), cyclinB1 (1:1000 Cell Signaling, #4138), cyclinD1 (1:2000 Cell Signaling, #2926), Tubulin (1:7000 Sigma, #T6199), GAPDH (1:10000 Sigma, #G8795). Horseradish peroxidase-conjugated secondary antibody (Jackson Immuno Research) was used to enhance the binding signal. Western Lightning Plus-ECL Enhanced Chemiluminescence (Perkin Elmer, NEL105001EA) was used as substrate to develop the membrane in a colorimetric detection. Image SXM software was used to quantify protein expression. For multiple staining the membranes were re-blotted with Re-Blot Plus Strong Solution (Millipore, #2504).

Data presentation and Statistical Analyses

Data are presented as mean±SEM. Statistical analyses were performed with GraphPad Prism version 7 software (GraphPad). Values were tested for Gaussian distribution using the D'Agostino-pearson normality test. If normally distributed, the data sets were analyzed using parametric testing. All non-normally distribuited data sets and all data sets with $n<8$ were analyzed using non-parametric testing, as indicated.

Two groups data sets were compared using unpaired t-test or Mann Whitney test, accordingly to parametric or non-parametric distribution.

For multiple comparison normally distribuited data sets were compared using ordinary one-way ANOVA followed by Hold-Sidak post hoc testing; non-normally distruibuited data sets were compared using Kruskal-Wallis test followed by Dunn post hoc testing.

Results

Chapter 1. Role of flt3 signaling in the regulation of the cardiac progenitor cell pool

SP-CPCs express functional flt3 receptor and secrete flt3L

Flt3 receptor is mainly expressed by hematopoietic progenitor cells. In the heart CMCs express functional flt3, which is up-regulated in response of oxidative stress (*3*). We therefore examined whether flt3 is also expressed by SP-CPCs. Consistent with previous findings in hematopoietic stem cells (*38*) we could not detect flt3 receptor expression using flow cytometry, probably due to the low numbers of flt3 receptor molecules on the cellular membrane (data not shown). Therefore, we verified the presence of functional flt3 receptor by exogenously activating intrinsic flt3-signaling. We treated SP-CPCs with recombinant flt3L and examined the flt3L-induced phosphorylation of Akt (pAkt), which has been shown to be a canonical downstream target of flt3-signaling (*127*). Following flt3L treatment we observed dose-dependent phosphorylation of Akt at 5 min, confirming the expression of functional flt3 receptor on SP-CPCs (n=4) (Fig.1A). We also observed Akt-phosphorylation in response to exogenous flt3L in flt3L-/- SP-CPCs, indicating that these cells still preserved receptor function and are responding to flt3L (n=3) (Fig.1B). Although to date, only one receptor for flt3L has been identified, we sought to exclude Akt-phosphorylation via unspecific mechanisms by treating wt and flk2-/- (flt3 receptor KO) SP-CPCs with 100ng/ml flt3L. As expected, flt3L induced Akt phosphorylation only in wt but not in flt3 receptor-deficient cells, confirming signal transduction through binding of flt3L to the flt3 receptor (Fig.2). These data suggest that SP-CPCs are a target of endogenous flt3L in the heart.

Flt3L is widely expressed in various tissues. In the hematopoietic system, Flt3L is secreted by stromal fibroblasts (*26, 128*) and T cells (*129*). With respect to cardiac cells, we found flt3L secretion by cardiac fibroblast (data not shown). We therefore tested whether SP-CPCs also secrete flt3L. We collected the supernatant from expanded SP-CPCs and were able to detect secretion of flt3L in wt SP-CPCs, whereas flt3L was absent in the supernatant from flt3L-/- CSP cultures. In addition, down-regulation of flt3L gene expression via siRNA treatment (siflt3L) resulted in significant reduction of flt3L secretion by wt SP-CPCs (n=3) (Fig.3).

In addition to being flt3L target cells, these data identify SP-CPCs as source of flt3L production, suggesting that activation of CSP by flt3L may occur in both an autocrine and paracrine fashion Fig.4).

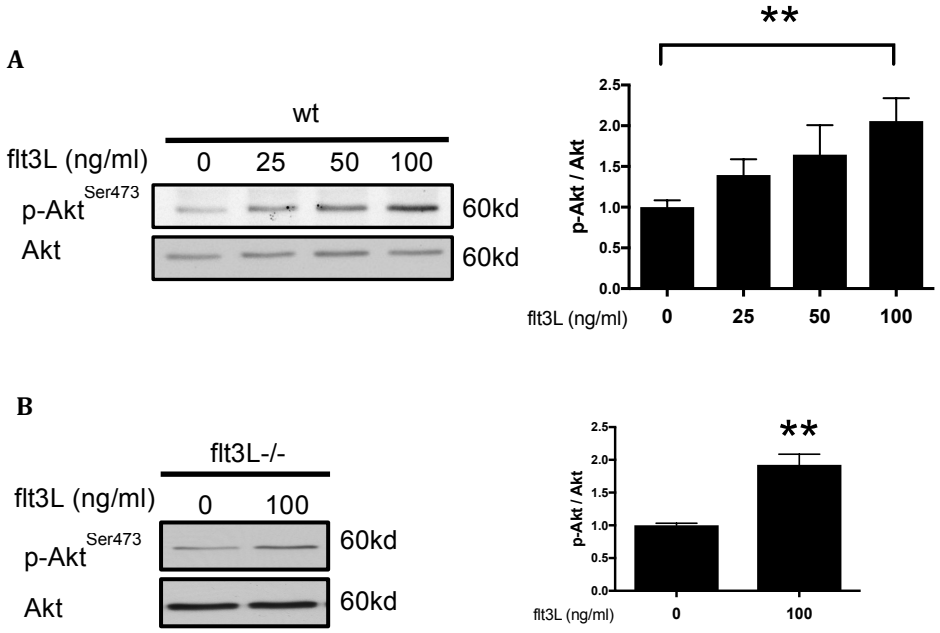

Fig.1: **A**. Akt phosphorylation in response to recombinant flt3L (0 - 100ng/ml) in expanded wt SP-CPCs (P7) in α-MEM 20%FCS medium. Representative blots are shown. Statistics: n=4, data are shown as mean±SEM, Kruskal-Wallis test, 0 vs. 100 ng/ml **p<0.01; **B**. Akt phosphorylation in response to recombinant flt3L (0 - 100ng/ml) in flt3L-/- expanded SP-CPCs (P7) in α-MEM 20%FCS medium. Representative blots are shown. Statistics: n=3, data are shown as mean±SEM. unpaired t-test, 0 vs. 100 ng/ml **p<0.01. P7 = passage7

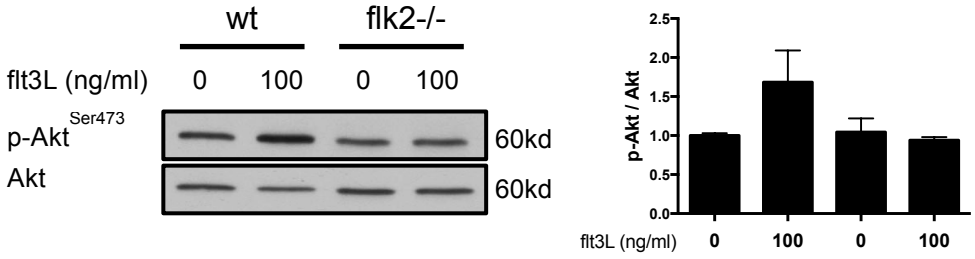

Fig.2: Akt phosphorylation in response to recombinant flt3L (0 - 100ng/ml)in wt and flk2-/- expanded SP-CPCs (P7) in α-MEM 20%FCS medium. Representative blots are shown. n=2, data are shown as mean±SEM. P7 = passage7

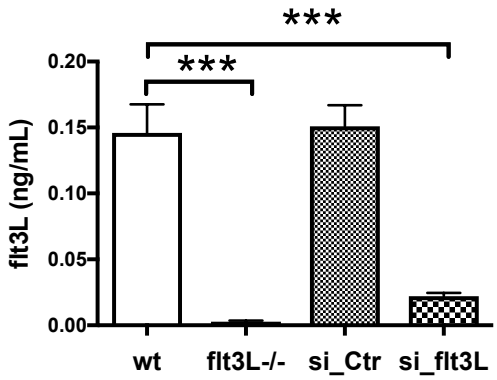

Fig.3: Flt3L in the supernatant from wt and flt3L-/- SP-CPCs (P7), and wt SP-CPCs treated with scrambled (si_Ctr) or flt3L-targeted siRNA (si_flt3L) after 48h in α-MEM 20%FCS medium as measured by ELISA. n=3, data are shown as mean±SEM. One-way ANOVA, ***p<0.001. P7 = passage7.

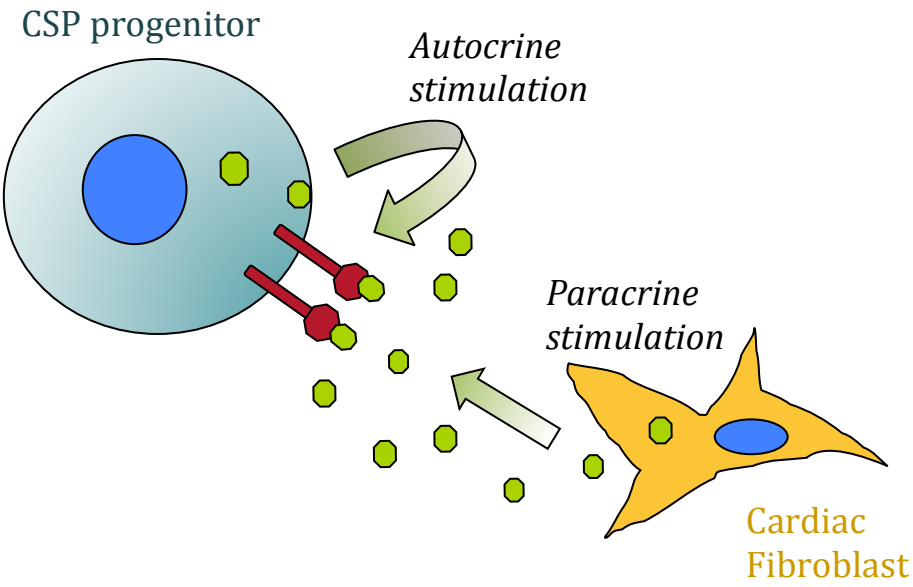

Fig.4: Proposed model of autocrine and paracrine flt3L stimulation of CPCs.

Absence of flt3L decreases the cardiac side population in the adult mouse heart

The CSP is a defined population of progenitor cells in the heart. Its size and function have to be tightly regulated to maintain cardiac cellular homeostasis and – hence – organ integrity. Since flt3 signaling has a major role in regulating hematopoietic stem/progenitor cell function, we examined how lack of flt3L affects the CSP *in vivo* and *in vitro*.

Flt3L-/- mice show a significant decrease of the CSP compared to age-matched 12 weeks-old wt mice (1.79% ± 0.21 vs. 1.01% ± 0.23, $p<0.05$; n=11) (Fig.5A and B), and this decrease is accentuated when considering only the distal portion of the tail

(tip CSP), the cells of which possess the most stringent progenitor phenotype (0.023% ± 0.004 vs. 0.007% ± 0.001, p<0.01; n=11) (Fig.5C).

The CSP exists as an heterogeneous population. We additionally broke down the CSP to isolate the fraction positive in Sca1 and negative in CD31 (Fig.6A), which has the highest cardiomyogenic potential (*5*) and the highest *in vitro* expansion capacity (*69*). We observed no significant difference of the percentages of this specific subpopulation between wt and flt3L-/- mice (0.61% ± 0.18 vs. 1.03% ± 0.26, ns; n=7) (Fig.6B).

To corroborate that our findings are related to the deficieny of Flt3-signaling, the same analyses were performed in mice lacking the flt3 receptor (flk2-/-). Similar to flt3L-/- mice, we also observed a depletion of the CSP in flk2-/- compared to wt mice (1.32% ± 0.19 vs. 0.63% ± 0.13, p<0.01; n=12) (Fig.7A) and this rarefaction is also accentuated in the distal portion of the tail (0.023% ± 0.009 vs. 0.011% ± 0.003, p<0.01; n=12) (Fig.7B).

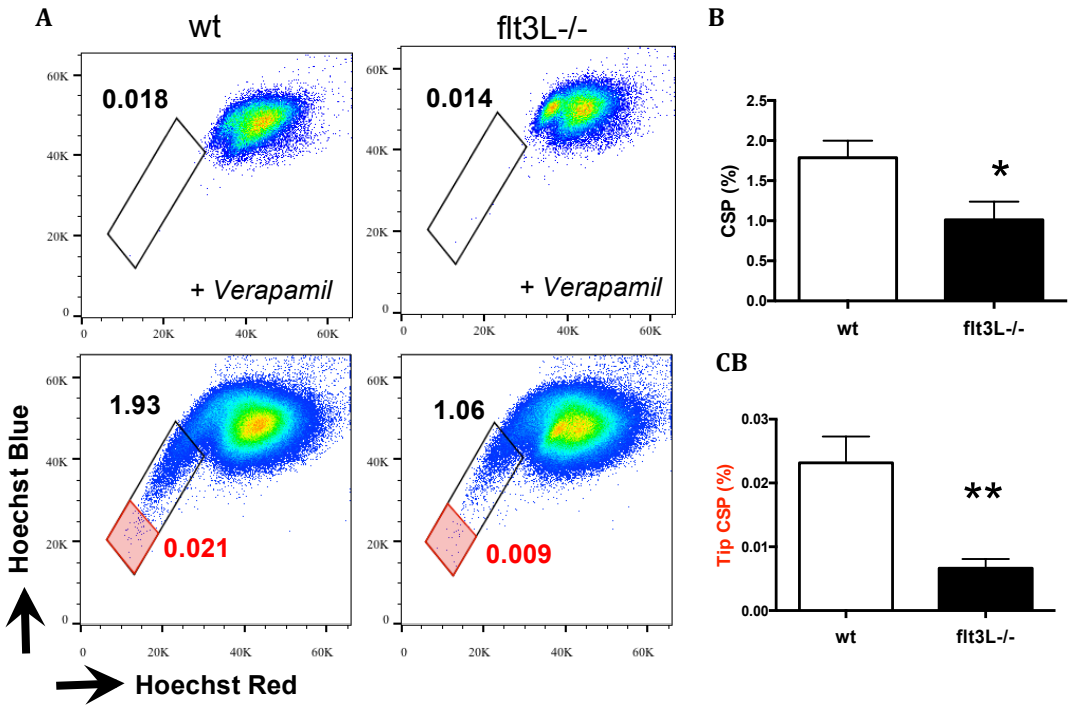

Fig.5: **A**. CMC- and erythrocyte-depleted population from digested hearts were stained with Hoechst and analysed by flow cytometry. Verapamil was used as negative control. Representative flow cytometry readouts of the CSP are shown. **B**. CSP% in the CMC- and erythrocyte-depleted population. Statistics: wt vs flt3L-/-, n=11 (pool of 4 mice for each "n"), data are shown as mean±SEM. Unpaired t-test, * p<0.05; **C**. Tip CSP % in the CMC- and erythrocyte-depleted population. Statistics: wt vs flt3L-/-, n=11 (pool of 4 mice for each "n"), data are shown as mean±SEM. Unpaired t-test, ** p<0.01

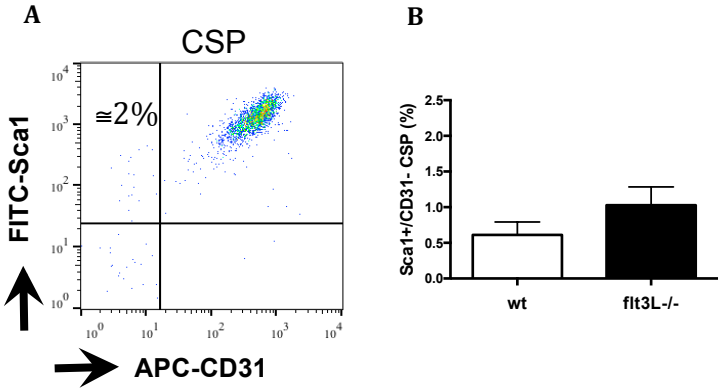

Fig.6: **A**. CMC- and erythrocyte-depleted population from digested hearts were stained firstly with Hoechst, subsequently with Sca1 and CD31 antibodies and then analysed by flow cytometry. Representative flow cytometry readouts of the CSP subfractions are shown; **B**. Sca1/CD31- CSP % in the CSP. Statistics: wt vs flt3L-/-, n=7 (pool of 4 mice for each "n"), data are shown as mean±SEM. Mann Whitney test, not significant (ns.).

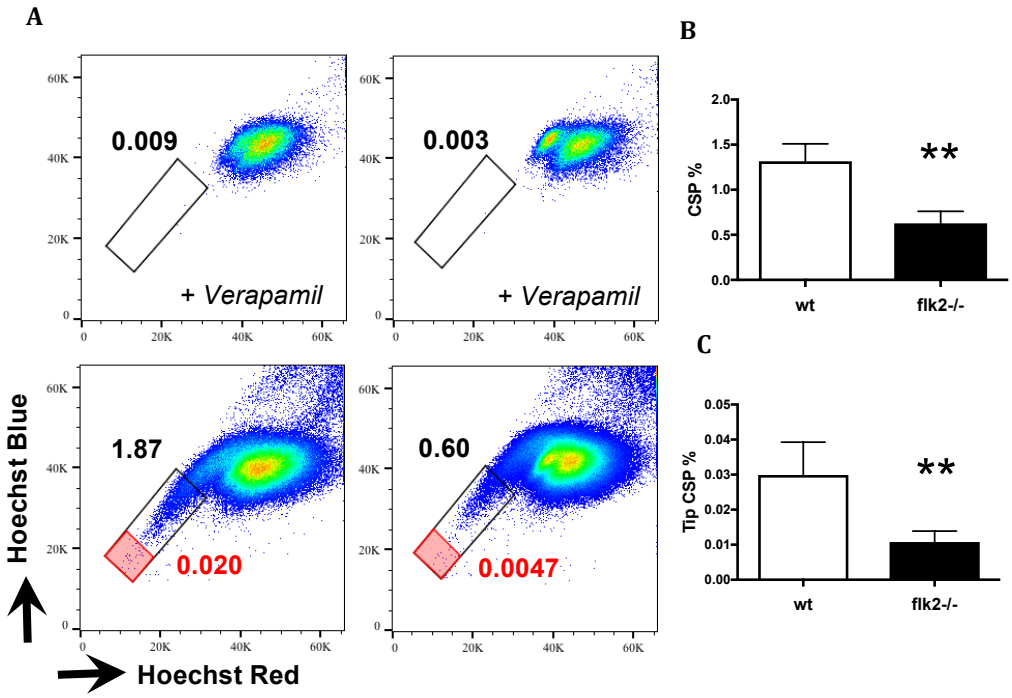

Fig.7: **A**. CMC- and erythrocyte-depleted population from digested hearts were stained with Hoechst and analysed by flow cytometry. Verapamil was used as negative control. Representative flow cytometry readouts of the CSP are shown. **B**. CSP% in the CMC- and erythrocyte-depleted population. Statistics: wt vs flk2-/-, n=12 (pool of 4 mice for each "n"), data are shown as mean±SEM. Unpaired t-test, ** $p<0.01$; **C**. Tip CSP % in the CMC- and erythrocyte-depleted population. Statistics: wt vs flk2-/-, n=12 (pool of 4 mice for each "n"), data are shown as mean±SEM. Unpaired t-test, ** $p<0.01$

Quizartinib inhibits flt3 signaling in CPCs in vitro

Quizartinib is a pharmacologic flt3-inhibitor, which exhibits a high binding affinity to both wild-type and mutated flt3 and is supposedly more specific for the flt3 receptor than previous TKIs (*45*). We assessed the efficiency of quizartinib to inhibit flt3L-induced signaling in SP-CPCs *in vitro*. After 2 hours pre-incubation, quizartinib inhibited flt3L-dependent phosphorylation of Akt (Fig.8), confirming the flt3L-responsiveness of SP-CPCs and the ability of quizartinib to inhibit the ligand-dependent signaling of wild-type flt3 in these cells.

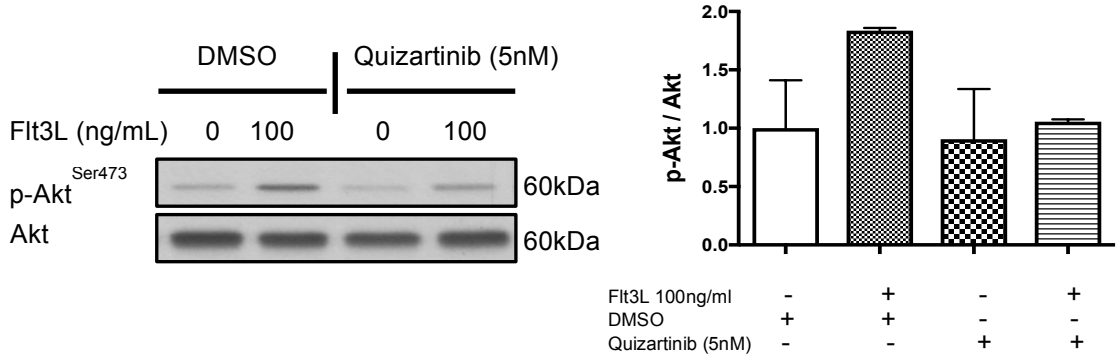

Fig.8: Flt3L (100ng/ml) treatment of wt SP-CPCs pre-treated with the flt3-inhibitor quizartinib (diluted in DMSO) or DMSO alone. Representative blots are shown. Data are shown as mean±SEM, n=2.

Quizartinib does not affect cardiac function but decreases CSP in healthy mice

We treated wt mice with 10 mg/kg quizartinib for 28 days in a row. We observed no change in body weight and behaviour in both vehicle and quizartinib-treated mice. Echocardiography analysis revealed no significant differences between vehicle and quizartinib-treated mice regarding left ventricular dimensions and function (table3; n=24). However, *ex vivo*, quizartinib-treated mice showed an increased heart weight (6.02 ± 0.09 vs. 6.36 ± 0.1, $p<0.05$; n=12) (Fig.9), suggesting a subclinical hypertrophic response. Importantly, treatment of wt mice with quizartinib leads to a decrease of the CSP similar to the one observed in flk2-/- and flt3L-/- mice (2.36% ± 0.32 vs. 1.98% ± 0.17, ns; n=6). This CSP depletion is again accentuated for the tip of the tail (0.07% ± 0.014 vs. 0.029% ± 0.06, $p<0.05$; n=6) (Fig.10). These data show that the flt3-inhibitor quizartinib affects the adult CSP progenitor pool *in vivo*.

	vehicle-treated		quizartinib-treated	
	Baseline	after treatment	Baseline	after treatment
LS (-%)	8.43 ± 0.35	8.85 ± 0.36	8.26 ± 0.35	8.85 ± 0.48
RS (%)	22.56 ± 1.03	19.86 ± 1.07	22.94 ± 1.55	20.23 ± 1.59
LVEF (%)	55.65 ± 1.27	56.69 ± 1.88	53.4 ± 1.16	57.56 ± 1.43
LVEDD (mm)	4.0 ± 0.04	3.9 ± 0.05	4.04 ± 0.03	3.95 ± 0.03

Table 3: Hemodynamic values from 2D-echocardiography. Vehicle-treated vs. quizartinib-treated mice, n=24, data are shown as mean±SEM. One-way ANOVA, ns. LS: longitudinal strain. RS: radial strain: LVEF: left ventricular ejection fraction. LVEDD: left ventricular end-diastolic diameter.

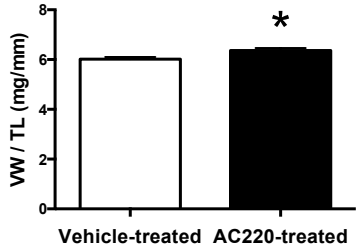

Fig.9: Comparison of ventricular weight/tibia length (VW/TL) ratio. Statistics: Vehicle-treated vs. quizartinib-treated mice, n=12, data are shown as mean±SEM. Unpaired t-test, * p<0.05

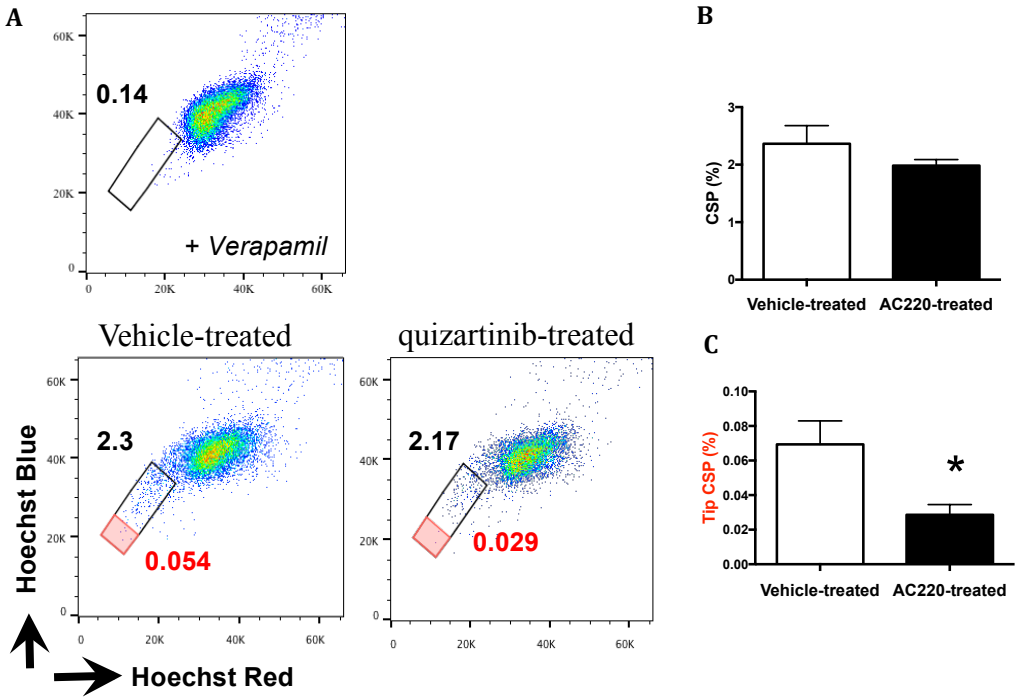

Fig.10: **A**. CMC- and erythrocyte-depleted population from digested hearts were stained with Hoechst and analysed by flow cytometry. Verapamil was used as negative control. Representative flow cytometry readouts of the CSP are shown. **B**. CSP% in the CMC- and erythrocyte-depleted population. Statistics: Vehicle-treated vs. quizartinib-treated mice, n=6, data are shown as mean±SEM. Mann Whitney test, ns.; **C**. Tip CSP % in the CMC- and erythrocyte-depleted population. Statistics: Vehicle-treated vs. quizartinib-treated mice, n=6,, data are shown as mean±SEM. Mann Whitney test, *p<0.05.

SP-CPCs are enriched in quiescent cells

Cellular quiescence is essential to prevent cellular damage and exhaustion of the proliferation capacity, and it is therefore pivotal for progenitor cell function *in vivo*. A quiescent state cannot be assessed by DNA-based cell cycle analysis since quiescent cells in G0 and active cells in G1 have the same amount of DNA and cannot be distinguished. To overcome this we used Pyronin Y (PY), which, similar as Hoechst, is a nucleic acid intercalant. When combined with Hoechst, PY is a molecule that binds only RNA (since Hoechst has a higher binding capacity for DNA) and through that cells in a quiescent state can be identified, since they have lower amounts of RNA (PY low-cells) compared to active cells (*130*). Compared to the main population (MP) the CSP is highly enriched in quiescent cells in G0 phase (Fig.11). We found that wt and flt3L-/- hearts have a similar percentage of quiescent cells in the CSP (68.97% ± 5.23 vs. 77.83% ± 6.78, ns; n=3) (Fig.12).

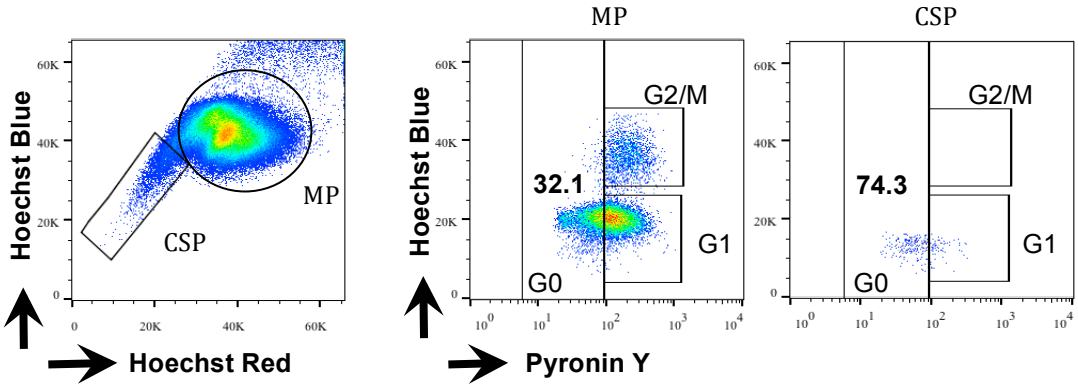

Fig.11: Analysis of the Pyronin Y content of the main population and the CSP within the CMC- and erythrocyte-depleted population. Representative flow cytometry readouts of the total Hoechst-stained population are shown.

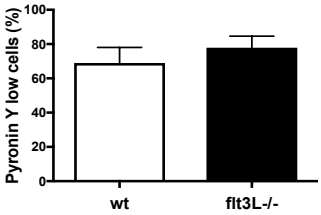

Fig.12: Analysis of the percentage of Pyronin Y low cells in the CSP. n=3, data are shown as mean±SEM. Mann Whitney test, ns.

Freshly isolated flt3L-/- SP-CPCs have a reduced CD31- progenitor cell signature

To compare the wt and flt3L-/- CSP cell transcriptomes, we purified RNA from freshly sorted SP-CPCs to avoid transcriptomic shifts deriving from the *in vitro* amplification. Prior to library preparation, RNA needed to be pre-amplified since SP-CPCs reside in a quiescent state and are transcriptionally inactive, and therefore low in RNA content.

29-35 millions reads were sequenced across samples (n=5), from which 19-28 millions reads mapped to the genome. Transcripts were firstly filtered according to number per read per million or count per million (cpm). Only transcripts presenting at least 1cpm in at least 5 samples (indistinctly wt or flt3L-/-) were considered for gene expression analysis. Sample correlation and Principal Component Analysis (PCA) showed a high inter- and intra-sample variation. This high variability might be associated to several factors, including the heterogeneity of the CSP and the time and modality of isolation/sorting of these progenitors.

Firstly we went through single gene comparison using a panel of genes, which characterized a CPC signature (*69*) (Table 4). Again we observed a high variability of expression of these transcripts between samples (data not shown) with no significant differences in expression between the two strains and no clustering of samples from the same strain (Fig.13). Specifically, we observed no detection of the most primitive stem cell transcripts POU domain, class 5, transcription factor 1 (Pouf51) and Nanog homeobox (Nanog), which are key genes for the maintenance of the pluripotency of stem cells. Instead, we observed high expression of the "less" primitive stemness markers kruppel-like factor (klf4), KIT proto-oncogene receptor tyrosine kinase (Kit) and lymphocyte antigen 6 complex, locus A (ly6a) (Table 4, flt3L-/- vs. wt, Log2A, pluripotency) confirming the progenitor signature of the CSP *in vivo*. Interestingly, between early and mature cardiac markers, the vascular markers showed the highest absolute expression, probably due to the high number of CD31+ cells (above 90%), i.e. endothelial progenitor cells, within the CSP (Table4, flt3L-/- vs. wt, Log2A, vascular).

Single gene analysis also showed detection of flt3 receptor in both strains but with higher expression in the wt freshly isolated SP-CPCs (2.3 ± 0.30 vs. -0.1 ± 0.27, cpm as log2 expression, wt vs flt3L-/-, $p<0.05$, n=4-5). Surprisingly, although enhanced in the wt SP-CPCs, we also observed expression of the flt3L transcript in the KO CSP

progenitors (3.4 ± 0.30 vs. 1.75 ± 0.07, cpm as log2 expression, wt vs flt3L-/-, p<0.01, n=5). However, a careful analysis of the sequencing showed that the reads are uniquely mapping the truncated part of the flt3L and not the deleted part of the gene (Fig. 14), hence confirming knock-out of flt3L in flt3L-/- CSP.

Setting a stringent false discovery rate (FDR) < 1e-6, we further proceeded with Gene Set Enrichment Analysis (GSEA), a computational comparison method based on defined sets of genes from MSigDB (version 5.2.) (*131-133*). Several curated gene sets were differentially regulated between wt and flt3L-/- RNA samples (Table 5). The gene set BOQUEST STEM CELL UP (223 genes) harbours the highest differentially expressed group of genes, with a false discovery rate (FDR) of 1.548e-25 and an absLog2FC of 0.97 (flt3L-/- vs- wt). The BOQUEST STEM CELL UP gene set identifies a stromal stem cell transcriptome, in which the transcripts involved in cell cycle arrest, stem cell biology, and development of mesodermal and ectodermal organs were up-regulated in CD31- stromal stem cells harbouring a stem cell signature and differentiation plasticity (*134*). These transcripts are down-regulated in freshly isolated flt3L-/- SP-CPCs suggesting a reduced CD31- progenitor cell signature.

EntrezID	Symbol	GeneName	log2FC	log2A	P.Value	adj.P.Val	
16600	Klf4	Kruppel-like factor 4 (gut)	0.23876484	7.63854939	0.53738402	0.85438847	
16590	Kit	KIT proto-oncogene receptor tyrosine kinase	0.07381807	4.86502996	0.78726395	0.94685232	
110454	Ly6a	lymphocyte antigen 6 complex, locus A	0.8787052	10.0556566	0.00801455	0.19364821	
26357	Abcg2	ATP-binding cassette, sub-family G (WHITE), member 2	0.69772869	7.69217985	0.01060976	0.21501598	
18669	Abcb1b	ATP-binding cassette, sub-family B (MDR/TAP), member 1B	0.1056543	5.94262856	0.65498644	0.90196111	pluripotency
	Pou5f1	POU domain, class 5, transcription factor 1		not detected			
	Nanog	Nanog homeobox		not detected			
	Tert	telomerase reverse transcriptase		not detected			
14465	Gata6	GATA binding protein 6	-0.5526344	4.04638693	0.49743085	0.83367049	
14463	Gata4	GATA binding protein 4	-0.9073911	5.65307629	0.09936888	0.46760184	
15111	Hand2	heart and neural crest derivatives expressed transcript 2	-0.6741429	1.12049544	0.10562492	0.4771259	
17258	Mef2a	myocyte enhancer factor 2A	0.31680683	8.3852946	0.17706368	0.58365757	
17260	Mef2c	myocyte enhancer factor 2C	0.32123108	7.63633302	0.22143149	0.63433806	
21385	Tbx2	T-box 2	0.05215746	1.19349644	0.91262837	0.98284482	
21388	Tbx5	T-box 5	-0.571984	1.72674254	0.21561119	0.62848291	cardiogenic transcription factor
76365	Tbx18	T-box18	-0.6505356	2.25175406	0.17512265	0.58091632	
57246	Tbx20	T-box 20	-0.8958965	6.302534	0.04465121	0.33715243	
	Hand1	heart and neural crest derivatives expressed transcript 1		not detected			
	Isl1	ISL1 transcription factor, LIM/homeodomain		not detected			
	Nkx2-5	NK2 homeobox 5		not detected			
17888	Myh6	myosin, heavy polypeptide 6, cardiac muscle, alpha	0.63527775	4.32115122	0.08634798	0.44161322	
17906	Myl2	myosin, light polypeptide 2, regulatory, cardiac, slow	0.90933167	4.20983874	0.00468837	0.16093517	
18821	Pln	phospholamban	0.65955835	5.06412778	0.01131595	0.21781181	cardiomyocytes
11464	Actc1	actin, alpha, cardiac muscle 1	1.0484367	5.07084203	0.00246175	0.12510156	
	Nppa	natriuretic peptide type A		not detected			
12562	Cdh5	cadherin 5	0.55147289	8.26983846	0.12601154	0.50653392	
16542	Kdr	kinase insert domain protein receptor	0.36884247	11.7100268	0.26728121	0.67459346	
12797	Cnn1	calponin 1	0.32938799	0.1778356	0.53919468	0.85523316	vascular
17880	Myh11	myosin, heavy polypeptide 11, smooth muscle	0.14306002	5.20593267	0.78922599	0.9474273	
22371	Vwf	Von Willebrand factor	-0.0074662	7.51983956	0.98248179	0.99652043	

Table 4: Cardiac progenitor cell gene expression (*69*). Statistics: flt3L-/- vs. wt, n=5 (pool of 4 mice for each "n").

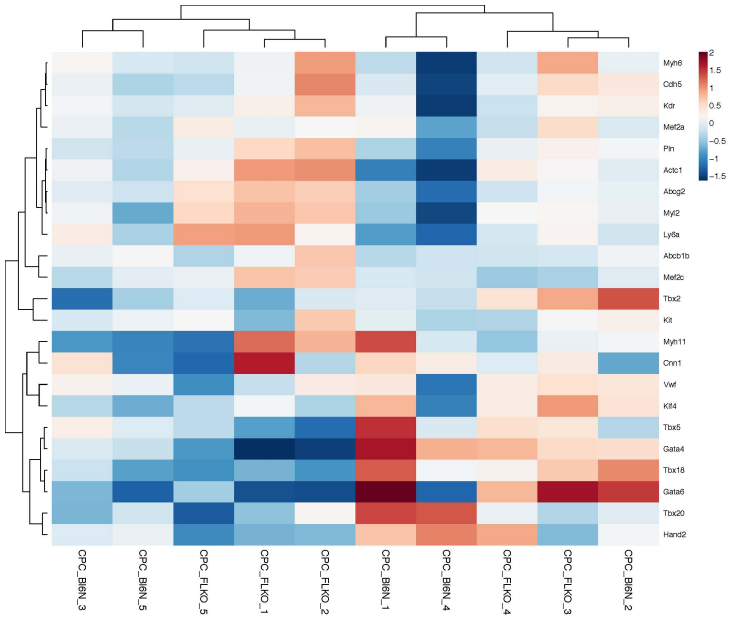

Fig.13: Heat Map visualization and clustering of cardiac progenitor cell genes (gene panel from Noseda *et al.(69)*) after transcriptional comparison between freshly isolated wt and flt3L-/- SP-CPCs.

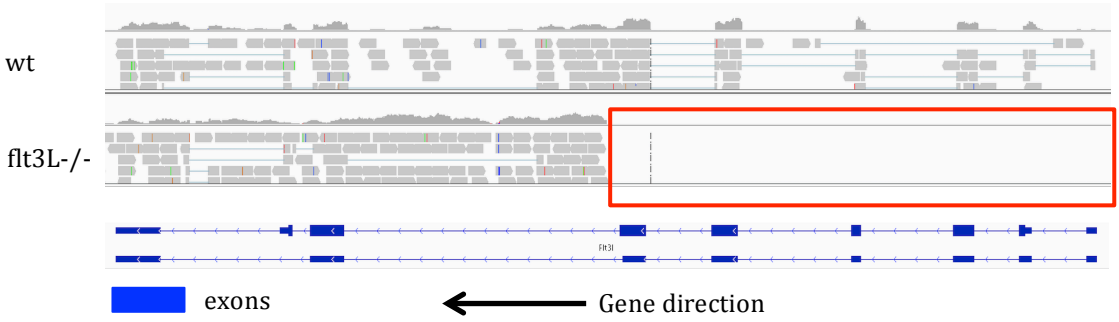

Fig.14: Visualization of the sequencing reads mapping in the flt3L gene in wt and flt3L-/- RNA samples. The Flt3L gene in the KO-sample is truncated in the initial part due to homologous recombination during flt3L-/- mice generation (red square).

GeneSet	NGenes	Correlation	Direction	absLog2FC	PValue	adj.P.Val
BOQUEST_STEM_CELL_UP	223	0.01	Down	0.9621744	3.800e-29	1.548e-25
CLASPER_LYMPHATIC_VESSELS_DURING_METASTASIS_DN	35	0.01	Down	1.1147762	2.381e-14	4.850e-11
ANASTASSIOU_CANCER_MESENCHYMAL_TRANSITION_SIGNATURE	56	0.01	Down	0.8874326	4.285e-14	5.820e-11
POOLA_INVASIVE_BREAST_CANCER_UP	204	0.01	Down	1.0580765	2.363e-13	2.407e-10
MCLACHLAN_DENTAL_CARIES_UP	191	0.01	Down	1.1220831	2.932e-12	2.389e-09
NABA_CORE_MATRISOME	176	0.01	Down	0.7706421	1.739e-11	1.181e-08
JAATINEN_HEMATOPOIETIC_STEM_CELL_DN	169	0.01	Down	1.1065485	3.141e-11	1.828e-08
NAKAYAMA_SOFT_TISSUE_TUMORS_PCA1_UP	59	0.01	Down	1.1811483	9.236e-11	4.703e-08
SMID_BREAST_CANCER_NORMAL_LIKE_UP	370	0.01	Down	1.0032941	2.812e-10	1.273e-07
SCHUETZ_BREAST_CANCER_DUCTAL_INVASIVE_UP	316	0.01	Down	0.8069481	5.983e-10	2.437e-07
TURASHVILI_BREAST_LOBULAR_CARCINOMA_VS_DUCTAL_NORMAL_UP	63	0.01	Down	0.8086498	9.173e-10	2.948e-07
WONG_ENDMETRIUM_CANCER_DN	68	0.01	Down	0.8681263	9.294e-10	2.948e-07
LEE_DIFFERENTIATING_T_LYMPHOCYTE	170	0.01	Down	0.9186551	9.406e-10	2.948e-07
HADDAD_T_LYMPHOCYTE_AND_NK_PROGENITOR_DN	43	0.01	Down	1.1969260	1.964e-09	5.716e-07
BOQUEST_STEM_CELL_DN	188	0.01	Up	0.5501095	2.248e-09	6.105e-07
NABA_MATRISOME	534	0.01	Down	0.7404168	3.882e-09	9.885e-07

Table 5: Gene Set Enrichment Analysis of curated gene sets. Statistics: flt3L-/- vs. wt, n=5 (pool of 4 mice for each "n"). Statistic filters: 1cmp in at least 5 samples (indistinctly wt or flt3L-/-); adj.P.Val < 1e-6.

Freshly isolated SP-CPCs show multipotential properties

As already investigated by several groups (*5, 69, 105, 106*), we assessed the multipotency of SP-CPCs with respect to the capacity to differentiate into the three major cardiac lineages, i.e., cardiomyocytes, vascular smooth muscle cells and endothelial cells.

Freshly isolated SP-CPCs are quiescent and this facilitates the commitment towards a more differentiated phenotype. We observed expression of α-sarcomeric-actinin in Sca1+/CD31- SP-CPCs when co-cultured with NRVM for 3 weeks (Fig.15A). Freshly isolated SP-CPCs also expressed the endothelial marker vWF when cultured for 2-3 weeks in endothelial differentiation medium (Fig.15B).

Of note, we found no differences in the percentage of vWF+ cells between wt and flt3L-/- SP-CPCs when freshly isolated and cultured in endothelial differentiation medium (9.69% ± 2.76 vs. 8.18% ± 2.58, ns; n=6) (data not shown).

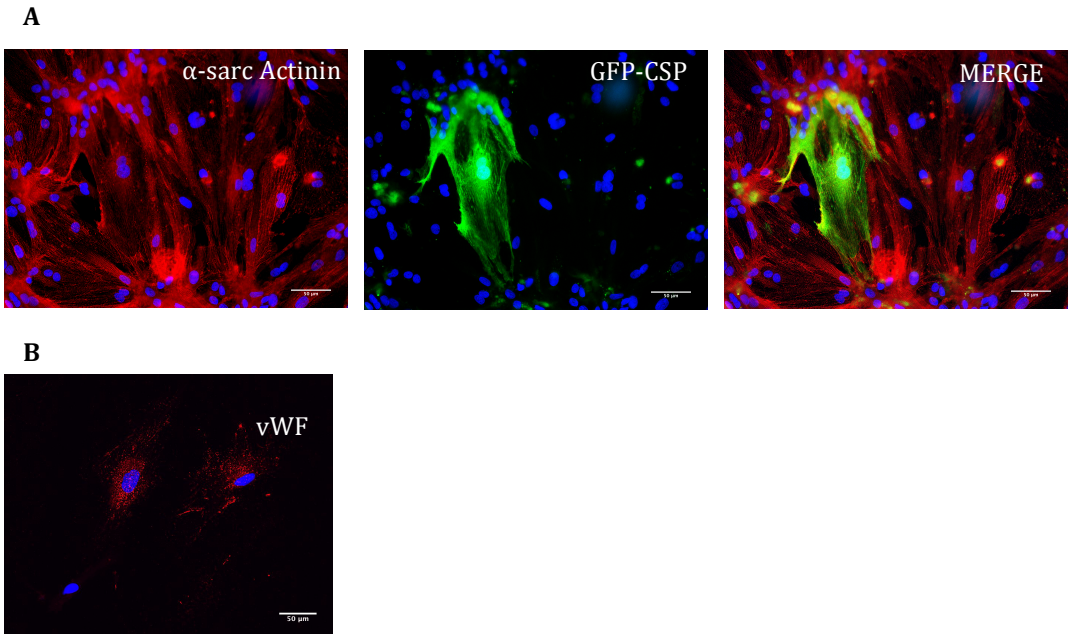

Fig.15: A. Sca1+/CD31- SP-CPCs were isolated from green-fluorescent protein (GFP) expressing mice and co-cultured with NRVM in DMEM 7%FCS medium for 3 weeks: SP-CPCs (green), α-sarcomeric-actinin (red), dapi/nuclei (blue); B. Freshly isolated SP-CPCs in EGM-2 medium for 2-3 weeks: vWF (red), dapi/nuclei (blue).

Expanded SP-CPCs maintain a cardiac progenitor signature

Sca1+/CD31- SP-CPCs are expandable *in vitro*, and this is the case for both wt and flt3L-/- SP-CPCs. Expanded wt and flt3L-/- SP-CPCs have a similar cardiac progenitor signature with respect to the expression of stem cell, early and late myogenic markers at the mRNA level (Fig.16A-B).

Independently from culturing the cells in Medium1 or Medium2 (see *material and methods*), expanded wt and flt3L-/- SP-CPCs maintained high positivity for the stem cell marker Sca1 and negativity for CD31 (76.95% ± 3.09 vs. 80.15% ± 3.19, ns; n=4 in Medium1; 55.56% ± 2.54 vs. 61.65% ± 8.86, ns; n=5-6 in Medium2) (Fig.17-18).

Two important features attributed (but not exclusive) to progenitor cells are the capacity to build clones and form spheres. We therefore assessed the capacity to generate cardiostem spheres and the clonogenicity of SP-CPCs. Expanded SP-CPCs from both strains were able to generate cardiostem spheres when cultured in bacteriological dishes (Fig.19A) and exhibited clonogenic capacity in the colony forming assay (Fig.14B). No significant differences were observed regarding the quantitiy of spheres or colonies between wt and flt3-/- SP-CPCs cultured over 2 weeks (n=5-6) (Fig.19B).

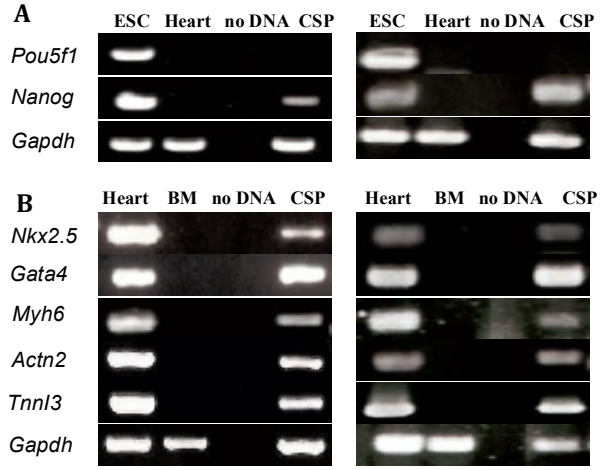

Fig.16: A. Gene expression of stemness and progenitor markers of wt and flt3L-/- expanded SP-CPCs (P7). Embryonic stem cells (ESC) and whole heart homogenate (Heart) were used as positive and negative controls, respectively; B. Gene expression of cardiac transcription factors and cardiomyogenic markers of wt and flt3L-/- expanded SP-CPCs (P7). Whole heart homogenate and bone marrow (BM) were used as positive and negative controls, respectively. P7 = passage7
Actn2: actinin alpha 2; Gapdh: glyceraldehyde-3-phosphate dehydrogenase; Gata4: GATA binding protein 4; Myh6: myosin, heavy chain 6, cardiac muscle, alpha; Nanog: Nanog homeobox; Nkx2.5: NK2 homeobox 5; Pou5f1: POU domain, class 5, transcription factor 1 (Oct-4); Tnni3: troponin I, cardiac 3.

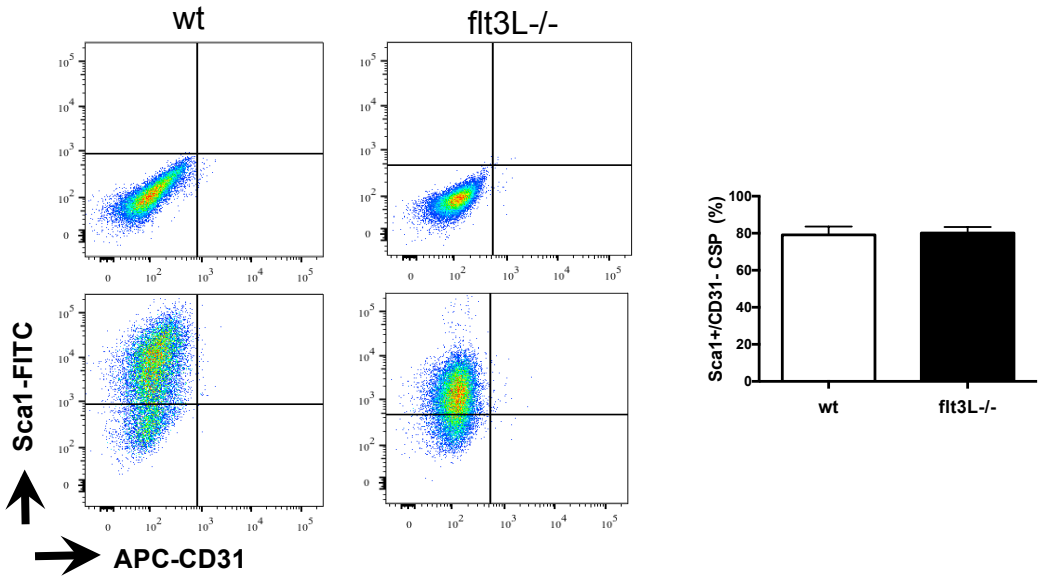

Fig.17: Analysis of Sca1 and CD31 expression in SP-CPCs (P7) expanded in α-MEM 20%FCS medium. Representative FACS readouts of the expanded SP-CPCs are shown. Statistics: wt vs. flt3L-/-, n=4, data are shown as mean±SEM. Mann Whitney test, ns. P7 = passage7

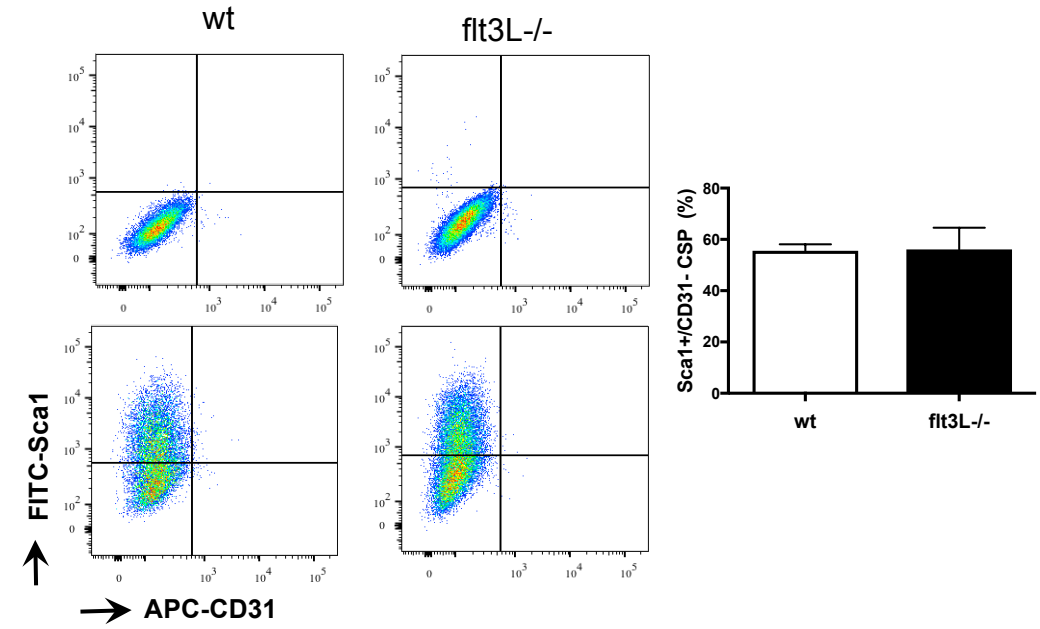

Fig.18: Analysis of Sca1 and CD31 expression in SP-CPCs (P7) expanded in stemness-preserving medium (Medium2). Representative FACS readouts of the expanded SP-CPCs are shown. Statistics: wt vs. flt3L-/-, n=5-6, data are shown as mean±SEM. Mann Whitney test, ns. P7 = passage7

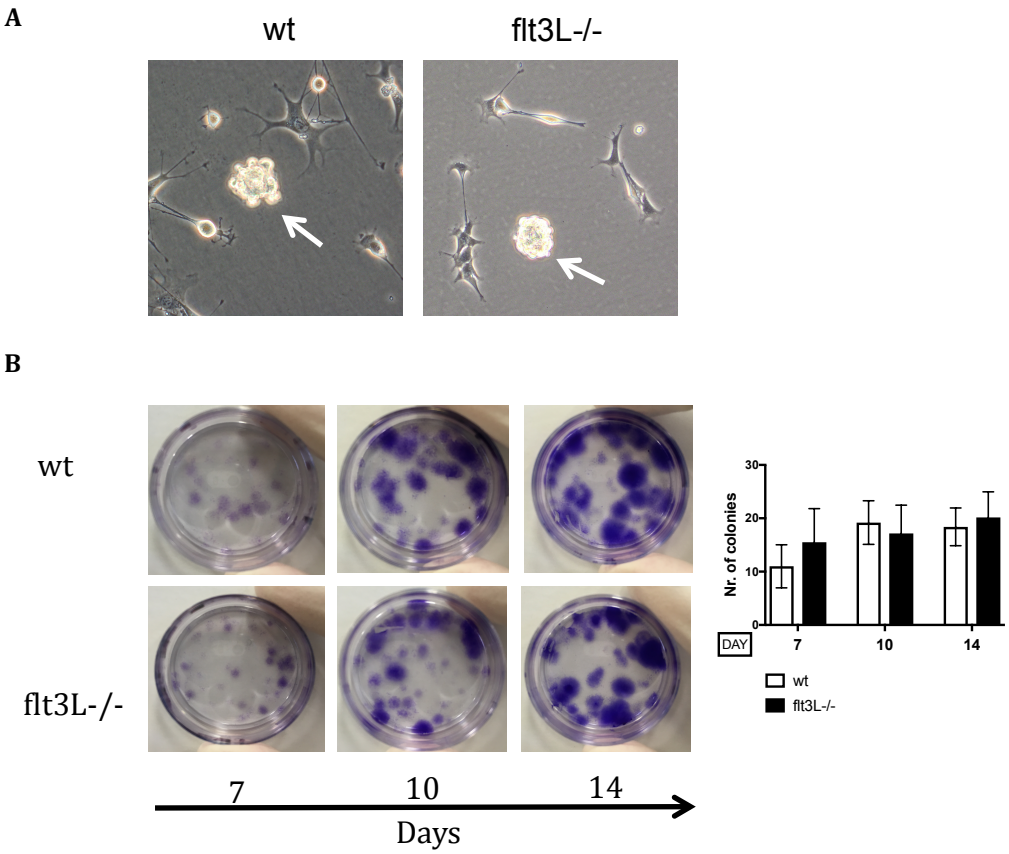

Fig.19: **A**. Cardiostem sphere formation assay in bacteriological dishes, 24h in medium without EGF and FGF supplement. **B**. Colony forming assay at 7, 10 and 14 days in stemness-preserving medium (Medium2). Representative experiment is shown. Statistics: wt vs. flt3L-/-, n=5-6, data are shown as mean±SEM. Mann Whitney test per each time point, ns.

Flt3-intrinsic pathways are down-regulated in flt3L-/- SP-CPCs in culture

We evaluated if lack of flt3L secretion in flt3L-/- SP-CPCs might affect flt3-related intracellular signalling pathways in culture. Using Medium1, which is not supplemented by additional growth factors, we observed a remarkable down-regulation of main intracellular pathways implicated in flt3-dependent signaling such as Akt, Erk, Stat3 and Stat5, either through decreased phosphorylation or decrease of expression or both (Fig.20A), resulting in a markedly decreased phosphorylation ratio of Akt and – to a lesser extent – ERK. Interestingly, following siRNA-mediated knock-down of flt3L (si_flt3L) (Fig.20B) in wt SP-CPCs, we observed a similar down-regulation of flt3-related pathways to the one observed in flt3L-/- SP-CPCs. (Fig.20B). These data suggest that secretion of flt3L by SP-CPCs is important to preserve functional flt3 signaling over time in culture in the absence of additional or

compensatory growth factors.

Surprisingly, we observed a different modulation of the flt3-related intracellular pathways in SP-CPCs cultured in medium supplemented with additional growth factors to preserve progenitor multipotency (Medium2) (Fig.21), in which case both phosphorylation and expression of signature signalling molecules was enhanced in the absence of intrinsic flt3-L, resulting in a maintained phosphorylation ratio. These data suggest that flt3L-signature signalling might be restored by compensatory factors supplemented to the medium, such as EGF and FGF, which share similar pathways.

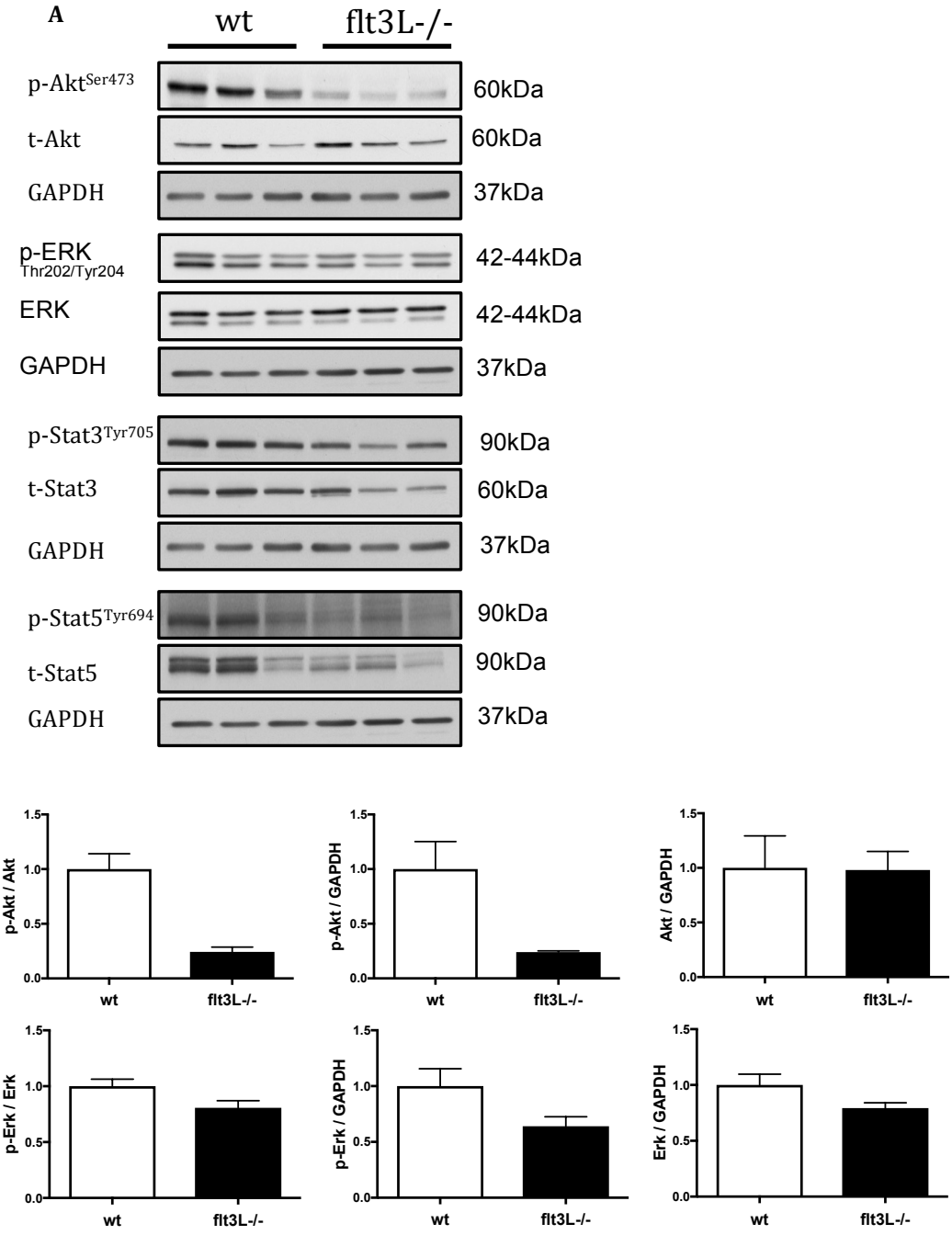

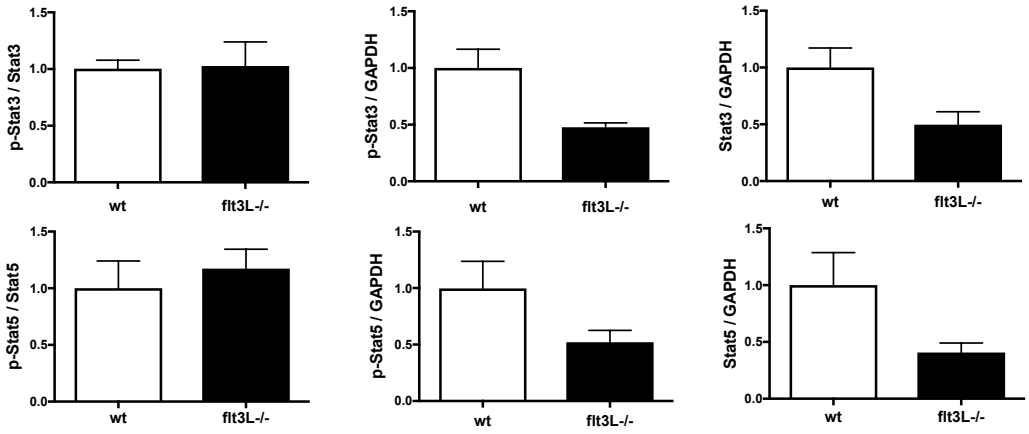
p-Stat3 / Stat3
p-Stat3 / GAPDH
Stat3 / GAPDH
p-Stat5 / Stat5
p-Stat5 / GAPDH
Stat5 / GAPDH
wt
flt3L-/-

B

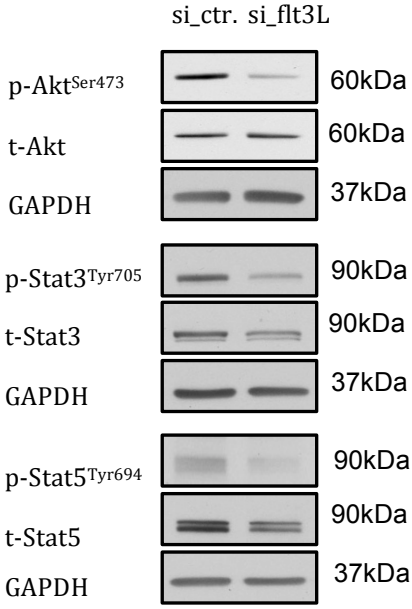
si_ctr.
si_flt3L
p-Akt Ser473
t-Akt
GAPDH
p-Stat3 Tyr705
t-Stat3
GAPDH
p-Stat5 Tyr694
t-Stat5
GAPDH
60kDa
60kDa
37kDa
90kDa
90kDa
37kDa
90kDa
90kDa
37kDa

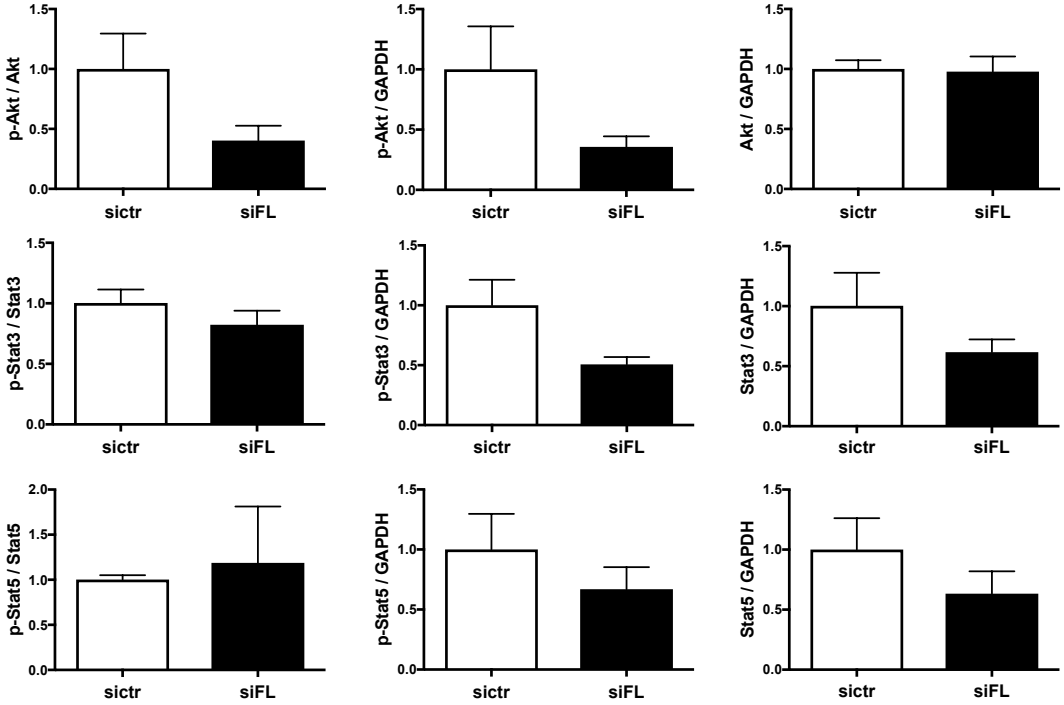
p-Akt / Akt
p-Akt / GAPDH
Akt / GAPDH
p-Stat3 / Stat3
p-Stat3 / GAPDH
Stat3 / GAPDH
p-Stat5 / Stat5
p-Stat5 / GAPDH
Stat5 / GAPDH
sictr
siFL

Fig.20: **A**. Protein expression and phosphorylation of Akt, Erk, Stat3 and Stat5 in expanded wt and flt3L-/- SP-CPCs (P7) cultured in α-MEM 20%FCS medium (Medium1) as assessed by Western blotting. Representative blots are shown. Statistics wt vs flt3L-/-, n=3. data are shown as mean±SEM. Mann Whitney test, ns. ;**B**. Protein quantification of Akt, Stat3 and Stat5 (total and phosphorylated form) in SP-CPCs (P7) treated with scrambled siRNA- (si_Ctr) or flt3L-targeting siRNA- (si_flt3L-/-) in α-MEM 20%FCS medium (Medium1). Representative blots are shown. Statistics: si_Ctr vs. si_flt3L-/-, n=3, data are shown as mean±SEM. Mann Whitney test, ns. P7 = passage7.

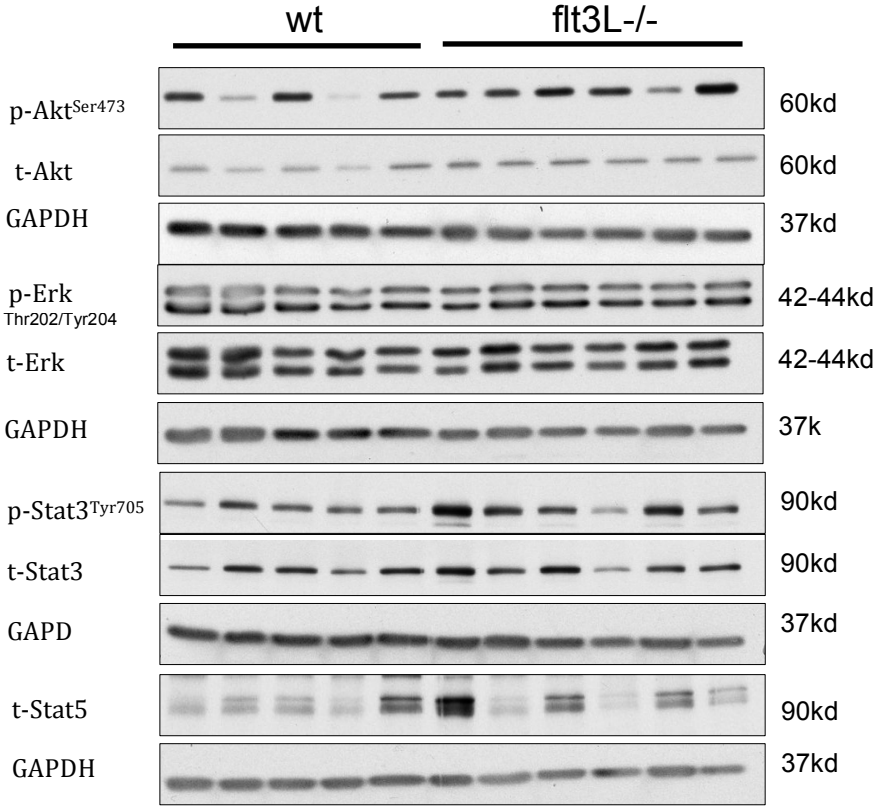

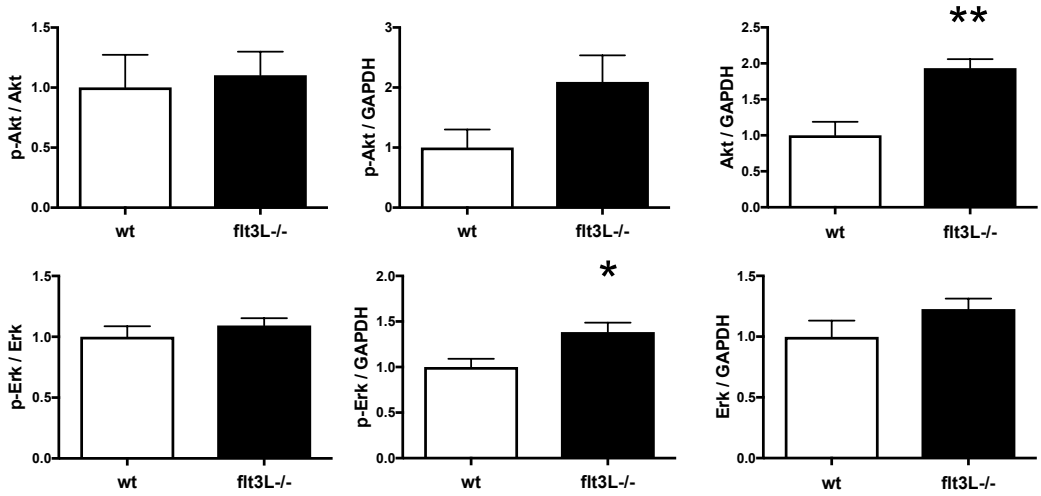

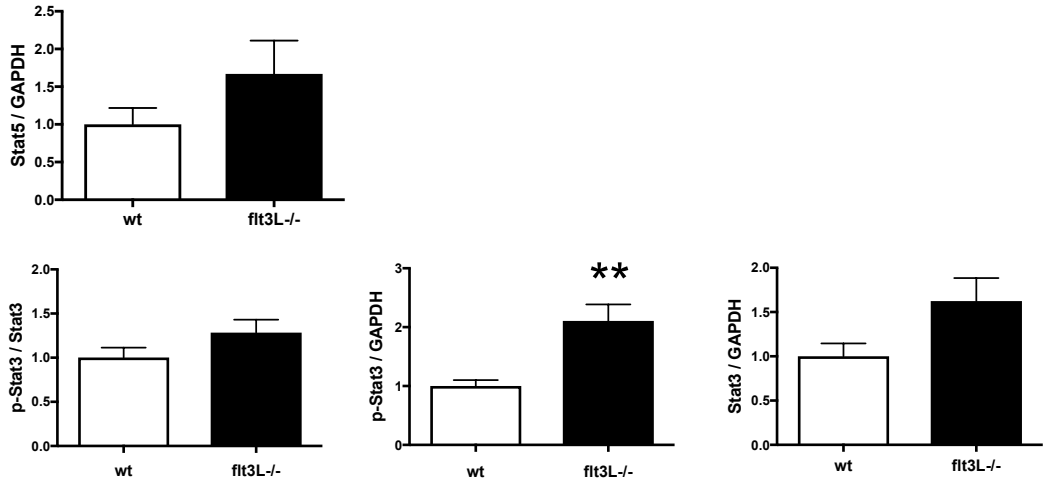

Fig.21:Protein quantification of Akt, Stat3 and Stat5 (total and phosphorylated form) in expanded wt and flt3L-/- SP-CPCs (P7) in medium supplemented with growth factors (Medium2). Representative blots are shown. Statistics: wt vs. flt3L-/-, n=5-6, data are shown as mean±SEM. Mann Whitney test, *p<0.05, **p<0.01. P7 = passage7.

In vitro characteristics of SP-CPCs from flt3L-deficient hearts

In Medium1 expanded flt3L-/- SP-CPCs exhibited an accelerated proliferation rate over time compared to wt SP-CPCs (3.5 fold at 5 days) (Fig.22). In addition, Flt3L-/- SP-CPCs showed enhanced Cyclin B1 expression 48h after G1-phase synchronization (1.00 ± 0.21 vs. 3.64 ± 0.51, ns, n=3) (Fig.23A), suggesting faster G2/M phase transition of flt3L-/- compared to wt cells. In contrast, we observed no significant difference in Cyclin D1 expression (1.00 ± 0.17 vs. 1.24 ± 0.1, ns, n=3) (Fig.23B).

Considering that differentiation and proliferation tend to follow distinct gene programs, differences in the proliferation rate may affect progenitor cell commitment and differentiation. Consistent with this hypothesis, we observed reduced mRNA expression of cardiomyogenic and endothelial lineage markers in flt3L-/- compared to wt SP-CPCs, and this difference was particularly pronounced for endothelial lineage genes (n=3) (Fig.24).

These results, together with the loss of quiescent SP-CPCs *in vivo,* suggest that ablation of flt3L promotes untimely activation and proliferation of CPCs, hence jeopardizing their functionality.

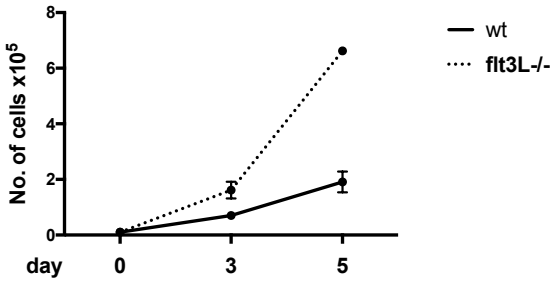

Fig.22: SP-CPC count in α-MEM 20%FCS medium (Medium1) at days 3 and 5 in culture. Starting cell number = $1x10^4$. Statistics: wt vs. flt3L-/-, n=3, data are shown as mean±SEM. Mann Whitney test, ns.

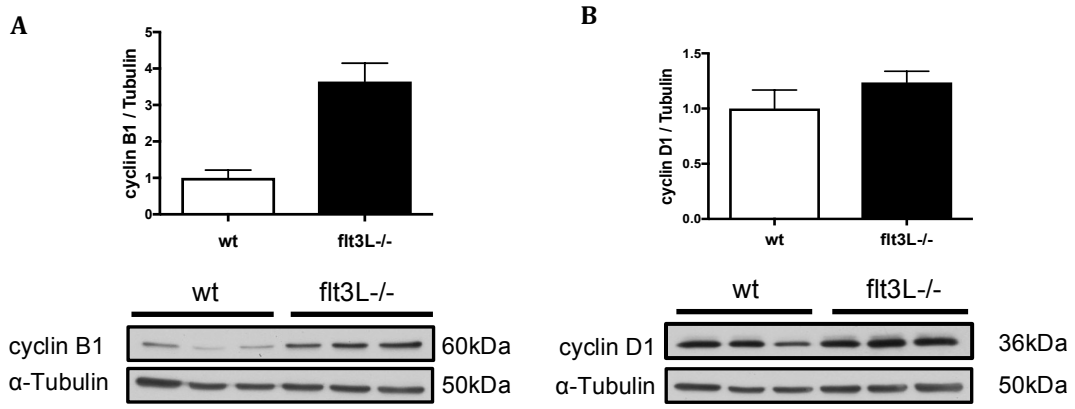

Fig.23: **A**-**B**: Protein expression of cyclin B1 and D1 after 24 hours in α-MEM 20%FCS medium following synchronization in 0.1% FCS for 24 hours. Statistics: wt vs. flt3L-/-, n=3, data are shown as mean±SEM. Mann Whitney test, ns.

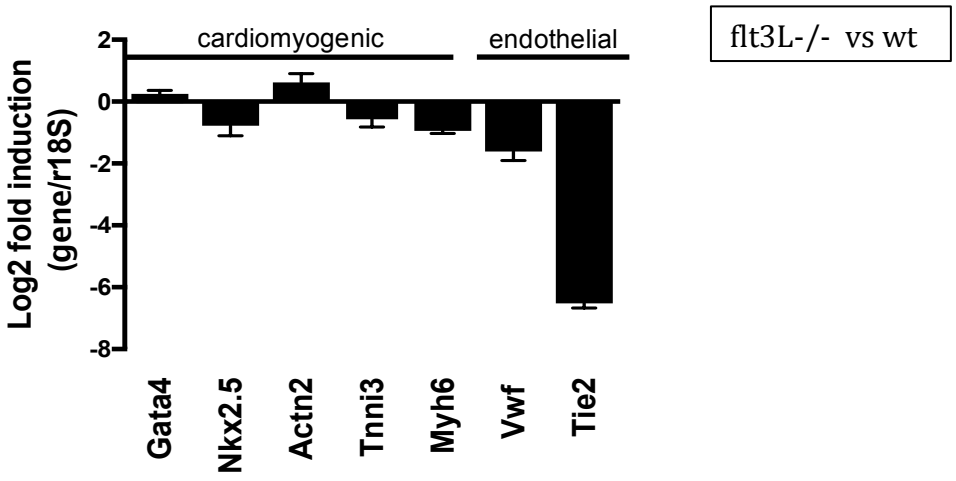

Fig.24: Relative mRNA expression of cardiomyogenic and endothelial lineage genes in flt3L-/- SP-CPCs compared to wt SP-CPCs in α-MEM 20%FCS medium. Statistics: flt3L-/- vs. wt, n=3, data are shown as mean±SEM, ns. P7 = passage7.
Actn2: actinin alpha 2; Gata4: GATA binding protein 4; Myh6: myosin, heavy chain 6, cardiac muscle, alpha; Nkx2.5: NK2 homeobox 5; Tie2: TEK receptor tyrosine kinase; Tnni3: troponin I, cardiac 3; Vwf: von Willebrand factor.

Expanded SP-CPCs preserve tri-lineage differentiation potential

The potential future use of SP-CPCs for cardiac cell therapy requires preservation of a multi-lineage differentiation potential during *ex vivo* expansion. We observed that Medium1-based culturing favours the *in vitro* transformation of SP-CPCs (irrespective of their genotype, i.e. wt or flt3L-/-), which is characterized by a high proliferation rate and loss of their capability to differentiate into any of the three major cardiac lineages. In contrast, culturing of the cells in Medium2, with lower concentrations of serum and enriched with growth factors such as EGF and FGF, which have been shown to preserve "stemness" in other types of stem/progenitor cells such as adipose-derived mesenchymal stem cells and neural stem cells (*135-137*), abolished the difference in proliferation rate between wt and flt3L-/- SP-CPCs (n=4 and 5) (Fig.25) while preserving the differentiation potential within expanded CSP cells of both genotypes.

Using distinct differentiation protocols (Table 6), we could observe expression of markers of all three major cardiac lineages from the same Sca1+/CD31- CSP progeny. Consistent with observations made by other investigators in a different CPC type (Plaisance I *et al*., JACC Basic Transl Med 2016), we found a higher propensity of Sca1+/CD31- SP-CPCs to differentiate towards the smooth muscle cell lineage than towards endothelial or cardiomyogenic lineages. When cultured in PDGF-β-enriched medium (and in the absence of EGF and FGF), SP-CPCs expressed mature filamentous structures of α-Smooth Muscle Actin (α-SMA) (Fig.26A).

Through cardiostem sphere formation in EGF/FGF-deprived medium and using Laminin-precoated dishes we could induce the expression of the cardiomyogenic marker troponinI, which could be detected in the cytosol of a limited number of cells, but mostly without fibrillar organization (Fig.26B), with few exceptions (Fig.26C).

To induce endothelial cell differentiation, we cultured CSP cells for two weeks in endothelial growth medium (EGM-2) using Fibronectin pre-coated dishes. In this context (although at low rate), expanded SP-CPCs expressed the endothelial marker vWF (Fig.27A). Additionally, they were able to form capillary-like structures in a tube formation assay within a matrigel scaffold (Fig.27B), supporting their endothelial potential.

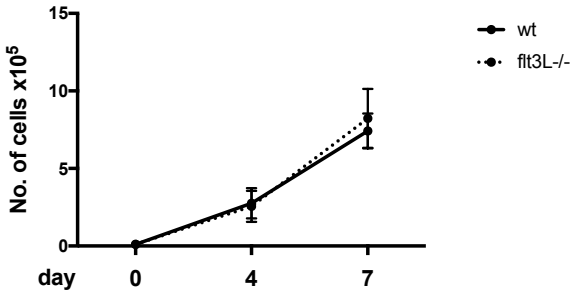

Fig.25: SP-CPC count in stemness-preserving medium (Medium2) at days 3 and 5 in culture. Starting cell number = $1x10^4$. Statistics: wt vs. flt3L-/-, n=4-5, data are shown as mean±SEM, ns. P7 = passage7.

	Myogenic	**Smooth muscle**	**Endothelial**
Expansion medium	Medium2	Medium2	Medium2
Sphere formation	Yes (-EGF, -FGF)	-	-
Coating	Laminin	-	Fibronectin
Serum starvation	-	48h Medium2 0.1%FCS	48h Medium2 0.1%FCS
Differentiation medium	DMEM 7%FCS	Medium2 (PDGF, -FGF, -EGF)	EGM-2
Culturing time	10-14 days	10-14 days	10-14 days

Table 6: Cell differentiation protocols for cardiomyogenic, smooth muscle cell and endothelial lineages.

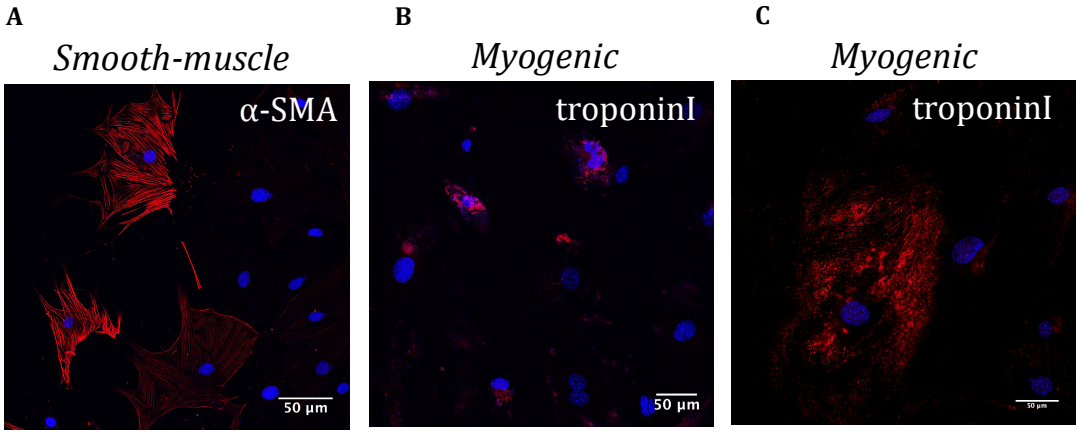

Fig.26: Expanded Sca1+/CD31- SP-CPCs (P7) cultured for 10-14 days in **A**: smooth muscle differentiation medium,. Representative pictures are shown: α-SMA (red), dapi/nuclei (blue). 20X magnification; **B-C**: cardiomyogenic differentiation medium. Representative pictures are shown: troponinI (red), dapi/nuclei (blue). 20X magnification. P7 = passage7.
α-SMA: α-Smooth Muscle Actin.

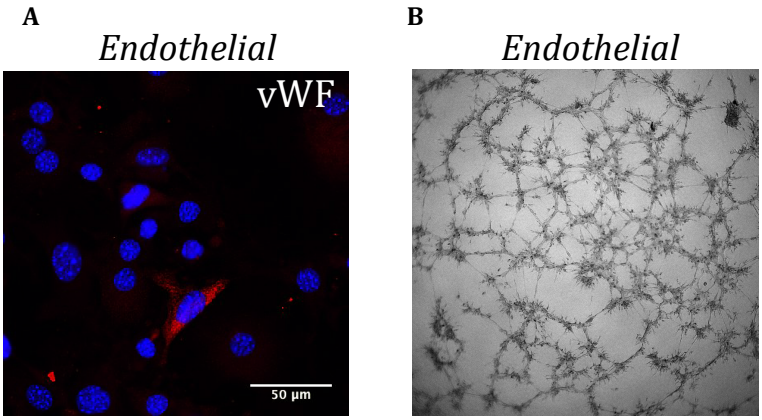

Fig.27: **A**. Expanded Sca1+/CD31- SP-CPCs (P7) cultured for 10-14 days in endothelial differentiation medium. Representative pictures are shown: vWF (red), dapi/nuclei (blue). 20X magnification; **B**. Expanded Sca1+/CD31- CSP cells after 24h in matrigel following 3 weeks of culturing in endothelial differentiation medium. BF, 2X magnification. P7 = passage7.
vWF: von Willebrand factor

Flt3L-/- CSP progenitor cells show a skewed proliferation - differentiation balance

Once we defined the differentiation protocol for the three main cardiac lineages we compared the behaviour of wt and flt3L-/- SP-CPCs under differentiation conditions.
With regard to smooth muscle cell differentiation, SP-CPCs from both genotpyes showed expression of mature structures of α-Smooth Muscle Actin (Fig.28A). However, whereas there was no difference with respect to the proliferation rate in Medium2 (Fig.25), but reminiscent of the proliferation behaviour in Medium1, flt3L-/- CSP cells proliferated much faster in smooth muscle differentiation medium as evidenced by the higher number of nuclei per field in flt3L-/- compared to wt cultures (201 ± 65 vs. 320 ± 52, ns; n=4-6, 20X magnification) (Fig.28B). This resulted in a lower percentage of cells undergoing differentiation for this specific lineage (34.5% ± 9.4 vs. 14.9% ± 8.4, p=0.066; n=4-6) (Fig.28C).
A similar observation was made when cells were cultured under cardiomyogenic differentiation conditions. Whereas SP-CPCs from both strains expressed troponinI (Fig.29A), flt3L-/- SP-CPCs also showed a high rate of proliferation (nuclei per field: 45 ± 4 vs. 98 ± 10, $p<0.01$; n=5-4, 10X magnification) (Fig.29B) and this resulted in a lower percentage of troponinI-positive cells in flt3L-/- cultures compared to wt (62.8% ± 5.9 vs. 42% ± 8.2, p=0.063; n=4-5) (Fig.29C). Of note, we observed a particularly high percentage of troponinI-positive cells compared to previous works (*5, 103*), which might be due to enrichment of the cardiomyogenic progenitor cell subfraction during cardiostem sphere formation.

These data suggest that flt3L might act as a regulator of the proliferation/differentiation balance of SP-CPCs.

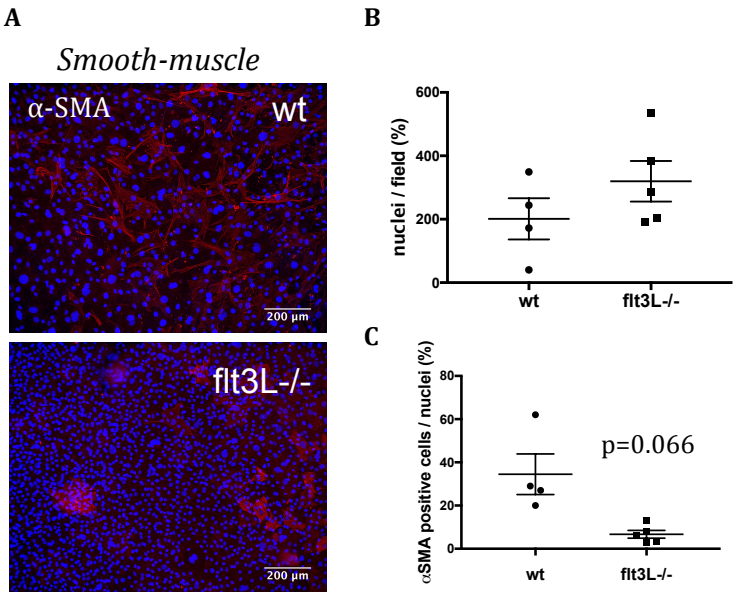

Fig.28: **A**: Expanded Sca1+/CD31- SP-CPCs (P7) cultured for 10-14 days in smooth muscle differentiation medium. Representative pictures are shown: α-SMA (red), dapi/nuclei (blue). 20X magnification; **B**. Numbers of cells per field. Wt vs. flt3L-/-, n=4-5, data are shown as mean±SEM. Mann Whitney test, ns.; **C**. % of α-SMA+ cells. Wt vs. flt3L-/-, n=4-6, data are shown as mean±SEM. Mann Whitney test, p=0.066. P7 = passage7.
α-SMA: α-Smooth Muscle Actin.

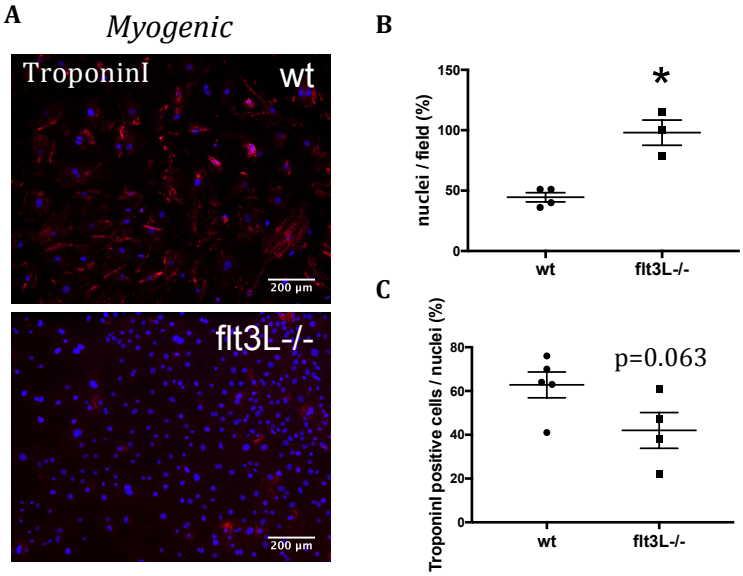

Fig.29: **A**: Expanded Sca1+/CD31- SP-CPCs (P7) cultured for 10-14 days in cardiomyogenic differentiation medium. Representative pictures are shown: troponinI (red), dapi/nuclei (blue). 20X magnification; **B**. Numbers of cells per field. Wt vs. flt3L-/-, n=4-3, data are shown as mean±SEM. Mann Whitney test, **p<0.01; **C**. % of α-SMA+ cells. Wt vs. flt3L-/-, n=5-4, data are shown as mean±SEM. Mann Whitney test, p=0.063. P7 = passage7.

Flt3L-/- CSP progenitor cells show no ability to organize in tube-like structures in matrigel upon endothelial differentiation

The tube formation assay measures the ability of the cells, supported by the appropriate extracellular matrix and conditioned media, to form capillary-like structures (a.k.a tubes) (*138*). We evaluated the tube formation ability of expanded wt and flt3L-/- cells upon endothelial differentiation using a growth factor reduced matrigel. Following 24h in 0.1% FCS-supplement-free medium2 , SP-CPCs were cultured for 3 weeks in endothelial differentiation medium. Upon culturing in endothelial differentiation medium, we observed subtle differences in cell morphology between wt and flt3L-/- SP-CPCs, whereby wt cells sported mostly a spindle-like shape and signs of cell alignment, which were both absent in flt3L-/- cells (Fig.30). Cells were then trypsinized and identical cell numbers were transferred on matrigel for additional 24h. Wt SP-CPCs were able to organize in capillary-like structures (Fig.31A), and this ability was completely absent in flt3L-/- cells (Fig.31B). These data show that flt3L-/- cells fail to differentiate into mature endothelial cells under appropriate differentiation conditions.

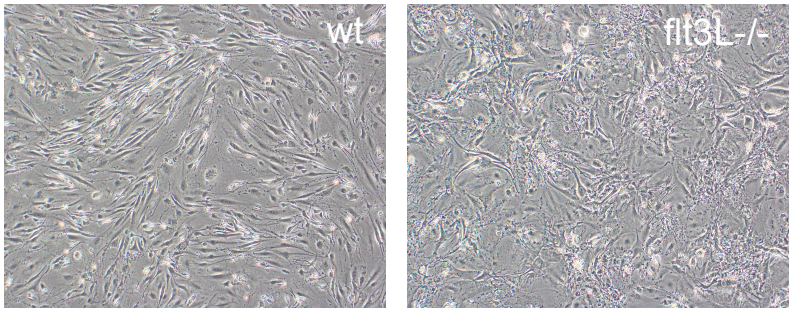

Fig.30: Expanded Sca1+/CD31- SP-CPCs (P7) cultured for 3 weeks in endothelial differentiation medium. Representative pictures are shown: BF, 4X magnification. P7 = passage7.

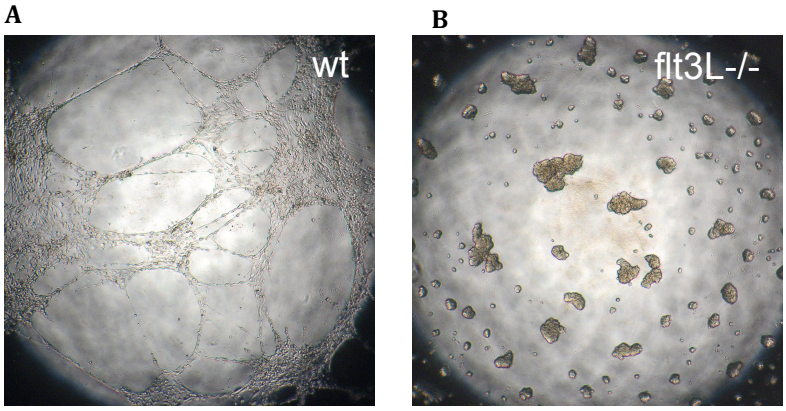

Fig.31: **A-B.** Expanded wt and flt3L-/- Sca1+/CD31- SP-CPCs (P7) after 24h in factor reduced-matrigel following 3 weeks in endothelial differentiation medium. Representative pictures are shown: BF, 2X magnification. P7 = passage7.

Chapter 2. Flt3 signaling in the healthy and injured heart

Flt3L-/- mice exhibit impaired cardiac function

Given that flt3 signaling appears important for cardiac progenitor cell maintenance and function, and that flt3L deficiency causes a disturbance of the adult cardiac progenitor cell homeostasis *in vivo*, we sought to test whether absence of functional flt3 signaling affects adult cardiac structure and function. Conventional echocardiography on age-matched 12 week-old wt and flt3L-/- mice showed a moderate but significant decrease in global systolic function in flt3L-/- mice as assessed by left ventricular (LV) ejection fraction (LVEF, 50.6% ± 1.7 vs. 43.3% ± 1.8, $p<0.01$; n=16-18, Fig.32A), whereas cardiac structure in terms of wall thicknesses and left ventricular (LV) diameters was virtually maintained (LV end-diastolic diameter: 4.50mm ± 0.07 vs. 4.36mm ± 0.06, ns; n=16-18) (Fig.32B). Using speckle-tracking echocardiography (*139*) we further evaluated deformation parameters of the myocardium in the long axis as longitudinal strain (LS) and radial strain (RS), which assess contraction strength of the myocardium and are considered early predictors of (subclinical) functional decline. As for conventional parameters, flt3L-/- mice showed reduced LS (-9.8Pk% ± 0.5 vs. -8.1Pk% ± 0.4, $p<0.05$; n=16-18) and RS values (20.8Pk% ± 1.0 vs. 17.5Pk% ± 1.2, $p<0.05$; n=16-18) (Fig.32C-D).

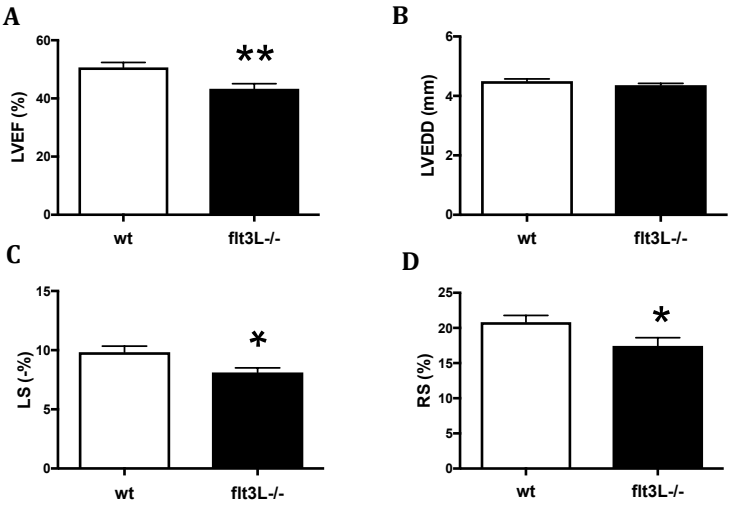

Fig.32: Echocardiographic measurements in 12 weeks-old mice of **A**. left ventricular ejection fraction (LVEF); **B**. left ventricular end-diastolic diameter (LVEDD); **C**. longitudinal strain (LS); **D**. radial strain (RS). Statistics: wt vs. flt3L-/-, n=16-18, data are shown as mean±SEM. Mann Whitney test for LVEF, unpaired t-test for LVEED,LS and RS, *$p<0.05$, **$p<0.01$.

Flt3L-/- mice have smaller hearts and smaller CMC size

Wt and flt3L-/- mice showed no significant difference with regard to body weight (29.1g ± 0.4 vs. 27.4g ± 0.4, p<0.05; n=12) (Fig.33A). In contrast, flt3L-/- mice had a reduced LV weight to tibia length ratio (6.96 ± 0.45 vs. 5.96 ± 0.16, p=0.088; n=6-8) (Fig.33B) and reduced CMC size according to the cross-sectional area (249.9µm^2 ± 13.5 vs. 213.8µm^2 ± 11.17, p=0.053; n=9-10), as assessed by wheat germ agglutinin (WGA) staining of cellular membranes (Fig.34). Of note, flt3L-/- mice had LV dysfunction and this might induce lung congestion. Surprisingly, we observed no accumulation of liquids in the flt3L-/- lungs, but instead the wet to dry lung weight ratio was reduced compared to wt mice (4.25 ± 0.06 vs. 4.09 ± 0.04, p=0.073; n=6-8) (Fig.35).

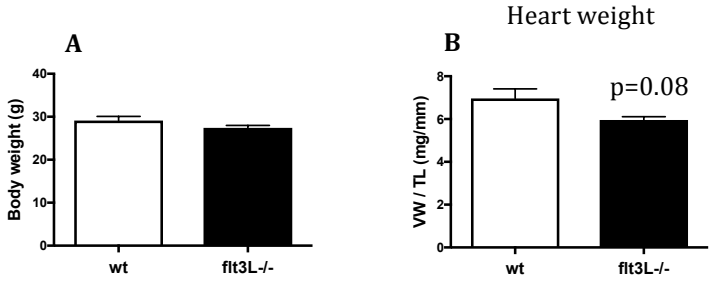

Fig.33: **A**. Measurement of 12 weeks-old mice body weight. Statistics: wt vs. flt3L-/-, n=12, data are shown as mean±SEM. Unpaired t-test, ns.; **B**. Measurement of the heart weight as ventricular weight/tibia length ratio (VW/TL). Statistics: wt vs. flt3L-/-, n=6-8, data are shown as mean±SEM. Mann Whitney test, p=0.08.

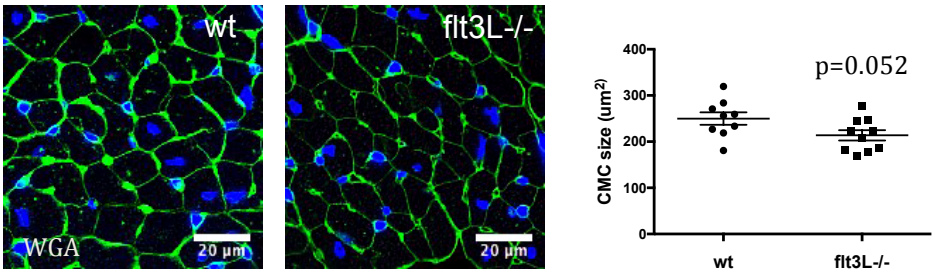

Fig.34: Analysis of the cross-sectional area of the CMCs in the free LV wall. Representative pictures are shown: WGA lectin (green), dapi/nuclei (blue). Statistics: wt vs. flt3L-/-, n=9-10, data are shown as mean±SEM. Unpaired t-test, p=0.053.
WGA: Wheat Germ Agglutinin

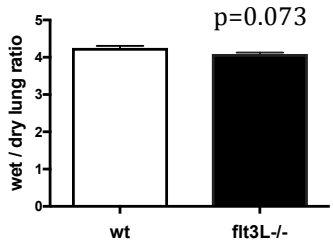

Fig.35: Analysis of the lung wet/dry ratio. Statistics: wt vs. flt3L-/-, n=6-8, data are shown as mean±SEM. Mann Whitney test, p=0.073.

Flt3L-/- mice show reduced capillary density

The smaller CMC size and the decreased cardiac function in the absence of cardiac injury suggest a developmental pathology in flt3L-/- mice. Given the reduced wet to dry lung ratio, which suggests lower perfusion and/or vascularization of the lungs of flt3L-/- mice, as well as the decreased capacity of flt3L-deficient SP-CPCs for endothelial differentiation and maturation, we primarily focused on myocardial vascularization, assessing the numbers of large and middle-sized vessels as well as the capillary density in the LV. We firstly analysed the cardiac vasculature using von Willebrand factor (vWF), a marker of mature endothelial cells. We found a moderately and non-significantly decreased number of medium to large-sized vessels (diameter > 20μm) in flt3L-/- compared to wt hearts (9.05 ± 0.88 vs. 6.39 ± 1.21, p=0.09; n=10) (Fig.36). To further analyse microvasculature in the heart, we used isolectin IB4, which recognises polysaccharides present in all endothelial cells (*140*). We observed a significantly reduced number of capillaries per myocyte in flt3L-/- mice (1.36 ± 0.07 vs. 1.14 ± 0.05, $p<0.05$; n=9-10) (Fig.37), suggesting a rarefaction of the microvascular bed. In contrast, we did not observe any microinjuries in terms of enhanced apoptosis or fibrosis in flt3L-/- hearts. Specifically, there was no difference in the number of TUNEL-positive nuclei (apoptotic nuclei) between flt3L-/- and wt hearts (0.53 ± 0.04 vs. 0.46 ± 0.03, ns; n=5) (Fig.38A) and no increase in fibrosis could be detected (Fig.38B). These data suggest microvascular rarefaction leading to malnutrition and decreased CMC size associated with subclinical systolic dysfunction of the flt3L-/- hearts.

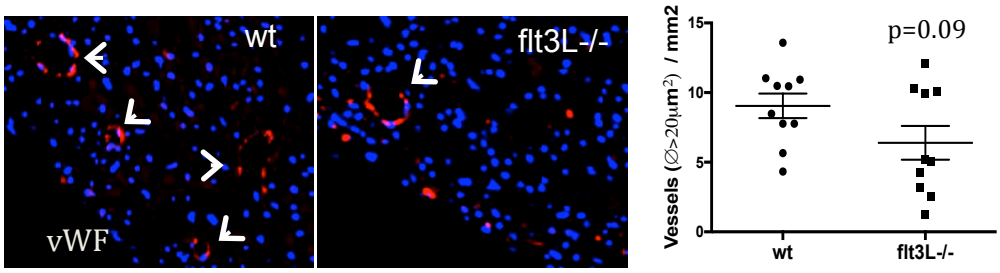

Fig.36: Analysis of the middle- to large-sized vessel density in the LV. Representative pictures are shown: vWF (red), dapi/nuclei (blue). Statistics: wt vs. flt3L-/-, n=10, data are shown as mean±SEM. Unpaired t-test, p=0.09.
vWF: von Willebrand factor

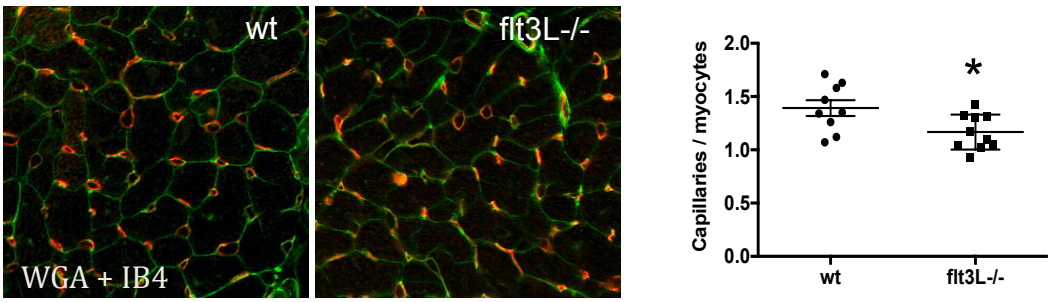

Fig.37: Analysis of the capillary density in the LV. Representative pictures are shown: IB4 (red), WGA (green). Statistics: wt vs. flt3L-/-, n=9-10, data are shown as mean±SEM. Unpaired t-test, *p<0.05.
WGA: Wheat Germ Agglutinin; IB4: isolectin B4

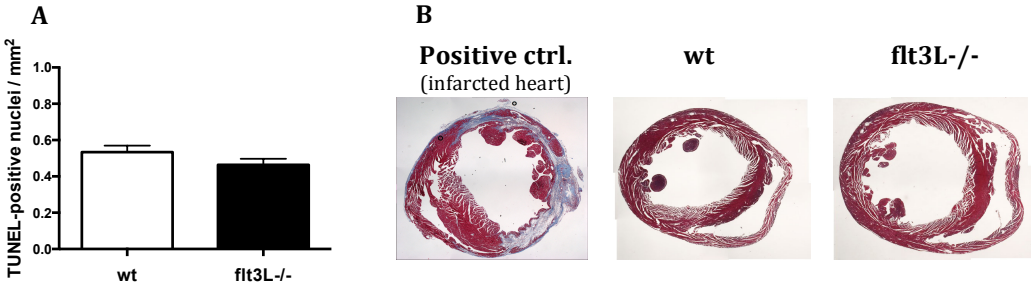

Fig.38: **A**. Detection and quantification of apoptotic CMCs via TUNEL staining. Statistics: wt vs. flt3L-/-, n=5, data are shown as mean±SEM. Mann Whitney test, ns.; **B**. Detection of fibrotic tissue via Masson's Trichrome staining. Representative pictures are shown: muscle tissue (red), collagen/fibrosis (blue). Infarcted heart was used a positive control.
TUNEL: Terminal deoxynucleotidyl transferase dUTP nick end labeling

Flt3L ablation is protective during post-MI cardiac remodelling

Flt3/flt3L is a cytoprotective system in the ischemically injured heart (*3*) and flt3L ablation is associated with disturbed cardiac progenitor cell homeostasis and function, microvascular rarefaction and subclinical cardiac dysfunction. In this context, we assessed the implications of flt3L-deficiency in the acute and post-acute phase after myocardial infarction (MI). We induced MI by LAD ligation (see methods) and followed-up on the mice clinically and echocardiographically over 7 days. We observed no difference in post-MI survival between the two strains (Fig.39). LV weight to tibia length ratio significantly increased after MI with no difference between the two strains (7.97 ± 0.55 vs. 7.64 ± 0.57, ns; n=8,10) (Fig.40). LVEF was significantly decreased in wt mice after MI compared to sham (43.35% ± 4.86 vs. 15.34% ± 1.78, $p<0.05$; n=6,8). Surprisingly, however, LVEF was less compromised in flt3L-/- mice, which showed only a non-significant decline in LVEF after MI compared to sham (43.32% ± 2.13 vs. 30.69% ± 5.32, ns; n=8-10) and to wt-MI mice (30.69% ± 5.32 vs. 15.34% ± 1.78, ns; n=8-10). (Fig.41A). Consistently, wt mice showed higher post-MI LV dilation as assessed by LVEDD compared to the flt3L-/- group (5.74mm ± 0.32 vs. 4.69mm ± 0.18, $p<0.01$; n=8-10) (Fig,41B). Deformation parameters supported a protective role of flt3L-/- during the early phase of remodelling as LS (4.07% ± 0.56 vs. 6.28% ± 0.75, ns; n=8-10) and – more pronounced – RS (7.92% ± 1.05 vs. 13.46% ± 2.41, ns; n=8-10) were higher in flt3L-/- mice compared to wt at 1 week after MI (Fig.41C-D).

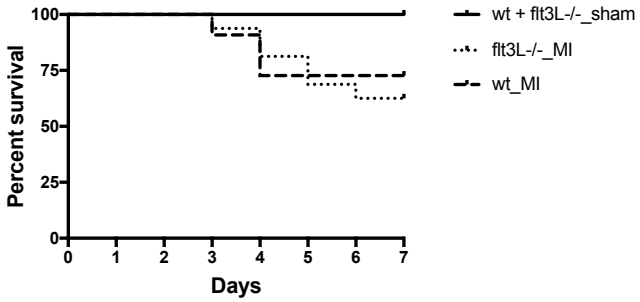

Fig.39: Post-MI percent survival over 7 days post-surgery in wt-infarcted (wt_MI), flt3L-/- infarcted (flt3L-/-_MI) and sham (wt+flt3L-/-_sham) mice. Statistics: wt_MI, flt3L-/-_MI, wt+flt3L-/-_sham, n=8, 10, 14, survival comparison test, ns.

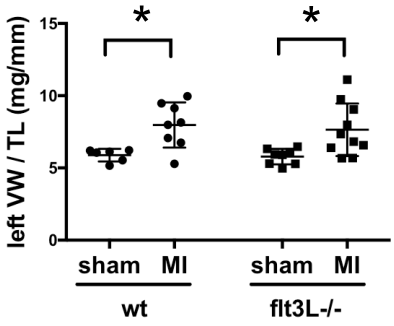

Fig.40: Ventricular weight to tibia length ratio (VW/TL). Statistics: wt sham (wt_sham), wt-infarcted (wt_MI), flt3L-/- sham (flt3L-/-_sham) flt3L-/- infarcted (flt3L-/-_MI) mice, n=6-8-8-10 data are shown as mean±SEM. 2way ANOVA, *p<0.05.

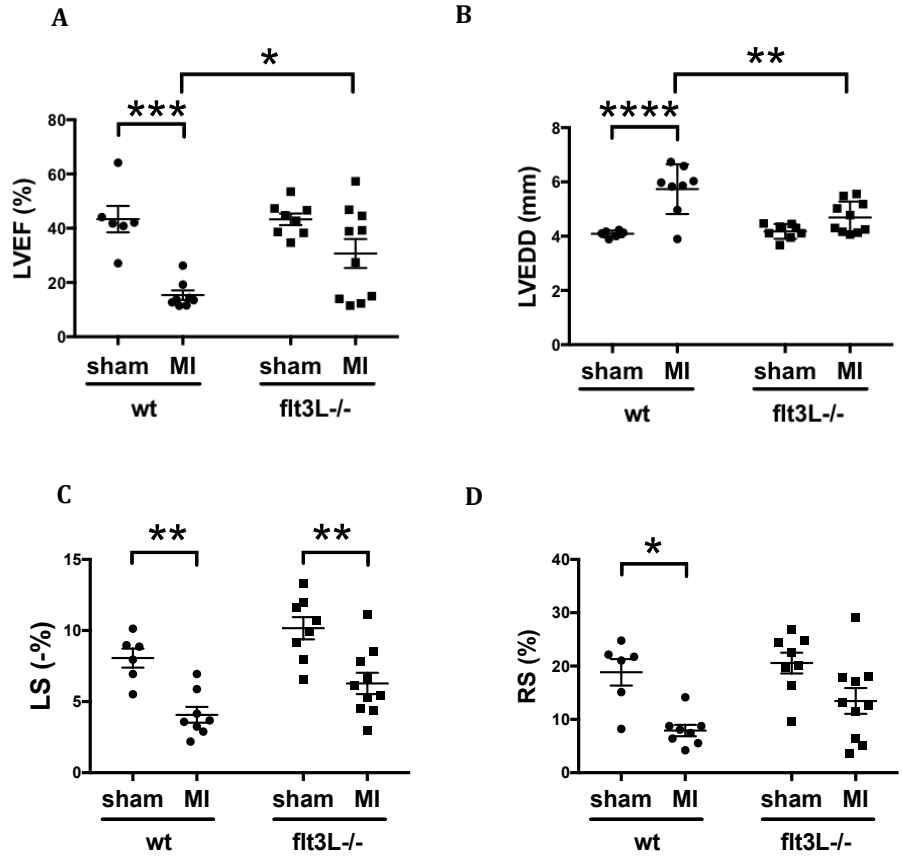

Fig.41: Echo-measurements in 9 week-old mice, 1 week after permanent occlusion of the left anterior descending coronary artery. **A**. left ventricular ejection fraction (LVEF); **B**. left ventricular end-diastolic diameter (LVEDD); **C**. longitudinal strain (LS); **D**. radial strain (RS). Statistics on wt sham (wt_sham), wt-infarcted (wt_MI), flt3L-/- sham (flt3L-/-_sham) flt3L-/- infarcted (flt3L-/-_MI) mice, n=6-8-8-10 data are shown as mean±SEM. 2way ANOVA, *p<0.05, **p<0.01, ***p<0.001, ****p<0.0001.

Flt3L-/- hearts appear to have an intrinsically enhanced inflammatory response

We compared the wt and flt3L-/- cardiac transcriptome using RNA isolated from whole heart homogenates. 60 to 70 millions reads were sequenced across samples (n=4), from which 27-32 millions reads mapped to the genome. As for CSP transcriptome analysis, only transcripts presenting at least 1cpm in at least 4 samples (indistinctly wt or flt3L-/-) were considered for gene expression analysis. In contrast to CSP cell samples, samples from wt and flt3L-/- whole hearts showed a remarkably high correlation within the group (0.987 and 0.986, respectively) and the PCA describing 55.05% of the observed differential expression between the samples is correlated with the KO of the flt3L gene.

As in the previous trascriptome analysis, flt3L transcript is detected in both strains but again only as truncated gene in the flt3L-/- hearts. Flt3 receptor is detected only by few reads.

Performing GSEA using a FDR < 1e-6, we focused on the Gene Ontology (GO) gene sets, in which genes are assigned to a set of predefined bins depending on their functional characteristics. Several GO gene sets were differentially regulated between wt and flt3L-/- (Table 5). The differential expression of these gene sets occurred in both direction (up-regulation or down-regulation) but the most differentially regulated GO gene sets were up-regulated in the flt3L-/- hearts. In particular, we found a profound up-regulation of gene sets involved in the inflammatory response and in immune cell migration (Table 7). These novel transcriptional findings suggest that flt3L-/- hearts have an intrinsically enhanced inflammatory response, which might be protective during the acute phase of the post-MI remodelling and might explain the partial preservation of LV function in flt3L-/- mice after MI (Fig.41).

GeneSet	NGenes	Correlation	Direction	absLog2FC	PValue	adj.P.Val
GO_REGULATION_OF_MONONUCLEAR_CELL_MIGRATION	11	0.01	Up	0.9652996	4.956e-11	6.196e-09
GO_REGULATION_OF_MACROPHAGE_CHEMOTAXIS	11	0.01	Up	0.9139747	1.944e-10	2.166e-08
GO_GRANULOCYTE_MIGRATION	38	0.01	Up	0.7693743	3.016e-09	2.712e-07
GO_REGULATION_OF_GRANULOCYTE_CHEMOTAXIS	28	0.01	Up	0.6629544	7.723e-09	5.909e-07
GO_LEUKOCYTE_CHEMOTAXIS	65	0.01	Up	0.6577073	8.190e-12	1.135e-09
GO_MYELOID_LEUKOCYTE_MIGRATION	55	0.01	Up	0.6127564	8.565e-09	6.456e-07
GO_CELL_CHEMOTAXIS	97	0.01	Up	0.5506670	4.026e-12	6.450e-10
GO_POSITIVE_REGULATION_OF_LEUKOCYTE_MIGRATION	67	0.01	Up	0.5133590	1.277e-08	9.216e-07
GO_INFLAMMATORY_RESPONSE	261	0.01	Up	0.4541596	2.721e-12	4.500e-10
GO_REGULATION_OF_LEUKOCYTE_MIGRATION	91	0.01	Up	0.4493215	3.699e-09	3.213e-07
GO_LEUKOCYTE_MIGRATION	165	0.01	Up	0.4463410	5.272e-10	5.404e-08
GO_CELLULAR_RESPONSE_TO_INTERFERON_GAMMA	86	0.01	Up	0.4299297	6.157e-11	7.514e-09
GO_RESPONSE_TO_INTERFERON_GAMMA	97	0.01	Up	0.4154306	8.177e-11	9.526e-09
GO_INTERFERON_GAMMA_MEDIATED_SIGNALING_PATHWAY	58	0.01	Up	0.3980250	1.203e-09	1.142e-07
GO_ADAPTIVE_IMMUNE_RESPONSE	135	0.01	Up	0.3676180	5.810e-09	4.582e-07
GO_MULTICELLULAR_ORGANISMAL_MACROMOLECULE_METABOLIC_PROCESS	56	0.01	Up	0.3577172	7.194e-09	5.587e-07
GO_INNATE_IMMUNE_RESPONSE	351	0.01	Up	0.3561577	4.865e-09	4.089e-07
GO_IMMUNE_RESPONSE	594	0.01	Up	0.3554412	6.268e-10	6.179e-08

Table 7: Gene Set Enrichment Analysis of Gene Ontology gene sets. Statistics: flt3L-/- vs wt, n=4. Statistics filters: 1: 1cmp in at least 4 samples (indistinctly wt or flt3L-/-); 2: adj.P.Val < 1e-6.

Discussion

Taken together, this thesis work contributes to an improved understanding of CPC biology and of the role of Flt3L, an early acting hematopoietic cytokine, in the heart. Firstly, we show that a tight control of CPC *ex vivo* expansion conditions together with the use of specific growth factors, i. e. EGF and FGF, are pivotal to maintain the CPC phenotype and differentiation potential, which may contribute to a better performance of such cells in the scope of regenerative cell therapy. Secondly, we uncover a so far unrecognized role of flt3/flt3L in the regulation of the adult cardiac progenitor pool. Specifically, we show that flt3L contributes to the maintenance of the CPC signature and the functionality of CPCs via a mechanism that includes the balancing of their proliferation and differentiation, pointing towards potentially important parallels between CPC and hematopoietic progenitor cell biology. Finally, we show that whereas non-conditional knock-out of Flt3L leads to reduced myocardial vascularization and subtle cardiac dysfunction, flt3L deficiency appears actually protective in the post-acute phase after myocardial infarction. In the following paragraphs, these three key observations of my thesis will be further discussed.

For the past decade, cell therapy has emerged as an appealing novel approach to regenerate lost cardiac tissue after major injury such as myocardial infarction. However, so far, proof of clinical benefit in large-scale randomized and double-blinded clinical trials is still missing. Current research is focusing on the many aspects of potential cell therapy that are still not understood and that include the search for the ideal cell type. Several endogenous precursors have been investigated in pre-clinical and clinical studies showing regenerative potential and functional improvement of the heart (*141, 142*). Still, survival and differentiation efficiency of transplanted cells remain poor.

An ideal cell type for replacing damaged myocardial tissue would have the ability to survive, integrate into an ischemic area, and stimulate endogenous regeneration via lineages-differentiation to support the pre-existing myocardium. So far different cell types have been explored in these regards. Several clinical trials using primitive cell population from heart or BM have shown safe delivery and functional improvement of cardiac output when administered to ischemic patients (*75, 76, 143*), but so far

none have met the ideal expectations.

Issues associated to cell therapy are multiple. Cell survival after transplantation is low regardless of the cell type and the injury model (*144*). Similarly, injected cells in murine MI-models have shown poor retention capacity: cell retention at day 1 varied from 1 to 8%, declining to 0.1–0.5% at 2 weeks (*69*). Several tissue engineering approaches such as the implantation of cell sheets, epicardial patches, or delivery in biomaterials have been described to increase the engraftment rate (*145-147*).

A second issue is defining the right timing of delivery of *ex vivo* expanded CPCs. The optimal maturation state of CMCs for transplantation is not fully understood yet. Mature adult CMCs do not survive transplantation and immature CMCs have slow conduction and may be cause of arrhythmias (*148*).

A last consideration points out that, despite the capability of these cells to migrate in the ischemic area and differentiate, only a small portion of engrafted cells express myogenic or vascular proteins and most of them lack complete maturation (*69, 106*). This partial loss of the multilineage differentiation potential might occur during the *ex-vivo* amplification, throughout which maintenance of CPC properties remains an obligatory step in order to use these progenitors for cell therapy.

Several factors might affect CPC properties during cell expansion. These could be stress factors such as the isolation procedure and the switch from a 3-dimensional to a 2-dimensional environment. But mainly the lack of signals such as paracrine factors or cell-cell contacts, which typically occur in the niche environment and are important for CPC quiescence and function, may affect *ex vivo* CPC behavior. All these factors might be responsible for a partial loss of differentiation efficiency during cell expansion and a consequent lack of complete maturation *in vitro* or *in vivo* when transplanted in the heart.

Different populations of CPCs have been identified in the heart, according to unique cell surface marker patterns. To investigate this final point we isolated a specific type of CPCs based on their ability to efficiently efflux Hoechst dye, knows as the CSP, which, as other candidate cells, has been well described in several animal models (*149*), and also in the adult human heart (*150*).

We showed that careful adjustments of culture conditions are necessary to preserve the multipotential properties of SP-CPCs expanded *in vitro*. In particular, SP-CPCs expressed specific lineage markers and preserved their differentiation potential, when expanded in low-serum conditions and in the presence of EGF and FGF, which are

commonly added into stem cell cultures to enhance their proliferation capacity while preserving their multipotency, a process also known as self-renewing proliferation (*135-137*).

Flt3/flt3L is an important regulator of hematopoietic progenitor cells, mainly controlling their proliferation and differentiation. Although its role is well known in the BM (*26, 31, 33*), it has also been implicated in the regulation of progenitor cell function from other organs, including neural and muscle-derived stem cells (*54, 55, 123*). In this context, we wanted to evaluate if and how flt3 signaling affects the adult progenitor cell pool in the heart.

Our *in vivo* findings suggest an untimely activation of a proportion of physiologically quiescent progenitor cells in flt3L-/- mice, prompting them to leave their quiescent state and, hence, the SP phenotype. In line with this finding, GSEA unveiled a reduced CD31- progenitor cell signature in flt3L-/- SP-CPCs, with downregulation of transcripts involved in cell cycle arrest and stemness.

Sorted wt and flt3L-/- Sca1+/CD31- SP-CPCs are expandable *in vitro*. In EGF/FGF-deprived medium, flt3L-/- SP-CPCs showed a hyperproliferative state compared to wt cells and lower expression of lineage markers. Considering that proliferation and differentiation tend to follow opposite pathways, these data point towards a lower differentiation efficiency of flt3L-/- SP-CPCs. Nevertheless, when pushed towards specific cardiac lineages with differentiation media, SP-CPCs of both genotypes (wt and flt3L-/-) failed to express lineage markers, suggesting that this expansion medium favours an *in vitro* transformation characterized by a high proliferation rate, in which SP-CPCs fail to exit the cell cycle and undergo differentiation.

In contrast, low serum and EGF/FGF-enriched medium abolished the phenotypic difference between wt and flt3L-/- SP-CPCs in terms of proliferation and helped preserve a primitive cellular state, which made CSP progenitors more prone to cell differentiation. However, differentiation media destabilized this state and unmasked strain differences with respect to proliferation and differentiation. Expanded Sca1+/CD31- flt3L-/- SP-CPCs showed a higher proliferation rate when cultured in differentiation media (irrespective of the targeted lineage and – hence – the composition of the medium). This increased cycling of flt3L-/- cells might negatively affect the commitment and differentiation capacity of a proportion of flt3L-/- SP-CPCs, which is reflected by a lower percentage of CPCs expressing smooth muscle

and cardiomyogenic proteins.

Differently from these two lineages, and although freshly isolated SP-CPCs showed between 10-15% of positivity for vWF (detected in cytoplasmatic vacuoles) (Fig.9B), we observed particularly low rates of vWF+ cells within expanded SP-CPCs when cultured in endothelial differentiation medium (Fig.24A). There are two possible explanations for the poor efficiency to differentiate towards the endothelial lineage: one is related to the fact that the highest capacity for endothelial differentiation is mainly linked to the CD31-positive fraction of Sca1+ SP-CPCs (*105*), while instead in our study expanded CD31-negative SP-CPCs were used. The second explanation may relate to technical issues (e.g. staining efficiency), which are currently still under investigation in the laboratory. Although expanded SP-CPCs exhibited low expression of mature endothelial markers, differentiated SP-CPCs from wt mice were able to organize in capillary-like structures in response to angiogenic factors (*138*). After 3 weeks of culturing in endothelial differentiation medium, wt SP-CPCs formed endothelial tube-like structures in matrigel, indicating successful endothelial differentiation despite low expression of vWF and favouring technical limitations for the low rate of vWF positivity after the differentiation procedure. In contrast, using an identical differentiation protocol, flt3L-/- SP-CPCs showed no ability to organize in capillary-like structures when cultured in matrigel upon three weeks in endothelial differentiation medium.

These data suggest that flt3-signaling is mandatory for the maintenance of a molecular signature that is required for adult cardiac progenitor cell quiescence and functionality, and propose flt3 as a so far unrecognized regulator of the adult cardiac progenitor pool. These findings are in part reminiscent of a recently uncovered role of Flt3 signaling in skeletal muscle precursors (*54, 55*). In both cell types flt3L appears important to balance proliferation and myogenic differentiation. Lack of functional flt3 signaling leads to increased proliferation and limited differentiation efficiency. These data suggest that flt3 signaling might be important for the coordinated repression of proliferation in favour of cell cycle exit, which is pivotal for promoting differentiation. In this regard, the role of flt3 signaling in myogenic progenitor and precursor cells shows both similarities and differences with respect to its role in the hematopoietic progenitor cell pool. Whereas the role of flt3 in the heart is consistent with the reported instructive role of flt3L in early lineage commitment of

lymphoid/myeloid progenitors (*33*), it diverges from the described pro-proliferative role of flt3L in lymphoid progenitors (*28, 29, 38*).

Flt3/flt3L is a cytoprotective system in the heart and exogenous delivery of recombinant flt3L directly into the myocardium ameliorates post-MI function (*3*). In this context, we investigated how flt3L ablation affects structure and function of the healthy and injured heart.

Non-conditional ablation of flt3L causes subclinical LV systolic dysfunction in flt3L-/- mice, although we observed no differences with regard to cardiac structure and dimensions as assessed echocardiographically. *Ex vivo*, however, Flt3L-/- hearts are lower in relative weight and exhibit reduced CMC size. In addition, Flt3L-/- mice show a rarefaction of the microvascular bed in the absence of detectable micro-injuries. Taken together, we hypothesize that the observed phenotype might be the result of a nutritional or supply problem, possibly originating in disturbed (micro)vasculogenesis already during the early stages of cardiac development.

Heart microvascularization is the result of complex angiogenic and vasculogenic processes occurring during heart development (*151, 152*). The healthy endothelium is turned-over approximately every three years (*153*). Renewal of the vascular cells in the adult heart does not occur exclusively by angiogenesis, circulating endothelial progenitor cells (*154*) or resident CPCs (*66*) represent at least two sources of vascular progenitors that actively contribute to new vessel growth.

In this work, we showed that CSP cells have the potential to commit towards the endothelial lineage and form capillary-like structures in matrigel, and this potential is clearly lost in expanded flt3L-/- cells. Although SP-CPCs do not represent the only type of progenitor cells with endothelial potential residing in the heart (*66, 78, 104, 105, 107*), the failure of flt3L-/- SP-CPCs to efficiently differentiate into endothelial cells might be one of the causes of the reduced number of capillaries per myocyte observed in flt3L-/- mice. However, it might be notable that other TK receptors, such as VEGF and Tie receptors, have been well described to directly mediate angiogenesis (*155*). Therefore, we cannot exclude a so far undiscovered role of flt3 signaling in the angiogenic processes during cardiac development or post-natal growth and homeostasis.

These findings demonstrate that, although these mice are viable with no previously described cardiac phenotype, ablation of flt3 signaling has an impact on cardiac organ and progenitor cell homeostasis.

As mentioned, intramyocardial activation of flt3 via exogenous flt3L is protective against adverse cardiac remodelling after MI (*3*) and flt3L ablation (via CPCs?) is responsible for a rarefaction of the microvascular bed in the ventricular wall. In this context, we assessed the implications of a lack of a functional flt3 system in the ischemically injured heart, in which cell survival and neovascularization are important features of cardiac tissue preservation and repair, hypothesizing that both of these features are impaired in flt3L-deficient hearts, hence leading to worse post-infarct remodelling and outcome.

Contrary to our hypothesis, however, we observed that flt3L ablation is protective rather than deleterious during the acute and post-acute phase after MI. In particular, both the reduction in LV pump function as well as LV dilation were both markedly mitigated in infarcted flt3L-/- compared to wt hearts. Whereas these findings suggest that additional mechanisms as discussed below are responsible for the beneficial effects in the early post-infarct phase, they do not exclude potential deleterious effects of flt3L ablation during the later, chronic phase of post-MI remodelling, when the inflammatory response subsides and function-preserving and regenerative processes are taking the lead (*108, 112*).

Flt3 signaling has a major role in normal haematopoiesis and it modulates immune cell homeostasis and function (*1*). The inflammatory response and the leucocyte chemotaxis at the injury site are major events during the acute phase of the post-MI remodelling. Their injury-mediated activation is pivotal to contain the ischemic damage and trigger an immediate repair process to retain cardiac function despite the newly-formed necrotic tissue (*108, 112, 113*). In this context we currently hypothesize that the protective effect observed in the flt3L-/- mice after 1 week post-MI (Fig.40) might be associated to a modulation of the inflammatory response, which occurs early in the repair process. Our hypothesis is supported by the transcriptome analysis of the heart tissue from wt and flt3L-/- mice, which revealed an endogenous up-regulation of genes involved in the inflammatory response and cell migration in the flt3L-/- hearts. These findings suggest that these mice might initiate a stronger and quicker inflammatory response following injury and that this appears to be consistent with the more favourable post-infarct cardiac function.

Anthracyclines are an important class of drugs in the treatment of cancer, but remain problematic chemotherapeutic agents given their cardiotoxic effects (*10, 156, 157*). Induction of cardiomyopathy and congestive heart failure (CHF) has stressed the need for proper prevention and alternative treatment strategies, as targeted cancer therapies including TKIs. As to date, little is known about the occurrence, timing and potential severity of TKI-related cardiac side effects (*12*).

Multi-kinase inhibitors, i. e. sunitinib and sorafenib target several kinase receptors, including flt3 (*158, 159*); they have shown efficacy in metastatic renal cell carcinoma and gastrointestinal stromal tumours but TKI-associated cardiotoxicity was reported in approximately 10% of the patients (*43*). In particular, aside inducing myocyte necrotic death, sorafenib significantly reduced the survival of mice undergoing MI after 1 week of treatment (*44*).

Second generation inhibitors, i. e. quizartinib (AC220), represent the state-of-the-art design for their high flt3-binding specificity, favouring a more targeted therapy and supposedly limiting off-target cardiotoxicity. In a phase II study, enrolling patients who were refractory to first-line chemotherapy or relapsed after hematopoietic stem cell transplantation (HSCT), quizartinib caused only transient QTc prolongation (13%) (*47*) and so far no late onset toxicity has been described. Still a profound gap of knowledge exists as to whether these new generation inhibitors targeting flt3 have cardiac side effects or not.

In our study, 4-weeks quizartinib treatment did not alter cardiac performance, but induced an increase in left ventricular dimensions, suggesting a subclinical hypertrophic response.

Cancer therapy may also negatively affect CPC function. In particular, administration of DOXO in rats leads to dilated cardiomyopathy with irreversible growth arrest and cellular senescence of CPCs (*72*). In a mouse model prone to developing heart failure as a result of anticancer therapies targeting Stat3 or DOXO (*78*), CPCs have a reduced endothelial differentiation capacity. These data suggest that an impairment of the CPC functionality might contribute to cancer therapy-induced cardiomyopathy and this could be the case for traditional chemotherapy (DOXO) as well as for targeted therapies (e.g., TKIs). Consistent with such hypothesis, in our *in vivo* study, 28 day-treatment with quizartinib caused a disturbance of the CPC homeostasis similar to the one observed in flt3L-/- SP-CPCs, suggesting that targeted (flt3-targeted in our case) short-term treatment may indeed cause potential cardiac side effects on the cellular

level, which may become relevant when co-inciding with an ischemic event (respective studies are currently ongoing in the lab).

Conclusions

In a context of a potential prospective use of CPCs in cardiac cell therapy, we show that careful adjustments of culturing conditions are pivotal to preserve progenitor potential, and thus the capability for multi-lineage commitment and differentiation, during *ex vivo* expansion.

With respect to its main focus, this work supports a novel role of flt3 signaling in the regulation of progenitor cells in the heart. Specifically, we show that flt3 contributes to the maintenance of a quiescent and functional cardiac progenitor cell pool *in vivo*. Flt3 is important for CPC lineage commitment and differentiation by regulating the balance between proliferation and differentiation in favour of differentiation. These findings reveal parallels between the roles of flt3 in the regulation of cardiac and the instructive role described in hematopoietic progenitor cells, and thus provide important novel insights into CPC biology. They also raise the possibility of a tighter relationship between cardiac and hematopoietic progenitor cells than previously thought that warrants further investigation.

We also found that flt3 contributes to the myocardial microvasculature, it is during development or postnatal growth and homeostasis. Although this could possibly be linked to the impaired endothelial differentiation potential of CPCs in the absence of flt3, additional mechanisms, including such related to angiogenesis rather than vasculogenesis may apply. Surprisingly, lack of endogenous flt3L was protective during the early, post-acute phase after myocardial infarction, as it mitigated the decline in cardiac function and ventricular dilation. With preliminary data pointing towards a potential modulation of the post-infarct inflammatory response investigation of the underling mechanism is currently ongoing in the laboratory.

This work was initiated against the background of cancer drug cardiotoxicity, as seen more and more often given the remarkable increase in lifespan through modern-day cancer therapies including receptor TKs. Better knowledge of the roles of cancer drug targets in the heart will help anticipate cardiac side effects, thus enabling early monitoring and interdisciplinary management of cancer patients. Our findings uncover so far unknown functions of flt3 in the heart, which are important in such context.

Future Perspective

As knowledge of CPC biology and their regulation is still limited, it will be important to understand the precise mechanisms through which flt3 regulates the balance between CPC proliferation and differentiation. Such findings will shed new light on how proliferation and differentiation are coordinated, and – hence – how differentiation is initiated, in CPCs. As previously shown for skeletal myoblasts, flt3 signaling is important for cell cycle exit and cell commitment towards a more differentiated phenotype (*54*) In our study, wt and flt3L-/- CPCs show a similar behaviour (in terms of proliferation) when expanded in stemness-preserving medium, suggesting that growth factors supplemented to the medium compensate for the lack of flt3L, thus maintaining the signalling signature necessary for keeping the cells in steady-state. Instead multiple types of differentiation media, irrespective of the targeted lineage, unmask strain differences and cause a striking increase of the proliferation rate in flt3L-/- cells, with consequently reduced differentiation efficiency (Fig.28-29). Although we used progenitor potential-preserving culturing conditions for expansion of CSP progenitors, we hypothesize the flt3L contributes to the preservation of a multipotent progenitor phenotype during *ex vivo* expansion. This also appears to be the case *in vivo* considering the reduced CD31- progenitor cell signature seen in freshly isolated flt3L-/- SP-CPCs. In this context, we recently tracked the transcriptional expression levels of primitive markers of multipotency in expanded wt and flt3L-/- SP-CPCs. We observed an overall passage-dependent down-regulation of some of these markers in both strains, suggesting a partial loss of multipotent properties during *in vitro* expansion. Interestingly, this down-regulation was more pronounced in flt3L-/- CPCs, suggesting an accelerated loss of progenitor characteristics that might affect their ability to commit and ultimately differentiate. We are currently working on corroborating this hypothesis by tracking stemness markers as well as cardiac lineage markers during CSP cell expansion and during the differentiation process into the different lineages in order to unveil differences between genotypes (i.e., wt versus flt3L-/-).

Regarding the molecular mechanisms that might regulate the behaviour of flt3L-/- CPCs, we identified the cell cycle regulator p63 (*160*) as markedly down-regulated in expanded (but not freshly isolated) ftl3L-/- CSP cells. P63 is a suppressor of

tumorigenesis and it affects several cellular mechanisms such as stemness, senescence, cell death and cell cycle arrest, which are all involved in cancer development (*161*). Interestingly, the p63 isoform TAp63 plays an important role in the maintenance and renewal of epidermal precursors. Loss of TAp63 leads to hyper-proliferation and senescence, and causes premature aging of these cells (*162*). TAp63 is also important for heart development and early embryonic stem cell (ESC) cardiogenesis. P63-deficient mice die soon after birth, but they show dilated cardiomyopathy at the embryonic stage. Compared to wt ESCs, ESCs deficient for p63 were unable to produce beating CMCs, likely due to a down-regulation of cardiac transcription factors and sarcomeric proteins (*163*). Using murine embryonic fibroblasts, Ma *et al.* identified the Stat3/p63/Notch cascade downstream of Akt as an important regulator of the balance between cell proliferation and differentiation (*164*).

We observed depletion of quiescent CPCs in systemically flt3L-deficient mice. We could reproduce a similar phenotype in mice treated with the flt3-inhibitor quizartinib for 28 consecutive days, suggesting that CSP homeostasis might be sensitive to the temporally restricted inhibition of flt3 in the adult heart, which would also raise the possibility of potential cardiac side effects of targeted, but short-lasting treatments as used for cancer therapy. In this context we want to treat wt and flt3L-/- mice with recombinant flt3L in order to rescue (at least partially) the CSP depletion and to verify that this phenotype directly depends on the availability of flt3L in the surroundings of the CPC niche.

We are also interested in a probable link between the rarefaction of the microvasculature and the CPC dysfunction, as suggested by the first results of the tube formation assay, showing an incapacity of flt3L-deficient progenitor cells to differentiate into endothelial cells capable to organize in tube-like structure.

We are also currently investigating the mechanisms, which are responsible for the apparently protective role of flt3L ablation in the early phase of post-MI cardiac remodelling. Interestingly, our most recent findings show a transcriptional pattern (Table 7) in favour of a stronger and possibly more efficient inflammatory response to MI in the flt3L-/- hearts. We are going to test the hypothesis that flt3L ablation is responsible for an immuno-modulation that enhances the early inflammatory response and facilitates leucocyte migration after injury.

Taken together, the presented results as well as the results from our still ongoing studies will advance our understanding of CPC biology and of heart-intrinsic as well as of systemic roles of cancer drug targets and how their inhibition is affecting the heart.

Other contributions

Cell therapy is a modern and still developing opportunity to treat cardiovascular disease. To promote myocardial regeneration, clinical trials have initially focused on the use of bone marrow-derived cells and have obtained very mixed results. Recent studies have switched the focus on cardiac-committed and/or cardiac resident progenitor cells. In the review article "Regenerative therapy for cardiovascular disease" we summarize current knowledge on different extracardiac as well as cardiac cell sources and highlight recent advances and backlashes in the field of cardiac cell therapy (*74*).

Over the past few years we deepened our studies on the regulation and role of the CSP, a specific progenitor cell population residing in the adult heart, and worked on adaptations and the fine-tuning of culture and differentiation techniques of these cells. Part of this work is reported in the chapter "Cell therapy for cardiac regeneration" enclosed in "Translating Regenerative Medicine to Clinics" (insert the following reference: Kuster GM, Della Verde G, Liao R, Pfister O. *Cell Therapy for Cardiac Regeneration*. In: J. Laurence, M. Van Beusekom, P. Baptista, A. Atala, eds. *Translating Regenerative Medicine to Clinics*. United States of America: Academic Press, Elsevier Inc., 2016; pp. 266-283.) and in the recently published work "Polo-like kinase 2 is dynamically regulated to coordinate proliferation and early lineage specification downstream of YAP in cardiac progenitor cells" (Mochizuki *et al.*, J Am Heart Assoc. 2017). In addition, a manuscript detailing adaptations in culture and differentiation techniques of CPCs is currently in preparation (invited submission to JoVE).

I was also involved in the overall management and the conduction of experiments within the scope of other studies ongoing in the laboratory, in particular *in vivo* work addressing the role of NOX1 in metabolic heart disease (manuscript submitted).

The work published or in preparation as well as congress contributions are listed below.

REVIEW ARTICLE

Regenerative therapy for cardiovascular disease

OTMAR PFISTER, GIACOMO DELLA VERDE, RONGLIH LIAO, and GABRIELA M. KUSTER

BASEL, SWITZERLAND; AND BOSTON, MASS

Recent insights into myocardial biology uncovered a hereto unknown regenerative capacity of the adult heart. The discovery of dividing cardiomyocytes and the identification and characterization of cardiac stem and progenitor cells with myogenic and angiogenic potential have generated new hopes that cardiac regeneration and repair might become a therapeutic option. During the past decade, multiple candidate cells have been proposed for cardiac regeneration, and their mechanisms of action in the myocardium have been explored. Initial clinical trials have focused on the use of bone marrow-derived cells to promote myocardial regeneration in ischemic heart disease and have yielded very mixed results, with no clear signs of clinically meaningful functional improvement. Although the efficiency of bona fide cardiomyocyte generation is generally low, stem cells delivered into the myocardium act mainly via paracrine mechanisms. More recent studies taking advantage of cardiac committed cells (eg, resident cardiac progenitor cells or primed cardiogenic mesenchymal stem cells) showed promising results in first clinical pilot trials. Also, transplantation of cardiomyogenic cells generated by induced pluripotent stem cells and genetic reprogramming of dividing nonmyocytes into cardiomyocytes may constitute attractive new regenerative approaches in cardiovascular medicine in the future. We discuss advantages and limitations of specific cell types proposed for cell-based therapy in cardiology and give an overview of the first clinical trials using this novel therapeutic approach in patients with cardiovascular disease. (Translational Research 2014;■:1–14)

Abbreviations: BMC = bone marrow-derived cell; BMSC = bone marrow stem cell; CADUCEUS = Cardiosphere-Derived Autologous Stem Cells to Reverse Ventricular Dysfunction; CD = Cluster of differentiation; SCF = stem cell factor; c-kit = receptor for SCF; CSC = cardiac stem cell; ESC = embryonic stem cells; HF = heart failure; iPS = induced pluripotent stem cell; MSC = mesenchymal stem cell; SCIPIO = Stem Cell Infusion in Patients With Ischemic Cardiomyopathy; SP = side population

Despite significant advances in the treatment of acute myocardial infarction, stroke, and hypertension, cardiovascular disease continues to remain the leading cause of death in developed countries.[1]

As the common final sequel of virtually all cardiac diseases, heart failure (HF) is the major contributor to cardiovascular morbidity and mortality. In the Western world, an estimated 1%–2% of the population experience HF,

From the Department of Biomedicine, University Hospital Basel and University of Basel, Basel, Switzerland; Division of Cardiology, University Hospital Basel, Basel, Switzerland; Cardiovascular Division, Department of Medicine, Brigham and Women's Hospital, Harvard Medical School, Boston, Mass.

Conflicts of Interest: All authors have read the journal's policy on disclosure of potential conflicts of interest and have none to declare.

Submitted for publication September 17, 2013; revision submitted November 4, 2013; accepted for publication December 5, 2013.

Reprint requests: Otmar Pfister, MD, Division of Cardiology, University Hospital Basel, Petersgraben 4, 4031 Basel, Switzerland; e-mail: otmar.pfister@usb.ch.

1931-5244/$ - see front matter

http://dx.doi.org/10.1016/j.trsl.2013.12.005

Chapter 18

Cell Therapy for Cardiac Regeneration

Gabriela M. Kuster, Giacomo Della Verde, Ronglih Liao, Otmar Pfister

Key Concepts

1. The heart is capable of very limited cell replacement through cardiomyocyte division and differentiation of heart-resident progenitor cells, but these endogenous regenerative resources are insufficient to compensate for major cell loss, which is at the core of heart failure. Novel therapeutic approaches including cell transplantation and cellular reprogramming aiming at the regeneration of lost cardiac tissue are currently in preclinical and early clinical testing.
2. A variety of extracardiac and heart-resident stem and progenitor cells have been characterized, all of them having their inherent strengths and limitations. These cells are transplanted through either intramyocardial or intracoronary application.
3. Bone marrow-derived cells act mainly through paracrine mechanisms. Despite promising preclinical and early clinical results, more rigorously designed clinical trials employing surrogate endpoints failed to prove clear efficacy, and a larger phase 3 mortality trial is currently ongoing.
4. Heart-resident cardiac stem and progenitor cells have cardiomyogenic differentiation potential, and preclinical and first small clinical trials yielded encouraging results. However, their availability is limited and amplification time-consuming, preventing their use in acute cardiac injury (acute myocardial infarction). A first study testing allogeneic cardiosphere-derived cells in humans is currently ongoing.
5. Embryonic stem cells (ESCs) and inducible pluripotent stem cells (iPS) have high plasticity, however, the suitability of cardiogenic cells derived from ESCs and iPS may be limited by yet unsolved safety issues including immunogenicity, tumorigenicity, and genetic instability.

List of Abbreviations

BCRP Breast cancer resistance protein
BMC Bone marrow-derived cell
BMMNC Bone marrow mononuclear cell
BMSC Bone marrow stem cells
CCTRN Cardiovascular cell therapy research network
CD Cluster of differentiation
c-kit Receptor for SCF
CSC Cardiac stem cell
CXCR4 Chemokine receptor 4
DNA Deoxyribonucleic acid
EPC Endothelial progenitor cell
ESC Embryonic stem cell
G-CSF Granulocyte-colony stimulating factor
HSC Hematopoietic stem cell
iPS Induced pluripotent stem cell
Isl-1 Islet 1
KLF4 Kruppel like factor 4
MDR Multidrug resistance protein
MSC Mesenchymal stem cell
Oct-4 Octamer binding transcription factor 4
RNA Ribonucleic acid
Sca-1 Stem cell antigen 1
SCF Stem cell factor

Translating Regenerative Medicine to the Clinic. http://dx.doi.org/10.1016/B978-0-12-800548-4.00018-8

ORIGINAL RESEARCH

American Heart Association | American Stroke Association

Polo-Like Kinase 2 is Dynamically Regulated to Coordinate Proliferation and Early Lineage Specification Downstream of Yes-Associated Protein 1 in Cardiac Progenitor Cells

Michika Mochizuki, PhD; Vera Lorenz, MSc; Robert Ivanek, PhD; Giacomo Della Verde, MSc; Emanuele Gaudiello, PhD; Anna Marsano, PhD; Otmar Pfister, MD; Gabriela M. Kuster, MD

***Background*—**Recent studies suggest that adult cardiac progenitor cells (CPCs) can produce new cardiac cells. Such cell formation requires an intricate coordination of progenitor cell proliferation and commitment, but the molecular cues responsible for this regulation in CPCs are ill defined.

***Methods and Results*—**Extracellular matrix components are important instructors of cell fate. Using laminin and fibronectin, we induced two slightly distinct CPC phenotypes differing in proliferation rate and commitment status and analyzed the early transcriptomic response to CPC adhesion (<2 hours). Ninety-four genes were differentially regulated on laminin versus fibronectin, consisting of mostly downregulated genes that were enriched for Yes-associated protein (YAP) conserved signature and TEA domain family member 1 (TEAD1)-related genes. This early gene regulation was preceded by the rapid cytosolic sequestration and degradation of YAP on laminin. Among the most strongly regulated genes was polo-like kinase 2 (*Plk2*). *Plk2* expression depended on YAP stability and was enhanced in CPCs transfected with a nuclear-targeted mutant YAP. Phenotypically, the early downregulation of *Plk2* on laminin was succeeded by lower cell proliferation, enhanced lineage gene expression (24 hours), and facilitated differentiation (3 weeks) compared with fibronectin. Finally, overexpression of Plk2 enhanced CPC proliferation and knockdown of Plk2 induced the expression of lineage genes.

***Conclusions*—**Plk2 acts as coordinator of cell proliferation and early lineage commitment in CPCs. The rapid downregulation of Plk2 on YAP inactivation marks a switch towards enhanced commitment and facilitated differentiation. These findings link early gene regulation to cell fate and provide novel insights into how CPC proliferation and differentiation are orchestrated. **(*J Am Heart Assoc*. 2017;6:e005920. DOI: 10.1161/JAHA.117.005920.)**

Key Words: cardiac progenitor cells • cell fate • extracellular matrix • polo-like kinase 2 • Yes-associated protein

The adult mammalian heart has a limited capacity of cell replacement, which in case of injury, such as myocardial infarction, is insufficient to restore cardiac cellularity and function. The resulting heart failure is a major cause of morbidity and mortality, and an intense search for therapeutic strategies to promote cardiac regeneration is currently ongoing. Such an approach, however, requires a clear understanding of the molecular mechanisms orchestrating cardiac cell replacement. It is now well established that the adult heart harbors cardiac progenitor cells (CPCs), which are —in principal—capable of self-renewal[1,2] and differentiation into cardiac lineages, including cardiomyocytes, endothelial cells, and vascular smooth muscle cells. A variety of markers and techniques for their identification and isolation have been reported.[3] In preclinical studies, various populations, including c-kit$^+$ CPCs, cardiosphere-derived cells, and cardiac side population (SP) CPCs, either endogenously or on in vitro expansion and transplantation, contribute to cardiac cell renewal after injury.[4–7] Clinical trials using c-kit$^+$ CPCs and cardiosphere-derived cells to induce regeneration of the postinfarct myocardium in humans have been initiated.[8,9]

Freshly isolated CPCs are low in numbers and require amplification before being transplanted into the injured heart for therapeutic application. Isolated CPCs can be readily expanded in vitro while keeping their multilineage

From the Department of Biomedicine (M.M., V.L., R.I., G.D.V., E.G., A.M., O.P., G.M.K.) and the Division of Cardiology (O.P., G.M.K.), University Hospital Basel, Basel, Switzerland; and University of Basel, Basel, Switzerland (M.M., V.L., R.I., G.D.V., E.G., A.M., O.P., G.M.K.).

Accompanying Tables S1, S2 and Figures S1 through S5 are available at http://jaha.ahajournals.org/content/6/10/e005920/DC1/embed/inline-supplementary-material-1.pdf

Correspondence to: Gabriela M. Kuster, MD, Department of Biomedicine and Division of Cardiology, University Hospital Basel, Hebelstrasse 20, 4031 Basel, Switzerland. E-mail: gabriela.kuster@usb.ch

Received May 16, 2017; accepted August 1, 2017.

References

1. P. Tsapogas, C. J. Mooney, G. Brown, A. Rolink, The Cytokine Flt3-Ligand in Normal and Malignant Hematopoiesis. *Int J Mol Sci* **18**, (2017).
2. S. A. Wander, M. J. Levis, A. T. Fathi, The evolving role of FLT3 inhibitors in acute myeloid leukemia: quizartinib and beyond. *Therapeutic advances in hematology* **5**, 65-77 (2014).
3. O. Pfister *et al.*, FLT3 Activation Improves Post-Myocardial Infarction Remodeling Involving a Cytoprotective Effect on Cardiomyocytes. *Journal of the American College of Cardiology* **63**, 1011-1019 (2014).
4. O. Pfister, A. Oikonomopoulos, K. I. Sereti, R. L. Liao, Isolation of Resident Cardiac Progenitor Cells by Hoechst 33342 Staining. *Methods Mol Biol* **660**, 53-63 (2010).
5. O. Pfister *et al.*, CD31- but Not CD31+ cardiac side population cells exhibit functional cardiomyogenic differentiation. *Circ Res* **97**, 52-61 (2005).
6. A. Torkamani, G. Verkhivker, N. J. Schork, Cancer driver mutations in protein kinase genes. *Cancer Letters* **281**, 117-127 (2009).
7. S. Gross, R. Rahal, N. Stransky, C. Lengauer, K. P. Hoeflich, Targeting cancer with kinase inhibitors. *J Clin Invest* **125**, 1780-1789 (2015).
8. H. Gharwan, H. Groninger, Kinase inhibitors and monoclonal antibodies in oncology: clinical implications. *Nat Rev Clin Oncol* **13**, 209-227 (2016).
9. H. Lal, K. L. Kolaja, T. Force, Cancer Genetics and the Cardiotoxicity of the Therapeutics. *Journal of the American College of Cardiology* **61**, 267-274 (2013).
10. E. A. Lefrak, J. Pitha, S. Rosenheim, J. A. Gottlieb, A clinicopathologic analysis of adriamycin cardiotoxicity. *Cancer* **32**, 302-314 (1973).
11. D. D. Vonhoff *et al.*, RISK-FACTORS FOR DOXORUBICIN-INDUCED CONGESTIVE HEART-FAILURE. *Annals of Internal Medicine* **91**, 710-717 (1979).
12. T. Force, D. S. Krause, R. A. Van Etten, Molecular mechanisms of cardiotoxicity of tyrosine kinase inhibition. *Nature Reviews Cancer* **7**, 332-344 (2007).
13. H. R. Mellor, A. R. Bell, J. P. Valentin, R. R. A. Roberts, Cardiotoxicity Associated with Targeting Kinase Pathways in Cancer. *Toxicological Sciences* **120**, 14-32 (2011).
14. A. C. Mertens *et al.*, Late mortality experience in five-year survivors of childhood and adolescent cancer: The childhood cancer survivor study. *Journal of Clinical Oncology* **19**, 3163-3172 (2001).
15. I. N. Daher, T. R. Daigle, N. Bhatia, J. B. Durand, The prevention of cardiovascular disease in cancer survivors. *Tex Heart Inst J* **39**, 190-198 (2012).
16. A. C. Mertens *et al.*, Cause-specific late mortality among 5-year survivors of childhood cancer: The childhood cancer survivor study. *J Natl Cancer I* **100**, 1368-1379 (2008).
17. S. E. Lipshultz, V. I. Franco, T. L. Miller, S. D. Colan, S. E. Sallan, Cardiovascular disease in adult survivors of childhood cancer. *Annu Rev Med* **66**, 161-176 (2015).

18. M. J. Adams, S. E. Lipshultz, Pathophysiology of anthracycline- and radiation-associated cardiomyopathies: implications for screening and prevention. *Pediatr Blood Cancer* **44**, 600-606 (2005).
19. S. E. Lipshultz *et al.*, Late Cardiac Effects of Doxorubicin Therapy for Acute Lymphoblastic-Leukemia in Childhood. *New Engl J Med* **324**, 808-815 (1991).
20. D. Cardinale *et al.*, Prevention of high-dose chemotherapy-induced cardiotoxicity in high-risk patients by angiotensin-converting enzyme inhibition. *Circulation* **114**, 2474-2481 (2006).
21. S. E. Lipshultz, Dexrazoxane for protection against cardiotoxic effects of anthracyclines in children. *Journal of Clinical Oncology* **14**, 328-331 (1996).
22. F. Shaikh *et al.*, Cardioprotection and Second Malignant Neoplasms Associated With Dexrazoxane in Children Receiving Anthracycline Chemotherapy: A Systematic Review and Meta-Analysis. *J Natl Cancer Inst* **108**, (2016).
23. P. A. Heidenreich *et al.*, Cost-effectiveness of screening with B-type natriuretic peptide to identify patients with reduced left ventricular ejection fraction. *Journal of the American College of Cardiology* **43**, 1019-1026 (2004).
24. D. Cardinale *et al.*, Prognostic value of troponin I in cardiac risk stratification of cancer patients undergoing high-dose chemotherapy. *Circulation* **109**, 2749-2754 (2004).
25. S. Takahashi, Downstream molecular pathways of FLT3 in the pathogenesis of acute myeloid leukemia: biology and therapeutic implications. *Journal of Hematology & Oncology* **4**, (2011).
26. A. Wodnar-Filipowicz, Flt3 ligand: Role in control of hematopoietic and immune functions of the bone marrow. *News in Physiological Sciences* **18**, 247-251 (2003).
27. K. C. Weisel, S. Yildirim, E. Schweikle, L. Kanz, R. Moehle, Regulation of FLT3 and its ligand in normal hematopoietic progenitor cells. *Annals of Hematology* **88**, 203-211 (2009).
28. K. Brasel *et al.*, Hematologic effects of flt3 ligand in vivo in mice. *Blood* **88**, 2004-2012 (1996).
29. L. S. Rusten, S. D. Lyman, O. P. Veiby, S. E. W. Jacobsen, The FLT3 ligand is a direct and potent stimulator of the growth of primitive and committed human CD34(+) bone marrow progenitor cells in vitro. *Blood* **87**, 1317-1325 (1996).
30. K. Mackarehtschian *et al.*, TARGETED DISRUPTION OF THE FLK2/FLT3 GENE LEADS TO DEFICIENCIES IN PRIMITIVE HEMATOPOIETIC PROGENITORS. *Immunity* **3**, 147-161 (1995).
31. H. J. McKenna *et al.*, Mice lacking flt3 ligand have deficient hematopoiesis affecting hematopoietic progenitor cells, dendritic cells, and natural killer cells. *Blood* **95**, 3489-3497 (2000).
32. H. Karsunky, M. Merad, A. Cozzio, I. L. Weissman, M. G. Manz, Flt3 ligand regulates dendritic cell development from Flt3(+) lymphoid and myeloid-committed progenitors to Flt3(+) dendritic cells in vivo. *Journal of Experimental Medicine* **198**, 305-313 (2003).

33. P. Tsapogas *et al.*, In vivo evidence for an instructive role of fms-like tyrosine kinase-3 (FLT3) ligand in hematopoietic development. *Haematologica* **99**, 638-646 (2014).
34. L. von Muenchow *et al.*, Permissive roles of cytokines interleukin-7 and Flt3 ligand in mouse B-cell lineage commitment. *Proc Natl Acad Sci U S A* **113**, E8122-E8130 (2016).
35. B. W. Parcells, A. K. Ikeda, T. Simms-Waldrip, T. B. Moore, K. M. Sakamoto, FMS-like tyrosine kinase 3 in normal hematopoiesis and acute myeloid leukemia. *Stem Cells* **24**, 1174-1184 (2006).
36. H. Kiyoi, FLT3 INHIBITORS: RECENT ADVANCES AND PROBLEMS FOR CLINICAL APPLICATION. *Nagoya Journal of Medical Science* **77**, 7-17 (2015).
37. D. B. Rosen *et al.*, Functional Characterization of FLT3 Receptor Signaling Deregulation in Acute Myeloid Leukemia by Single Cell Network Profiling (SCNP). *Plos One* **5**, (2010).
38. S. H. Chu *et al.*, FLT3-ITD Knockin Impairs Hematopoietic Stem Cell Quiescence/Homeostasis, Leading to Myeloproliferative Neoplasm. *Cell Stem Cell* **11**, 346-358 (2012).
39. R. Roskoski, Classification of small molecule protein kinase inhibitors based upon the structures of their drug-enzyme complexes. *Pharmacological Research* **103**, 26-48 (2016).
40. T. F. Chu *et al.*, Cardiotoxicity associated with tyrosine kinase inhibitor sunitinib. *Lancet* **370**, 2011-2019 (2007).
41. A. Al-Kali *et al.*, Patterns of Molecular Response to and Relapse After Combination of Sorafenib, Idarubicin, and Cytarabine in Patients With FLT3 Mutant Acute Myeloid Leukemia. *Clinical Lymphoma Myeloma & Leukemia* **11**, 361-366 (2011).
42. C. Rollig *et al.*, Addition of sorafenib versus placebo to standard therapy in patients aged 60 years or younger with newly diagnosed acute myeloid leukaemia (SORAML): a multicentre, phase 2, randomised controlled trial. *Lancet Oncology* **16**, 1691-1699 (2015).
43. M. Schmidinger *et al.*, Cardiac Toxicity of Sunitinib and Sorafenib in Patients With Metastatic Renal Cell Carcinoma. *Journal of Clinical Oncology* **26**, 5204-5212 (2008).
44. J. M. Duran *et al.*, Sorafenib Cardiotoxicity Increases Mortality After Myocardial Infarction. *Circulation Research* **114**, 1700-+ (2014).
45. P. P. Zarrinkar *et al.*, AC220 is a uniquely potent and selective inhibitor of FLT3 for the treatment of acute myeloid leukemia (AML). *Blood* **114**, 2984-2992 (2009).
46. K. M. Kampa-Schittenhelm *et al.*, Quizartinib (AC220) is a potent second generation class III tyrosine kinase inhibitor that displays a distinct inhibition profile against mutant-FLT3, -PDGFRA and -KIT isoforms. *Molecular Cancer* **12**, (2013).
47. J. E. Cortes *et al.*, Final Results of a Phase 2 Open-Label, Monotherapy Efficacy and Safety Study of Quizartinib (AC220) in Patients >= 60 Years of Age with FLT3 ITD Positive or Negative Relapsed/Refractory Acute Myeloid Leukemia. *Blood* **120**, (2012).
48. E. Weisberg, M. Sattler, A. Ray, J. D. Griffin, Drug resistance in mutant FLT3-positive AML. *Oncogene* **29**, 5120-5134 (2010).

49. C. C. Smith *et al.*, Validation of ITD mutations in FLT3 as a therapeutic target in human acute myeloid leukaemia. *Nature* **485**, 260-U153 (2012).
50. J. K. Randhawa *et al.*, Results of a Phase II Study of Crenolanib in Relapsed/Refractory Acute Myeloid Leukemia Patients (Pts) with Activating FLT3 Mutations. *Blood* **124**, (2014).
51. A. Galanis *et al.*, Crenolanib is a potent inhibitor of FLT3 with activity against resistance-conferring point mutants. *Blood* **123**, 94-100 (2014).
52. T. M. Cooper *et al.*, A Phase I Study Of AC220 (Quizartinib) In Combination With Cytarabine and Etoposide In Relapsed/Refractory Childhood ALL and AML: A Therapeutic Advances In Childhood Leukemia & Lymphoma (TACL) Study. *Blood* **122**, (2013).
53. T. Sato *et al.*, FLT3 ligand impedes the efficacy of FLT3 inhibitors in vitro and in vivo. *Blood* **117**, 3286-3293 (2011).
54. Y. Ge, R. J. Waldemer, R. Nalluri, P. D. Nuzzi, J. Chen, Flt3L is a novel regulator of skeletal myogenesis. *Journal of Cell Science* **126**, 3370-3379 (2013).
55. B. M. Deasy, Z. Qu-Peterson, J. S. Greenberger, J. Huard, Mechanisms of muscle stem cell expansion with cytokines. *Stem Cells* **20**, 50-60 (2002).
56. B. B. Ayach *et al.*, Stem cell factor receptor induces progenitor and natural killer cell-mediated cardiac survival and repair after myocardial infarction. *Proceedings of the National Academy of Sciences of the United States of America* **103**, 2304-2309 (2006).
57. B. Dawn *et al.*, Postinfarct cytokine therapy regenerates cardiac tissue and improves left ventricular function. *Circulation Research* **98**, 1098-1105 (2006).
58. M. Lisovsky *et al.*, Flt3 ligand stimulates proliferation and inhibits apoptosis of acute myeloid leukemia cells: Regulation of Bcl-2 and Bax. *Blood* **88**, 3987-3997 (1996).
59. G. Tian, J. Y. Lu, H. Q. Guo, Q. Liu, H. W. Wang, Protective effect of Flt3L on organ structure during advanced multiorgan dysfunction syndrome in mice. *Molecular Medicine Reports* **11**, 4135-4141 (2015).
60. O. Bergmann *et al.*, Evidence for Cardiomyocyte Renewal in Humans. *Science* **324**, 98-102 (2009).
61. K. Malliaras *et al.*, Cardiomyocyte proliferation and progenitor cell recruitment underlie therapeutic regeneration after myocardial infarction in the adult mouse heart. *Embo Molecular Medicine* **5**, 191-209 (2013).
62. M. H. Soonpaa, L. J. Field, Assessment of cardiomyocyte DNA synthesis in normal and injured adult mouse hearts. *Am J Physiol-Heart C* **272**, H220-H226 (1997).
63. S. E. Senyo *et al.*, Mammalian heart renewal by pre-existing cardiomyocytes. *Nature* **493**, 433-U186 (2013).
64. A. P. Beltrami *et al.*, Evidence that human cardiac myocytes divide after myocardial infarction. *New Engl J Med* **344**, 1750-1757 (2001).
65. J. Kajstura *et al.*, Myocyte proliferation in end-stage cardiac failure in humans. *Proceedings of the National Academy of Sciences of the United States of America* **95**, 8801-8805 (1998).
66. A. P. Beltrami *et al.*, Adult cardiac stem cells are multipotent and support myocardial regeneration. *Cell* **114**, 763-776 (2003).

67. F. Mouquet *et al.*, Restoration of cardiac progenitor cells after myocardial infarction by self-proliferation and selective homing of bone marrow-derived stem cells. *Circulation Research* **97**, 1090-1092 (2005).
68. H. Oh *et al.*, Cardiac progenitor cells from adult myocardium: Homing, differentiation, and fusion after infarction. *Proceedings of the National Academy of Sciences of the United States of America* **100**, 12313-12318 (2003).
69. M. Noseda *et al.*, PDGFR alpha demarcates the cardiogenic clonogenic Sca1(+) stem/progenitor cell in adult murine myocardium. *Nature Communications* **6**, (2015).
70. D. Torella, G. A. Ellison, B. Nadal-Ginard, C. Indolfi, Cardiac stem and progenitor cell biology for regenerative medicine. *Trends in Cardiovascular Medicine* **15**, 229-236 (2005).
71. E. Piegari *et al.*, Doxorubicin induces senescence and impairs function of human cardiac progenitor cells. *Basic Research in Cardiology* **108**, (2013).
72. A. De Angelis *et al.*, Anthracycline Cardiomyopathy Is Mediated by Depletion of the Cardiac Stem Cell Pool and Is Rescued by Restoration of Progenitor Cell Function. *Circulation* **121**, 276-U188 (2010).
73. T. H. She *et al.*, Hyperglycemia suppresses cardiac stem cell homing to peri-infarcted myocardium via regulation of ERK1/2 and p38 MAPK activities. *International Journal of Molecular Medicine* **30**, 1313-1320 (2012).
74. O. Pfister, G. Della Verde, R. Liao, G. M. Kuster, Regenerative therapy for cardiovascular disease. *Translational Research* **163**, 307-320 (2014).
75. A. R. Chugh *et al.*, Administration of Cardiac Stem Cells in Patients With Ischemic Cardiomyopathy: The SCIPIO Trial Surgical Aspects and Interim Analysis of Myocardial Function and Viability by Magnetic Resonance. *Circulation* **126**, S54-S64 (2012).
76. K. Malliaras *et al.*, Intracoronary Cardiosphere-Derived Cells After Myocardial Infarction. *Journal of the American College of Cardiology* **63**, 110-122 (2014).
77. K. Matsuura *et al.*, Adult cardiac Sca-1-positive cells differentiate into beating cardiomyocytes. *Journal of Biological Chemistry* **279**, 11384-11391 (2004).
78. M. Hoch *et al.*, Erythropoietin Preserves the Endothelial Differentiation Capacity of Cardiac Progenitor Cells and Reduces Heart Failure during Anticancer Therapies. *Cell Stem Cell* **9**, 131-143 (2011).
79. M. A. Izquierdo *et al.*, Overexpression of the ABC transporter TAP in multidrug-resistant human cancer cell lines. *British Journal of Cancer* **74**, 1961-1967 (1996).
80. M. A. Goodell, K. Brose, G. Paradis, A. S. Conner, R. C. Mulligan, Isolation and functional properties of murine hematopoietic stem cells that are replicating in vivo. *Journal of Experimental Medicine* **183**, 1797-1806 (1996).
81. R. W. Storms, M. A. Goodell, A. Fisher, R. C. Mulligan, C. Smith, Hoechst dye efflux reveals a novel CD7(+)CD34(-) lymphoid progenitor in human umbilical cord blood. *Blood* **96**, 2125-2133 (2000).
82. A. P. Meeson *et al.*, Cellular and molecular regulation of skeletal muscle side population cells. *Stem Cells* **22**, 1305-1320 (2004).

83. A. Asakura, P. Seale, A. Girgis-Gabardo, M. A. Rudnicki, Myogenic specification of side population cells in skeletal muscle. *Journal of Cell Biology* **159**, 123-134 (2002).
84. F. Montanaro *et al.*, Demystifying SP cell purification: viability, yield, and phenotype are defined by isolation parameters. *Experimental Cell Research* **298**, 144-154 (2004).
85. B. E. Welm *et al.*, Sca-1(pos) cells in the mouse mammary gland represent an enriched progenitor cell population. *Developmental Biology* **245**, 42-56 (2002).
86. H. Clayton, I. Titley, M. D. Vivanco, Growth and differentiation of progenitor/stem cells derived from the human mammary gland (vol 297, pg 444, 2004). *Experimental Cell Research* **300**, 257-257 (2004).
87. L. Gremeaux, Q. L. Fu, J. H. Chen, H. Vankelecom, Activated Phenotype of the Pituitary Stem/Progenitor Cell Compartment During the Early-Postnatal Maturation Phase of the Gland. *Stem Cells and Development* **21**, 801-813 (2012).
88. R. Summer *et al.*, Side population cells and Bcrp1 expression in lung. *American Journal of Physiology-Lung Cellular and Molecular Physiology* **285**, L97-L104 (2003).
89. A. Giangreco, H. M. Shen, S. D. Reynolds, B. R. Stripp, Molecular phenotype of airway side population cells. *American Journal of Physiology-Lung Cellular and Molecular Physiology* **286**, L624-L630 (2004).
90. S. M. Majka *et al.*, Identification of novel resident pulmonary stem cells: Form and function of the lung side population. *Stem Cells* **23**, 1073-1081 (2005).
91. K. Shimano *et al.*, Hepatic oval cells have the side population phenotype defined by expression of ATP-binding cassette transporter ABCG2/BCRP1. *American Journal of Pathology* **163**, 3-9 (2003).
92. A. Terunuma, K. L. Jackson, V. Kapoor, W. G. Telford, J. C. Vogel, Side population keratinocytes resembling bone marrow side population stem cells are distinct from label-retaining keratinocyte stem cells. *Journal of Investigative Dermatology* **121**, 1095-1103 (2003).
93. C. Triel, M. E. Vestergaard, L. Bolund, T. G. Jensen, U. B. Jensen, Side population cells in human and mouse epidermis lack stem cell characteristics. *Experimental Cell Research* **295**, 79-90 (2004).
94. M. Kim, C. M. Morshead, Distinct populations of forebrain neural stem and progenitor cells can be isolated using side-population analysis. *Journal of Neuroscience* **23**, 10703-10709 (2003).
95. B. Lassalle *et al.*, 'Side Population' cells in adult mouse testis express Bcrp1 gene and are enriched in spermatogonia and germinal stem cells. *Development* **131**, 479-487 (2004).
96. I. Falciatori *et al.*, Identification and enrichment of spermatogonial stem cells displaying side-population phenotype in immature mouse testis. *Faseb Journal* **17**, 376-+ (2003).
97. H. Iwatani *et al.*, Hematopoietic and nonhematopoietic potentials of Hoechst(low)/side population cells isolated from adult rat kidney. *Kidney International* **65**, 1604-1614 (2004).

98. K. Watanabe *et al.*, Human limbal epithelium contains side population cells expressing the ATP-binding cassette transporter ABCG2. *Febs Letters* **565**, 6-10 (2004).
99. T. Umemoto *et al.*, Limbal epithelial side-population cells have stem cell-like properties, including quiescent state. *Stem Cells* **24**, 86-94 (2006).
100. R. I. Bhatt *et al.*, Novel method for the isolation and characterisation of the putative prostatic stem cell. *Cytometry Part A* **54A**, 89-99 (2003).
101. J. Xu *et al.*, Effect of estradiol on proliferation and differentiation of side population stem/progenitor cells from murine endometrium. *Reproductive Biology and Endocrinology* **9**, (2011).
102. A. M. Hierlihy, P. Seale, C. G. Lobe, M. A. Rudnicki, L. A. Megeney, The post-natal heart contains a myocardial stem cell population. *Febs Letters* **530**, 239-243 (2002).
103. T. Oyama *et al.*, Cardiac side population cells have a potential to migrate and differentiate into cardiomyocytes in vitro and in vivo. *Journal of Cell Biology* **176**, 329-341 (2007).
104. J. Yoon, S. C. Choi, C. Y. Park, W. J. Shim, D. S. Lim, Cardiac side population cells exhibit endothelial differentiation potential. *Experimental and Molecular Medicine* **39**, 653-662 (2007).
105. S. X. Liang *et al.*, In vitro and in vivo proliferation, differentiation and migration of cardiac endothelial progenitor cells (SCA1(+)/CD31(+) side-population cells). *Journal of Thrombosis and Haemostasis* **9**, 1628-1637 (2011).
106. S. X. Liang, T. Y. L. Tan, L. Gaudry, B. Chong, Differentiation and migration of Sca1+/CD31-cardiac side population cells in a murine myocardial ischemic model. *International Journal of Cardiology* **138**, 40-49 (2010).
107. X. Z. Wang *et al.*, Proliferation, differentiation and migration of SCA1(-)/CD31(-) cardiac side population cells in vitro and in vivo. *International Journal of Cardiology* **227**, 378-386 (2017).
108. N. G. Frangogiannis, The inflammatory response in myocardial injury, repair, and remodelling. *Nature Reviews Cardiology* **11**, 255-265 (2014).
109. Y. Feng *et al.*, MicroRNAs are Released During Myocardial Ischemia Reperfusion Injury and Induce Inflammation via Toll-like Receptor 7 in vitro. *Circulation* **134**, (2016).
110. L. Timmers *et al.*, Toll-like receptor 4 mediates maladaptive left ventricular remodeling and impairs cardiac function after myocardial infarction. *Circulation Research* **102**, 257-264 (2008).
111. J. Oyama *et al.*, Reduced myocardial ischemia-reperfusion injury in toll-like receptor 4-deficient mice. *Circulation* **109**, 784-789 (2004).
112. N. G. Frangogiannis, The Immune System and the Remodeling Infarcted Heart: Cell Biological Insights and Therapeutic Opportunities. *J Cardiovasc Pharm* **63**, 185-195 (2014).
113. N. G. Frangogiannis, The immune system and cardiac repair. *Pharmacological Research* **58**, 88-111 (2008).
114. L. Fang, X. L. Moore, A. M. Dart, L. M. Wang, Systemic inflammatory response following acute myocardial infarction. *Journal of Geriatric Cardiology* **12**, 305-312 (2015).

115. B. Cheng, H. C. Chen, I. W. Chou, T. W. Tang, P. C. Hsieh, Harnessing the early post-injury inflammatory responses for cardiac regeneration. *J Biomed Sci* **24**, 7 (2017).
116. M. G. Sutton, N. Sharpe, Left ventricular remodeling after myocardial infarction: pathophysiology and therapy. *Circulation* **101**, 2981-2988 (2000).
117. M. Ikeuchi *et al.*, Inhibition of TGF-beta signaling exacerbates early cardiac dysfunction but prevents late remodeling after infarction. *Cardiovasc Res* **64**, 526-535 (2004).
118. M. Dobaczewski, W. Chen, N. G. Frangogiannis, Transforming growth factor (TGF)-beta signaling in cardiac remodeling. *J Mol Cell Cardiol* **51**, 600-606 (2011).
119. N. G. Frangogiannis *et al.*, IL-10 is induced in the reperfused myocardium and may modulate the reaction to injury. *J Immunol* **165**, 2798-2808 (2000).
120. K. T. Keyes *et al.*, Resolvin E1 protects the rat heart against reperfusion injury. *Am J Physiol-Heart C* **299**, H153-H164 (2010).
121. X. X. Yan *et al.*, Temporal dynamics of cardiac immune cell accumulation following acute myocardial infarction. *J Mol Cell Cardiol* **62**, 24-35 (2013).
122. M. Shiraishi *et al.*, Alternatively activated macrophages determine repair of the infarcted adult murine heart. *J Clin Invest* **126**, 2151-2166 (2016).
123. C. Y. Brazel, M. H. Ducceschi, B. Pytowski, S. W. Levison, The FLT3 tyrosine kinase receptor inhibits neural stem/progenitor cell proliferation and collaborates with NGF to promote neuronal survival. *Mol Cell Neurosci* **18**, 381-393 (2001).
124. B. C. Schaefer, M. L. Schaefer, J. W. Kappler, P. Marrack, R. M. Kedl, Observation of antigen-dependent CD8(+) T-cell/dendritic cell interactions in vivo. *Cell Immunol* **214**, 110-122 (2001).
125. N. M. Degabriele *et al.*, Critical appraisal of the mouse model of myocardial infarction. *Experimental Physiology* **89**, 497-505 (2004).
126. L. H. Michael *et al.*, Myocardial ischemia and reperfusion: a murine model. *Am J Physiol* **269**, H2147-2154 (1995).
127. A. Markovic, K. L. MacKenzie, R. B. Lock, FLT-3: a new focus in the understanding of acute leukemia. *Int J Biochem Cell B* **37**, 1168-1172 (2005).
128. M. Lisovsky *et al.*, Flt3-ligand production by human bone marrow stromal cells. *Leukemia* **10**, 1012-1018 (1996).
129. E. Chklovskaia *et al.*, Cell-surface trafficking and release of flt3 ligand from T lymphocytes is induced by common cytokine receptor gamma-chain signaling and inhibited by cyclosporin A. *Blood* **97**, 1027-1034 (2001).
130. Y. Morita, H. Ema, S. Yamazaki, H. Nakauchi, Non-side-population hematopoietic stem cells in mouse bone marrow. *Blood* **108**, 2850-2856 (2006).
131. A. Subramanian *et al.*, Gene set enrichment analysis: A knowledge-based approach for interpreting genome-wide expression profiles. *Proceedings of the National Academy of Sciences of the United States of America* **102**, 15545-15550 (2005).
132. A. Liberzon *et al.*, The Molecular Signatures Database Hallmark Gene Set Collection. *Cell Syst* **1**, 417-425 (2015).

133. A. Liberzon *et al.*, Molecular signatures database (MSigDB) 3.0. *Bioinformatics* **27**, 1739-1740 (2011).
134. A. C. Boquest *et al.*, Isolation and transcription profiling of purified uncultured human stromal stem cells: Alteration of gene expression after in vitro cell culture. *Mol Biol Cell* **16**, 1131-1141 (2005).
135. D. L. Coutu, J. Galipeau, Roles of FGF signaling in stem cell self-renewal, senescence and aging. *Aging-Us* **3**, 920-933 (2011).
136. M. Otsu, T. Nakayama, N. Inoue, Pluripotent stem cell-derived neural stem cells: From basic research to applications. *World J Stem Cells* **6**, 651-657 (2014).
137. F. H. Hu *et al.*, Effects of Epidermal Growth Factor and Basic Fibroblast Growth Factor on the Proliferation and Osteogenic and Neural Differentiation of Adipose-Derived Stem Cells. *Cell Reprogram* **15**, 224-232 (2013).
138. K. L. DeCicco-Skinner *et al.*, Endothelial Cell Tube Formation Assay for the In Vitro Study of Angiogenesis. *Jove-J Vis Exp*, (2014).
139. M. Bauer *et al.*, Echocardiographic Speckle-Tracking Based Strain Imaging for Rapid Cardiovascular Phenotyping in Mice. *Circulation Research* **108**, 908-U933 (2011).
140. D. Hilfiker-Kleiner *et al.*, A cathepsin D-cleaved 16 kDa form of prolactin mediates postpartum cardiomyopathy. *Cell* **128**, 589-600 (2007).
141. K. A. Gerbin, C. E. Murry, The winding road to regenerating the human heart. *Cardiovasc Pathol* **24**, 133-140 (2015).
142. J. H. van Berlo, J. D. Molkentin, An emerging consensus on cardiac regeneration. *Nat Med* **20**, 1386-1393 (2014).
143. J. M. Hare *et al.*, Randomized Comparison of Allogeneic vs Autologous Mesenchymal Stem Cells in Patients With Non-Ischemic Dilated Cardiomyopathy-The POSEIDON-DCM Trial. *Circulation* **134**, E709-E710 (2016).
144. E. Abdelwahid *et al.*, Stem cell death and survival in heart regeneration and repair. *Apoptosis* **21**, 252-268 (2016).
145. G. Vunjak-Noyakovic, K. O. Lui, N. Tandon, K. R. Chien, Bioengineering Heart Muscle: A Paradigm for Regenerative Medicine. *Annu Rev Biomed Eng* **13**, 245-267 (2011).
146. L. Ye, W. H. Zimmermann, D. J. Garry, J. Y. Zhang, Patching the Heart Cardiac Repair From Within and Outside. *Circulation Research* **113**, 922-932 (2013).
147. K. L. K. Coulombe, V. K. Bajpai, S. T. Andreadis, C. E. Murry, Heart Regeneration with Engineered Myocardial Tissue. *Annual Review of Biomedical Engineering, Vol 16* **16**, 1-28 (2014).
148. H. Reinecke, M. Zhang, T. Bartosek, C. E. Murry, Survival, integration, and differentiation of cardiomyocyte grafts - A study in normal and injured rat hearts. *Circulation* **100**, 193-202 (1999).
149. A. Yellamilli, J. H. van Berlo, The Role of Cardiac Side Population Cells in Cardiac Regeneration. *Front Cell Dev Biol* **4**, 102 (2016).
150. J. Sandstedt *et al.*, Left atrium of the human adult heart contains a population of side population cells. *Basic Research in Cardiology* **107**, (2012).

151. P. R. Riley, N. Smart, Vascularizing the heart. *Cardiovasc Res* **91**, 260-268 (2011).
152. A. Luttun, P. Carmeliet, De novo vasculogenesis in the heart. *Cardiovasc Res* **58**, 378-389 (2003).
153. D. C. Sane, The endothelial life insurance plan. *Blood* **104**, 2615-2616 (2004).
154. T. Asahara *et al.*, Isolation of putative progenitor endothelial cells for angiogenesis. *Science* **275**, 964-967 (1997).
155. M. Jeltsch, V. M. Leppanen, P. Saharinen, K. Alitalo, Receptor Tyrosine Kinase-Mediated Angiogenesis. *Csh Perspect Biol* **5**, (2013).
156. M. Volkova, R. Russell, 3rd, Anthracycline cardiotoxicity: prevalence, pathogenesis and treatment. *Curr Cardiol Rev* **7**, 214-220 (2011).
157. J. V. McGowan *et al.*, Anthracycline Chemotherapy and Cardiotoxicity. *Cardiovasc Drug Ther* **31**, 63-75 (2017).
158. S. M. Wilhelm *et al.*, BAY 43-9006 exhibits broad spectrum oral antitumor activity and targets the RAF/MEK/ERK pathway and receptor tyrosine kinases involved in tumor progression and angiogenesis. *Cancer Res* **64**, 7099-7109 (2004).
159. D. B. Mendel *et al.*, In vivo antitumor activity of SU11248, a novel tyrosine kinase inhibitor targeting vascular endothelial growth factor and platelet-derived growth factor receptors: Determination of a pharmacokinetic/pharmacodynamic relationship. *Clin Cancer Res* **9**, 327-337 (2003).
160. B. Testoni, R. Mantovani, Mechanisms of transcriptional repression of cell-cycle G2/M promoters by p63 (vol 34, pg 928, 2006). *Nucleic Acids Res* **42**, 1391-1391 (2014).
161. G. Melino, p63 is a suppressor of tumorigenesis and metastasis interacting with mutant p53. *Cell Death Differ* **18**, 1487-1499 (2011).
162. X. H. Su *et al.*, TAp63 Prevents Premature Aging by Promoting Adult Stem Cell Maintenance. *Cell Stem Cell* **5**, 64-75 (2009).
163. M. Rouleau *et al.*, TAp63 Is Important for Cardiac Differentiation of Embryonic Stem Cells and Heart Development. *Stem Cells* **29**, 1672-1683 (2011).
164. J. H. Ma *et al.*, Mammalian target of rapamycin regulates murine and human cell differentiation through STAT3/p63/Jagged/Notch cascade. *J Clin Invest* **120**, 103-114 (2010).

Giacomo Della Verde

Myocardial Research
Department of Biomedicine, University Hospital
Hebelstrasse 20, CH-4031Basel
Tel: ++41 +61 265 23 46
Fax: ++41 +61 265 23 50
giacomo.dellaverde@gmail.com

Italian
2nd September 1987
Orbetello

Education

February 2013 – March 2018	PhD Program, Biomedical Research, Natural Sciences Faculty, University of Basel, Switzerland
October 2009 – July 2012	Faculty of Mathematical, Physical and Natural Sciences, Pisa M. Sc., Molecular and Cellular Biology
October 2006 - October 2009	Faculty of Mathematical, Physical and Natural Sciences, Pisa B. Sc., Molecular Biological Sciences

Research Experience

March 2018 – now

Post-Doctoral Research
Research topic: "*Role of fms-like tyrosine kinase 3 in cardiac health and disease"*
Advisors: PD Dr. med. Gabriela Kuster Pfister
Department of Biomedicine, University Hospital Basel, Switzerland

February 2013 – March 2018

Doctoral Research
Research topic: "*Role of fms-like tyrosine kinase 3 (flt3) in cardiac health and disease"*
Advisors: PD Dr. med. Gabriela Kuster Pfister, PD Dr. med. Otmar Pfister
Department of Biomedicine, University Hospital Basel, Switzerland

October 2011 – July 2012

Undergraduate Research
Thesis title: *"Phenotyping of cardiac side population (CSP) progenitor cells and comparison between wild-type CSP and CSP from mice deficient in fms-like tyrosine kinase 3 (flt3) or flt3 ligand (FL)"*
Advisors: PD Dr. med. Gabriela Kuster Pfister, PD Dr. med. Otmar Pfister
Department of Biomedicine, University Hospital Basel, Switzerland

January 2011 - May 2011

Scientific Apprentice
Research topic: *"Investigation on the targeting and localization of the Na+-K+ ATPase in eukaryotic cells and mouse embryos"*
Advisor: Prof. Karin Lykke-Hartmann
Department of Medical Biochemistry, Aarhus University, Denmark

March 2009 - June 2009

Undergraduate Research
Thesis title: *"Characterization of the expression pattern of specific RNA in Xenopus laevis retinal cells"*
Advisor: Prof. Luciana Dente
Laboratory of Molecular and Cellular Biology. Ghezzano, Pisa.

Awards and Fellowships

May 2014	Young Investigator Award Basic Science (Runner-Up Prize), European Society of Cardiology Heart Failure Association, Athens
October 2011 – July 2012	Erasmus Placement Scholarship, (University and University Hospital Basel, Switzerland)
January 2011 - June 2011	Erasmus Study Scholarship, (Aarhus University, Denmark)

Presentations, Congress Contributions

Oral

15.01.2016	Cardiovascular and Metabolic Research Conference 2016 Fribourg, Switzerland
28.05.2015	DBM Scientific Summer PhD Retreat 2015 Schwarsee, Switzerland
18.05.2014	Heart Failure 2014 of the European Society of Cardiology, Athens
16.01.2014	Cardiovascular and Metabolic Research Conference 2014 Fribourg, Switzerland
14.06.2012	Scientific Sessions, Swiss Society of Cardiology (SGK), 2012 Lausanne, Switzerland

Posters

22.03.2013	DBM Scientific Winter PhD Retreat 2013 Hasliberg, Switzerland
11.01.2013	AGLA & Cardiovascular Biology Meeting 2013 Bern, Switzerland

Publications

1	Kuster GM, **Della Verde G**, Liao R. and Pfister O. "Cell therapy for cardiac regeneration". Chapter for " Translating Regenerative Medicine to Clinic". Academic Press. 2015 Dec. ISBN: 978-0-12-800548-4
2	Pfister O, **Della Verde G**, Liao R, Kuster GM. "Regenerative therapy for cardiovascular disease". Transl Res. 2014 Apr; 163(4):307-320.
3	Michika Mochizuki, Vera Lorenz, Robert Ivanek, **Giacomo Della Verde**, Emanuele Gaudiello, Anna Marsano, Otmar Pfister, Gabriela M. Kuster. "Polo-Like Kinase 2 is Dynamically Regulated to Coordinate Proliferation and Early Lineage Specification Downstream of Yes-Associated Protein 1 in Cardiac Progenitor Cells". Journal of the American Heart Association. 2017;6:e005920, originally published October 24, 2017